

Response to RC2

(responses in blue)

The authors simulate the pre-industrial, mid-Holocene, LGM, and Pliocene climates using the ECHAM5 general circulation model. The motivation is to understand how past climatic states may change regional climatologies, particularly over mountainous areas that have been the focus of much erosion and geomorphic work. The authors find that past climatic states (particularly the LGM and Pliocene) do produce changes in absolute temperature and precipitation and in the annual ranges of these two climatic variables.

Overall, I did not find the manuscript to be a particularly useful addition to the literature. Though the motivation is potentially novel, the analysis is not complete and needs substantially more work. Most of the manuscript focuses on simply describing climatic changes, while neglecting novel analyses. Consequently, at this point, I recommend reject, though perhaps with substantial work (including more modeling, comparison with existing models, and/or comparison with data), it may become publishable in the future in *ESurf*.

We thank the reviewer for their constructive feedback on our manuscript. We found the reviewer's comment very useful in the improvement of this manuscript and hope that the modifications we made do the reviewer's thorough review justice. Most importantly, we followed the reviewer's suggestion to deepen the comparison of our model simulation results with data, specifically proxy-based reconstructions, as we believe this suggestion is of most relevance to the earth surface science community targeted by *ESurf*. While it was not possible to create a complete overview of all proxy-based studies everywhere and for all time periods, we included an extensive compilation of site specific reconstructions of precipitation for our largest areas (South America and Tibet). In prioritizing the compilation of precipitation reconstructions, we also hope to address the reviewer's concerns about the GCM's performance regarding this variable, and are happy to report that the model shows satisfactory to good performance in predicting the direction of changes in MH and LGM.

First, the authors need to decide what the point of the paper is. Most of the paper reads as a description of climatological changes for 3 periods in the geologic past (MH, LGM, and Plio) (indeed, most of the text is written this way). However, this work has already been done, most prominently by the PMIP and PlioMIP set of model intercomparisons. What does this manuscript offer that these model intercomparisons have not already analyzed? A case could be made that these model intercomparisons are typically of a global nature (though there has been some work on changes in the Asian Monsoon systems using both PlioMIP and PMIP results (Jiang et al., 2013; Jiang and Lang, 2010; Zhang et al., 2013)), so that the analysis of the orogens in this study is useful. However, given that GCMs have difficulty simulating precipitation and in particular simulating precipitation over complex topography, the usefulness of simply describing changes over the Himalaya, Andes, Cascades, and St. Elias ranges is somewhat muted. For example, why should readers believe that ECHAM5 produces reasonable results over the St. Elias range? Why not use (or at least compare with) the existing model intercomparisons to look at changes in these locations? Most of the PlioMIP simulations are of a lower resolution than the model simulations presented here, though not all (Haywood et al., 2013). Many of the newer PlioMIP2 simulations are being run at a higher resolution and permit at least some comparison with the data here (Chandan and Peltier, 2017). Having myself tried to access PlioMIP data, I understand that it can be difficult to get access to the PlioMIP output, but if the point of the paper is to quantify actual climatological change, then comparison with other models is a must (or at least a thorough treatment of possible boundary condition uncertainties and additional ECHAM5 model runs to establish the sensitivity of precipitation/temperature in these areas); otherwise, we have no reason to believe that ECHAM5 presents anything resembling a proper picture of climatic change in the past.

Summary Response: We appreciate this assessment and hope to have enhanced the usefulness of the manuscript with modifications we've made throughout the results and discussion sections. While GCM simulations for the time slices we chose already exist and individual studies were also conducted at a relatively high resolution, we believe (contrary to the reviewer's suggestion) that the usefulness of our results lies in both the high resolution combined with the consistency in model choice, resolution, output frequency (and methods of descriptive statistics). We emphasise this point in the revised manuscript. We acknowledge in the text (methods section 2.1 and introduction) the shortcomings of GCMs in predicting orographic precipitation in the discussion and in the revised text now compare the simulated precipitation with readily available proxy-based reconstructions for specific locations in Tibet and South America where we were able to compile data (this was a large undertaking). The revised manuscript now demonstrates the shortcomings of GCMs and provides an additional data compilation that *ESurf* readers interested in

palaeoclimate effects on denudation may find useful. The changes we have made to address this reviewers suggestions are contained in the revised introduction, and extensively throughout the Discussion section (4.0), as well as the addition of two new (concluding figures).

In More Detail: While we appreciated the reviewer's comments, we note that what he/she is asking for in the above comments is a manuscript that either focuses on an inter-model comparisons, or a comparison to proxy data. We see merits in both, but both are not possible in a single manuscript. An inter-model comparison is not really well suited to the aims of this journal and our target community to bring attention to the magnitude of palaeoclimate changes that have occurred in different active orogens. Our intended audience is not the palaeoclimate modelling community (and journals associated with it), but rather the surface processes community. We specifically chose this journal to provide this community with palaeoclimate predictions that may be of interest to them. In our own experience in trying to interpret palaeodenudation rates from data we produce, our first goal is always trying to find predictions or observations of climate change for a region. Thus, we set out to write this paper to provide what we find in our research as the first, most useful, step in understanding the surface process history of a region. Furthermore, one major aspect of this study that we want to retain is the statistical analysis of the climatology of each time slice as this is what is most useful for the ESurf community in terms of knowing if a region they are working is has experienced a signal change in climate through time.

Thus, we are left with the conundrum that what the review requests and we want would normally be three full manuscripts that include: 1) a statistical analysis of climatological changes over active orogens (our previous focus of the text), or 2) a comparison of a suite of similarly set up and common code (ECHAM5) simulations of palaeoclimate time slices to other GCM models (one of the suggestions by this reviewer), or 3) a model-data comparisons for model evaluation at the time slices investigated (also suggested by this reviewer).

In an attempt to hopefully reach a compromise with this reviewer – the revised manuscript is now structured around points 1 and 3 above (statistical analysis of climatological changes, and model-data comparison where possible). These changes have been manifested in a now expanded discussion section, and through the addition of model-data comparison figures at the end of the text (see section 4.1.2 , 4.2.2, and 4.4). These changes hopefully reach a happy middle-ground between our aims and the reviewer's suggestions. The changes have significantly expanded the manuscript, and we hope that the reviewer also recognizes that implementation of all the suggested changes is not possible within a single manuscript of typical length for this journal. The revised manuscript now has 18 figures (including 1 in the supplemental section) and 21 pages of manuscript text (not including references / captions).

Some parts of the paper address actual causes for climatic change (for example, discussion of the Pacific North American Teleconnection (no citation given). Is this related to the PDO? Lines 493-495). Again, if this is the primary point of the paper, then substantially more work needs to be done to address why precipitation, for example, increases in the Himalaya in the Pliocene. If this was the point of the paper, it would obviate the need to compare with other model simulations (see paragraph above), but would then require substantially more work to identify how various atmospheric phenomenon change through time. A generalized description of changes in the past is not particularly useful (most of this information can be communicated fairly effectively with figures), so addressing the causes of these changes (or comparison with proxies – see below) is worthwhile.

Parts of the discussion showcase comparisons with terrestrial proxy data, though this is limited to citing previous work and stating that there is general agreement with previous, proxy-model work. If a proxy-model comparison is the point of the paper, then more work needs to be done actually compiling the proxies and doing a proper statistical test to see if there is agreement between modelled precip/temperature changes in each of these orogens and existing data. This would be a useful contribution to the literature, but, again, would require substantially more work.

We address the suggestions in the previous 2 paragraphs in the following ways: **First**, as was mentioned earlier, we maintain that for this journal and the community that reads it there is value in demonstrating climate change events in commonly studied active orogens where denudation studies (sensitive to climate change) are conducted. This requires that we maintain our current statistical characterisations of the climate change. With this approach, it then becomes intractable to focus on the climate dynamics associated with change in each region because typically a thorough investigation of the climate dynamics associate with

change in each region could be a paper for each region in itself, and the broader picture of change in a range would be missed. We try to meet the reviewer half way in this suggestion by including additional comments on possible causes for climatic change in different regions.

The PNA (citation now included) is related to the PDO, and Alaskan precipitation and temperature is to some degree controlled by it. In order to properly address these questions, however, further analyses looking at dominant atmospheric variability modes, trajectories and other aspects of atmosphere would have to be carried out, which are beyond the scope of this study. We have modified the manuscript in text at the end of section 2.1 to clarify (and justify) why we do not conduct an inter model comparison, as well as some of the caveats associated with our approach.

However, **(second)**, we like the reviewer's suggestions of adding additional comparisons to proxy data, and we heavily invested time in compiling this information in this revised version for locations where spatially distributed data are available for the time slices available.

Unfortunately, changes from proxy studies are often reported in terms of relative changes compared to modern (e.g., wetter/drier, warmer/colder) and are sometimes contradictory for the same location, making the application of otherwise suitable statistical tests (e.g. t-test and even non-parametric tests) difficult. There are, in some cases (see final figures in paper), even contradictions between the proxy data themselves in neighbouring locations, a reality often underappreciated by the surface processes community. Furthermore, terrestrial proxy data are not available for all the time slices and locations we investigate. This is particularly true for the Pliocene time slice. **With these limitations of available proxies, we do the best we can to compare available observations to proxy data. These comparisons are now provided in revisions to the discussion section, and the addition of 2 figures at the end of the manuscript.**

We note that for the Alaska and Cascadia (NW USA) study areas, which are heavily and repeatedly glaciated, that limited - to no proxy data are available (due to poor preservation of proxies over glacial-interglacial cycles). Although some marine proxy records and records of past glaciations have been published for these regions, they are not useful for our purposes because they do not record if terrestrial locations in the regions were wetter/drier or warmer/colder during our time slices. Marine proxy records are of limited use for comparison to the terrestrial changes investigated in this study. Thus, despite the lack of terrestrial proxy comparisons available for two of the regions (Alaska, Cascadia), we maintain that presentation of the model predicted changes for these data poor regions is extremely useful because the model predictions augment existing terrestrial data gaps, and provide a starting point for future studies to formulate testable hypotheses of climate change and potential denudation impacts.

Much of the motivation for the manuscript appears to be to understand how climatic changes may change denudation/geomorphic analyses, but this is done in only a superficial way. If this is the point of the paper, then, again, much more work needs to be done, rather than simply stating that erosion depends on climate (lines 416-423 are a good example of statements that serve to motivate a paper, but don't provide any actual analysis). For example, can the authors take some of the climate model output and, given a potential 2000 mm/yr change in precipitation in the Himalaya since the Pliocene, actually re-interpret some of the existing exhumation/denudation data? If not, why not? What additional data is necessary? And if such a reanalysis isn't possible, then how does knowledge of such a change in precipitation facilitate future work?

This is a great suggestion and we are indeed doing this as ongoing work. But what the reviewer is asking for here simply cannot be included in this paper without making it an extremely long manuscript. For example, in the surface processes community, comparisons of river profiles to modern precipitation, or temperature changes to frost cracking histories for **one** catchment / study area (e.g. <100x100 km²) is typically a full manuscript in itself (e.g. Marhsall et al., 2015 Science Advances; Schaller et al. 2004 Journal of Geology). So, we respectfully disagree with the reviewer that this should be done within this manuscript. It's simply not possible to do in a way that would be convincing to the surface processes community.

I agree with the generalized statements made throughout the paper (i.e., that denudation and landscape evolution depend on climate), but these are somewhat self-evident and, as currently written, the manuscript does not make a fundamental contribution to improving our knowledge on this subject except to state that climate changed in the past. Assumptions of stationarity are indeed a problem in interpreting modern datasets that have a component of geologic history, but a really nice contribution of this paper would be to show how these assumptions can be mitigated when one knows the history of precipitation or temperature.

We agree with the reviewer that it is “self-evident” that palaeoclimate can impact the denudation history of an orogen, but how many palaeodenudation rate studies actually make a comparison to spatial distributed predictions of palaeoclimate? Very few in our experience, and we cite the robust ones in the manuscript. What most palaeodenudation rate studies do is compare some set of observation to the nearest set of proxy observations, but this approach does not provide a sense of spatial variability in terrestrial climate change that models predict (furthermore, proxy observations are often far removed from the denudation rate observations). In our manuscript, we specifically avoid picking on previous publications that follow this ‘conventional’ approach to show how this commonly used approach ignores spatial variability in climate change. We don’t think this is a productive way to advance the science. Instead, we maintain that providing spatially continuous model predictions at different time slices in a self-consistent set of simulations is extremely useful for documenting the magnitude of climate change (which is not self-evident), and for formulating testable hypotheses for future work and to identify where the best locations are in the world to investigate climate change impacts on a regions denudation history. Thus, the way in which our research group usually conducts palaeodenudation rate studies is to first run model simulations to formulate testable hypotheses, and then to investigate/test these hypotheses with field studies and geochemical observations of denudation histories. This approach to investigating palaeoclimate-palaeodenudation interactions is definitely not self-evident in the literature in our opinion.

We very much agree that in order for our simulations to ultimately be useful in actually quantifying denudation much more work needs to be done. Translating any of the changes observed here (or by other studies) to erosion rates remains a big problem in the Earth surface science community. It is one that we are actively working on and includes the application and comparison of different models for quantifying frost cracking [Anderson et al., 1998, Hales and Roering, 2007, and Andersen et al. 2015] and possible improvements on them, different measures for precipitation extremes and testing how well they are captured in modern day simulations (by comparison with indices derived from observation based datasets), etc.. However, the format and length of a typical article does not allow thorough investigation of any of these as part of this manuscript and we believe that an arbitrary selection of these efforts would ultimately be very misleading. Instead, we hope to offer these consistently set up simulations as a useful framework for the earth surface science community to build on. We added further descriptions and discussion to convey this.

Because ESurf is not a climate modeling journal, more discussion needs to be given as to the limitations of ECHAM5 in a way that Earth surface process folks can understand. For example, what are the uncertainties associated with simulating orographic precipitation? Though T159 is high-resolution, it still requires substantially smoothing topography, which presumably introduces some uncertainty in to the results. What uncertainties are associated with the PRISM reconstruction? (on a side note, which PRISM reconstruction is used? PRISM3D? PRISM2? I mention this because the topographies between different PRISM reconstructions are substantially different.)

We thank the reviewer for raising this important point. We emphasised the problem of simulating orographic precipitation, and included the recommendation for downscaling where it may be required. We used the PRISM3D reconstruction (as in Haywood et al. 2010), and commented on some of its uncertainties.

I found the use of the cluster analysis to be not intuitively helpful. If the authors want to keep using it, then the authors need to at least walk the reader through an example of how to understand Figures 6, 9, 12, and 15. Is C1 always the same climate zone in each figure and in each time-slice? If so, why are different colors used? Why don’t the authors use something more intuitive, like Köppen’s climate classification scheme (Peel et al., 2007) to classify climates? As best I understand it, the clustering analysis is used to show the spatial extent of a given climate in a given time-slice and in a given location, but it’s not clear how one should interpret these results.

We have modified the text in the results and discussion sections to help clarify this. In short, the clustering analysis essentially fulfills a similar synoptic purpose, but optimises classification and is more fine-tuned to this study’s purpose in its selection of variables. This is now reflected in text changes we made to the end of the methods section 2.2. The climate clusters do indeed show the spatial extent of a given climate (described by the mean vectors represented graphically in the raster plots and by numbers in the table included in the supplementary material). The idea is to provide an overview of regional climate without the need to study maps of individual variables, on which these patterns and the climatic homogeneity may not be seen as easily. Each plot represents an optimal classification and thus cluster 1, for example, is not always described by the same mean vector (though usually is usually very similar). The different colours are used to avoid the

interpretation that cluster 1, for example, is always characterised by the exact same mean vector. We have included a more elaborate explanation in our revised manuscript to avoid confusion. While readers may be more familiar with the Köppen climate classification scheme, we are more interested in providing an overview not forcefully tied to the categories of this classification scheme. Clustering by various methods (such as this one or PCA) as a synoptic tool are not uncommon (e.g. Paeth 2004, Mannig et al. 2013), but we acknowledge that many readers may not be use to these tools and therefore elaborate explanations.

Minor Comments: Are the topographies for any of these ranges modified at all (it's unclear from the PRISM reference (Line 131), whether this has been done).

Yes, the topographies are different and we now specify the reconstruction we use (PRISM3D) in the methods section.

Lines 57-59: "Cold-temperature island" is not a climatic term in widespread use. What precisely do you mean? Also, Boos and Kuang, 2010 specifically refute the idea that Plateau surface elevation matters for the South Asian Monsoon and rather focus on the Himalaya instead.

Yes, this matters only regionally, but not for the South Asian Monsoon. We have corrected this sentence.

Line 61: Zhisheng et al. (2001) don't actually present any new geological data. Instead, it is all from cited literature. The focus of their study was GCM results. Dettman et al. (2003) is not the only study to look at this. Please see the following studies (which are just a sampling): (Caves et al., 2017; Kent-Corson et al., 2006; Lechler et al., 2013; Lechler and Niemi, 2011; Licht et al., 2016; Methner et al., 2016; Mulch et al., 2015, 2008; Pingel et al., 2016).

Thank you for pointing out this inaccuracy and pointing us to additional studies we ought to list here. We modified the text accordingly.

Lines 77 and 78: "documenting the magnitude" appears twice.

Thank you for pointing this out. We corrected this.

Lines 96-97: Though, importantly, several recent studies have run ECHAM5 at a higher resolution ((Feng et al., 2016; Feng and Poulsen, 2016).

That is true, of course. We mention these in our revised manuscript.

Lines 102-103: This statement is somewhat odd, since the authors are specifically investigating climatological changes over mountain ranges, where resolution typically tends to matter.

Thank you for noticing this apparent inconsistency. We corrected the text accordingly.

Lines 114-133: For all simulations, stating the pCO₂ used in the experiment would be most helpful, particularly since it won't take up much room. Also, how is the land-surface treated? For example, the authors state that they are using vegetation reconstructions, but it's unclear if this is then being fed into a "built-in" land-surface model or if they are explicitly using JSBACH.

This is a good point. We included these values in the text. We used the built-in land surface scheme (LSS) and clarified this in the revised text.

Lines 126: "for the" used twice.

This has been corrected.

Lines 203-204: Changes in Greenland and Antarctica are almost certainly unreliable. Because PRISM uses a reconstructed ice-sheet extent, changes in temperature in Greenland and Antarctica are almost certainly reflecting the imposed boundary condition, which itself has quite a bit of uncertainty. It's hard to get around this, except to note that the change in temperature is entirely dependent upon the ice-sheet boundary condition (see discussion in and of de Boer et al. (2015)).

Thank you for pointing this out. We comment on the Pliocene uncertainty in ice sheet reconstructions in the method section of the revised manuscript.

Lines 416-423: Are runoff changes in these models coupled to precipitation changes? In all cases, does P-E (precipitation minus evaporation) scale with changes in precipitation. I'm not particularly familiar with JSBACH (presuming this is the land-surface model used), but if it has a CO₂ fertilization parameterization, then runoff may be decoupled from precip. Some of these erosion processes may depend more on runoff than precip.

We use the built in LSS and the runoff is coupled to precipitation. Also, ECHAM5's runoff is not particularly useful in river discharge modelling (see Weiland et al. 2011), which would be of interest in context of erosion. Given this, we refrain from using the model predicted runoff in the global GCM (even

though it's conducted at relatively high resolution compared to previous work) to calculate changes in fluvial incision. This would be better done by mapping the predicted precipitation changes onto higher resolution (<90 m) DEMs and solving the kinematic wave equation for each fluvial erosion in each catchment, for the changes in precipitation. However, as we repeatedly mention above, this is not possible to include in this manuscript without first characterising how the precipitation has changed in each region (the current manuscript goals). Work in progress we are conducting is trying to apply the kinematic wave equation and palaeoprecipitation to selected areas, but it's proving difficult to implement meaningfully without temporally continuous (e.g. LGM to present) simulations of precipitation change. We hope this brings to the readers attention the complications associated with doing full erosion history calculations based on these results. We have expanded the last paragraph in the instruction to convey the above perspective better, and more clearly articulate (and justify) the scope and limitations of the manuscript.

Figure 1: Would be nice to also plot the topography of the St. Elias range and the Cascades.

This is a good idea. We included ECHAM5 topographies for Alaska and the Pacific Northwest in Fig. 1 in the revised manuscript.

Figure 7b-Precip-PLIO: Why does precipitation appear to follow a wave-like pattern over tropical South America? Is this due to the spectral nature of ECHAM5?

This may indeed be due to the spectral nature of ECHAM5.

References used in review:

Thank you for being thoughtful enough to provide these. We have added many of them to the revised text.

An, Z., Kutzbach, J.E., Prell, W.L., Porter, S.C., 2001. Evolution of Asian monsoons and phased uplift of the Himalaya-Tibetan plateau since Late Miocene times. *Nature* 411, 62–66. doi:10.1038/35075035

Caves, J.K., Bayshashov, B.U., Zhamangara, A., Ritch, A.J., Ibarra, D.E., Sjostrom, D.J., Mix, H.T., Winnick, M.J., Chamberlain, C.P., 2017. Late Miocene uplift of the Tian Shan and Altai and reorganization of Central Asia climate. *GSA Today* 27, 19–26.

Chandan, D., Peltier, W.R., 2017. Regional and global climate for the mid-Pliocene using CCSM4 and PlioMIP2 boundary conditions. *Clim. Past* 13, 919–942. doi:10.5194/cp-2017-21

de Boer, B., Dolan, A.M., Bernales, J., Gasson, E., Goelzer, H., Golledge, N.R., Sutter, J., Huybrechts, P., Lohmann, G., Rogozhina, I., Abe-Ouchi, A., Saito, F., van de Wal, R.S.W., 2015. Simulating the Antarctic ice sheet in the Late-Pliocene warm period: PLISMIP-ANT, an ice-sheet model intercomparison project. *Cryosph.* 9, 881–903. doi:10.5194/tc-9-881-2015

Dettman, D.L., Fang, X., Garzione, C.N., Li, J., 2003. Uplift-driven climate change at 12 Ma: a long $\delta^{18}\text{O}$ record from the NE margin of the Tibetan plateau. *Earth Planet. Sci. Lett.* 214, 267–277. doi:10.1016/S0012-821X(03)00383-2

Feng, R., Poulsen, C.J., 2016. Refinement of Eocene lapse rates, fossil-leaf altimetry, and North American Cordilleran surface elevation estimates. *Earth Planet. Sci. Lett.* doi:10.1016/j.epsl.2015.12.022

Feng, R., Poulsen, C.J., Werner, M., 2016. Tropical circulation intensification and tectonic extension recorded by Neogene terrestrial $\delta^{18}\text{O}$ records of the western United States. *Geology* 44. doi:10.1130/G38212.1

Haywood, A.M., Hill, D.J., Dolan, A.M., Otto-Bliesner, B.L., Bragg, F., Chan, W.L., Chandler, M.A., Contoux, C., Dowsett, H.J., Jost, A., Kamae, Y., Lohmann, G., Lunt, D.J., Abe-Ouchi, A., Pickering, S.J., Ramstein, G., Rosenbloom, N.A., Salzmann, U., Sohl, L., Stepanek, C., Ueda, H., Yan, Q., Zhang, Z., 2013. Large-scale features of Pliocene climate: Results from the Pliocene Model Intercomparison Project. *Clim. Past* 9, 191–209. doi:10.5194/cp-9-191-2013

Jiang, D., Lang, X., 2010. Last glacial maximum East Asian monsoon: Results of PMIP simulations. *J. Clim.* 23, 5030–5038. doi:10.1175/2010JCLI3526.1

Jiang, D., Lang, X., Tian, Z., Ju, L., 2013. Mid-Holocene East Asian summer monsoon strengthening: Insights from Paleoclimate Modeling Intercomparison Project (PMIP) simulations. *Palaeogeogr. Palaeoclimatol. Palaeoecol.* 369, 422–429. doi:10.1016/j.palaeo.2012.11.007

- Kent-Corson, M.L., Sherman, L.S., Mulch, A., Chamberlain, C.P., 2006. Cenozoic topographic and climatic response to changing tectonic boundary conditions in Western North America. *Earth Planet. Sci. Lett.* 252, 453–466. doi:10.1016/j.epsl.2006.09.049
- Lechler, A.R., Niemi, N.A., 2011. Sedimentologic and isotopic constraints on the Paleogene paleogeography and paleotopography of the southern Sierra Nevada, California. *Geology* 39, 379–382. doi:10.1130/G31535.1
- Lechler, A.R., Niemi, N. a., Hren, M.T., Lohmann, K.C., 2013. Paleoelevation estimates for the northern and central proto-Basin and Range from carbonate clumped isotope thermometry. *Tectonics* 32. doi:10.1002/tect.20016
- Licht, A., Quade, J., Kowler, A., Santos, M. de los S., Hudson, A., Schauer, A., Huntington, K., Copeland, P., Lawton, T., 2016. Impact of the North American Monsoon on isotope paleoaltimeters: Implications for the paleoaltimetry of the American Southwest. *Am. J. Sci.* 317.
- Methner, K., Fiebig, J., Wacker, U., Umhoefer, P., Chamberlain, C.P., Mulch, A., 2016. Eo-Oligocene proto-Cascades topography revealed by clumped ($\Delta 47$) and oxygen isotope ($\delta 18\text{O}$) geochemistry (Chumstick Basin, WA, USA). *Tectonics* 35, 546–564. doi:10.1002/2015TC003984
- Mulch, A., Chamberlain, C.P., Cosca, M.A., Teyssier, C., Methner, K., Hren, M.T., Graham, S.A., 2015. Rapid change in high-elevation precipitation patterns of western North America during the Middle Eocene Climatic Optimum (MECO). *Am. J. Sci.* 315, 317–336. doi:10.2475/04.2015.02
- Mulch, A., Sarna-Wojcicki, A.M., Perkins, M.E., Chamberlain, C.P., 2008. A Miocene to Pleistocene climate and elevation record of the Sierra Nevada (California). *Proc. Natl. Acad. Sci. U. S. A.* 105, 6819–6824. doi:10.1073/pnas.0708811105
- Peel, M.C., Finlayson, B.L., McMahon, T.A., 2007. Updated world map of the Köppen-Geiger climate classification. *Hydrol. Earth Syst. Sci.* 11, 1633–1644.
- Pingel, H., Mulch, A., Alonso, R.N., Cottle, J., Hynke, S.A., Poletti, J., Rohrmann, A., Schmitt, A.K., Stockli, D.F., Strecker, M.R., 2016. Surface uplift and convective rainfall along the southern Central Andes (Angastaco Basin, Argentina). *Earth Planet. Sci. Lett.* 440, 33–42. doi:10.1016/j.epsl.2016.02.009
- Zhang, R., Yan, Q., Zhang, Z.S., Jiang, D., Otto-Bliesner, B.L., Haywood, a. M., Hill, D.J., Dolan, a. M., Stepanek, C., Lohmann, G., Contoux, C., Bragg, F., Chan, W.-L.,
- Chandler, M.a., Jost, a., Kamae, Y., Abe-Ouchi, a., Ramstein, G., Rosenbloom, N. a., Sohl, L., Ueda, H., 2013. East Asian monsoon climate simulated in the PlioMIP. *Clim. Past Discuss.* 9,1135-1164. doi:10.5194/cpd-9-1135-2013

2 **Where is Late Cenozoic climate change most likely to impact**
3 **denudation?**

4
5 Sebastian G. Mutz¹, Todd A. Ehlers¹, Martin Werner², Gerrit Lohmann², Christian Stepanek²,
6 Jingmin Li^{1,3}

7 ¹Department of Geosciences, University Tübingen, D-72074 Tübingen, Germany

²Department of Paleoclimate Dynamics, Alfred Wegener Institute, Helmholtz Centre for Polar and Marine Research, D-27570 Bremerhaven, Germany

8 ³[now at](#) Institute for Geography and Geology, University of Würzburg, Würzburg, D-97074 Germany

9 Correspondence to: Sebastian G. Mutz (sebastian.mutz@uni-tuebingen.de)

10
11 **Abstract**

12 The denudation history of active orogens is often interpreted in the context of modern climate and vegetation gradients.
13 Here we address the validity of this approach and ask the question: what are the spatial and temporal variations in
14 palaeo-climate for a latitudinally diverse range of active orogens? We do this using high-resolution (T159, ca. 80 x 80
15 km at the equator) palaeo-climate simulations from the ECHAM5 global Atmospheric General Circulation Model and a
16 statistical cluster analysis of climate over different orogens (Andes, Himalaya, SE Alaska, Pacific NW USA). Time
17 periods and boundary conditions considered include the Pliocene (PLIO, ~3 Ma), the Last Glacial Maximum (LGM,
18 ~21 ka), Mid Holocene (MH, ~6 ka) and Pre-Industrial (PI, reference year 1850). The regional simulated climates of
19 each orogen are described by means of cluster analyses based on the variability of precipitation, 2m air temperature, the
20 intra-annual amplitude of these values, and monsoonal wind speeds where appropriate. Results indicate the largest
21 differences to the PI climate ~~are observed~~ existed for the LGM and PLIO climates in the form of widespread cooling and
22 reduced precipitation in the LGM and warming and enhanced precipitation during the PLIO. The LGM climate shows
23 the largest deviation in annual precipitation from the PI climate, and shows enhanced precipitation in the temperate
24 Andes, and coastal regions for both SE Alaska and the US Pacific Northwest ~~Pacific~~. Furthermore, LGM precipitation
25 is reduced in the western Himalayas and enhanced in the eastern Himalayas, resulting in a shift of the wettest regional
26 climates eastward along the orogen. The cluster-analysis results also suggest more climatic variability across latitudes
27 east of the Andes in the PLIO climate than in other time-slice experiments conducted here. Taken together, these results
28 highlight significant changes in Late Cenozoic regional climatology over the last ~3 Ma. [Comparison of simulated](#)
29 [climate with proxy-based reconstructions for the MH and LGM reveal satisfactory to good performance of the model in](#)

[reproducing precipitation changes, although in some cases discrepancies between neighbouring proxy observations](#)
[highlight contradictions between proxy observations themselves.](#) Finally, we document regions where the largest
magnitudes of Late Cenozoic changes in precipitation and temperature occur and offer the highest potential for future
observational studies ~~interested in quantifying~~ that quantify the impact of climate change on denudation and weathering
rates.

Keywords: Cenozoic climate, ECHAM5, Last Glacial Maximum, Mid-Holocene, Pliocene, cluster analysis, Himalaya,
Tibet, Andes, Alaska, Cascadia

1. Introduction

Interpretation of orogen denudation histories in the context of climate and tectonic interactions is often hampered
by a paucity of terrestrial palaeo-climate proxy data needed to reconstruct spatial variations in palaeo-climate. [While it](#)
[is self-evident that palaeoclimate changes could influence palaeodenudation rates, it is not always self-evident what the](#)
[magnitude of climate change over different geologic time scales is, or what geographic locations offer the greatest](#)
[potential to investigate palaeoclimate impacts on denudation.](#) Palaeoclimate reconstructions are particularly beneficial
when denudation rates are determined using geo- and thermo-chronology techniques that integrate over timescales of
 10^3 - 10^6 years (e.g. cosmogenic radionuclides or low-temperature thermochronology) [e.g., Kirchner et al., 2001;
Schaller et al., 2002; Bookhagen et al., 2005; Moon et al., 2011; Thiede and Ehlers, 2013; Lease and Ehlers, 2013].
However, few studies using denudation rate determination methods that integrate over longer timescales have access to
information about past climate conditions that could influence these palaeo-denudation rates. Palaeo-climate modelling
offers an alternative approach to sparsely available proxy data for understanding the spatial and temporal variations in
precipitation and temperature in response to changes in orography [e.g. Takahashi and Battisti, 2007a, b; Insel et al.,
2010; Feng et al., 2013] and global climate change events [e.g. Salzmann, 2011; Jeffery et al., 2013]. In this study, we
characterize the climate at different times in the [Late](#) Cenozoic, and the magnitude of climate change for a range of
active orogens. Our emphasis is on identifying changes in climate parameters relevant to weathering and catchment
denudation to illustrate the potential importance of various global climate change events on surface processes.

Previous studies of orogen-scale climate change provide insight into how different tectonic or global climate
change events influence regional climate change. For example, sensitivity experiments demonstrated significant
changes in regional and global climate in response to landmass distribution and topography of the Andes, including
changes in moisture transport, [the north-south asymmetry of the Intertropical Convergence Zone and the north-south](#)
[asymmetry of the Inter-Tropical Convergence Zone](#) [e.g. Takahashi and Battisti, 2007a, ; Insel et al., 2010] [and](#)

(tropical) precipitation [Maroon et al., 2015, ; ~~Maroon et al.~~ 2016]. Another example is the regional and global climate changes induced by the Tibetan Plateau surface uplift due to its role as a ~~cold-temperature island and~~ physical obstacle to circulation [Raymo and Ruddiman, 1992; Kutzbach et al., 1993; Thomas, 1997; Böhner, 2006; Molnar et al., 2010; Boos and Kuang, 2010]. The role of tectonic uplift in long term regional and global climate change remains a focus of research and continues to be assessed with geologic datasets [e.g. ~~Zhisheng, 2001;~~ Dettman et al., 2003; ~~Caves et al., 2017;~~ Kent-Corson et al., 2006; Lechler et al., 2013; Lechler and Niemi, 2011; Licht et al., 2016; ~~Methner et al., 2016;~~ Mulch et al., 2015, 2008; Pingel et al., 2016] and climate modelling [e.g. Kutzbach et al., 1989; Kutzbach et al., 1993; ~~Zhisheng, 2001;~~ Böhner, 2006; Takahashi and Battisti, 2007a; Ehlers and Poulsen, 2009; Insel et al., 2010; Boos and Kuang, 2010]. Conversely, climate influences tectonic processes through erosion [e.g. Molnar and England, 1990; Whipple et al., 1999; Montgomery et al., 2001; Willett et al., 2006; Whipple, 2009]. Quaternary climate change between glacial and interglacial conditions [e.g. Braconnot et al., 2007; Harrison et al., 2013] resulted in not only the growth and decay of glaciers and glacial erosion [e.g. Yanites and Ehlers, 2012; Herman et al., 2013; Valla et al., 2011] but also global changes in precipitation and temperature [e.g. Otto-Bliesner et al., 2006; Li et al., 2017] that could influence catchment denudation in non-glaciated environments [e.g. Schaller and Ehlers, 2006; Glotzbach et al., 2013; Marshall et al., 2015]. These dynamics highlight the importance of investigating how much climate has changed over orogens that are the focus of studies of climate-tectonic interactions and their impact on erosion.

Despite recognition by previous studies that climate change events relevant to orogen denudation are prevalent throughout the Late Cenozoic, few studies have critically evaluated how different climate change events may, or may not, have affected the orogen climatology, weathering and erosion. Furthermore, recent controversy exists concerning the spatial and temporal scales over which geologic and geochemical observations can record climate-driven changes in weathering and erosion [e.g. Whipple, 2009; von Blanckenburg et al., 2015; Braun, 2016]. For example, the previous studies highlight that although palaeoclimate impacts on denudation rates are evident in some regions and measurable with some approaches, they are not always present (or detectable) and the spatial and temporal scale of climate change influences our ability to record climate sensitive denudation histories. This study contributes to our understanding of the interactions between climate, weathering, and erosion by bridging the gap between the palaeoclimatology and surface processes communities by documenting the magnitude and distribution of climate change over tectonically active orogens. ~~Our focus is on documenting the magnitude of paleoclimateclimate and climate change in different locations with the intent of informing past and ongoing paleodenudation studies of these regions. The application of these results to predicted changes in denudation rates is beyond the scope of this study and the focus of future work.~~

~~We~~ In this study, we employ the ECHAM5 global Atmospheric General Circulation Model and document climate and climate change for time slices ranging between the Pliocene (PLIO, ~3 Ma) to pre-industrial (PI) times for

the St. Elias Range of South East Alaska, the US Pacific Northwest (Olympic and Cascade Range), western South America (Andes) and South Asia (incl. parts of Central- and East Asia). Our approach is two-fold and includes:

1. An empirical characterisation of palaeo-climates in these regions based on the covariance and spatial clustering of monthly precipitation and temperature, the monthly change in precipitation and temperature magnitude, and wind speeds where appropriate.

2. Identification of changes in annual mean precipitation and temperature in selected regions ~~over in the following time, specifically from the~~ for four time periods: (PLIO, ~~to the~~ Last Glacial Maximum (LGM), the Mid-Holocene (MH) and PI)- and subsequent validation of the simulated precipitation changes for MH and LGM.

Our focus is on documenting climate and climate change in different locations with the intent of informing past and ongoing palaeodenudation studies of these regions. The results presented here also provide a means for future work to formulate testable hypotheses and investigations into whether or not regions of large palaeoclimate change produced a measurable signal in denudation rates. In this study, we intentionally refrain from applying predicted palaeoclimate changes to predict denudation rate changes. Such a prediction is beyond the scope of this study because a convincing (and meaningful) calculation of climate-driven transients in fluvial erosion (e.g. via the kinematic wave equation), variations in frost cracking intensity, or changes in hillslope sediment production and transport at the large regional scales considered here is not tractable within a single manuscript, and instead is the focus of our ongoing work. Instead, our emphasis lies on addressing the first question we are confronted with in our own research into denudation rate studies around world, namely - where is Late Cenozoic climate change most likely to impact denudation?

2. Methods: Climate modelling and cluster analyses for climate characterisation

2.1 ECHAM5 simulations

The global Atmospheric General Circulation Model ECHAM5 [Roeckner et al., 2003] has been developed at the Max Planck Institute for Meteorology and is based on the spectral weather forecast model of the ECMWF [Simmons et al., 1989]. In the context of palaeoclimate applications, the model has been used mostly at lower resolution (T31, approximately ca. 3.75°x3.75°; T63, ca. 1.9°x1.9° in case of Feng et al. [2016] and T106 in the case of Li et al. [2016] and Feng and Poulsen [2016]). The performed studies are not limited to the last millenium [e.g. Jungclaus et al., 2010] but also include research in the field of both warmer and colder climates, at orbital [e.g. Gong et al., 2013; Lohmann et al., 2013; Pfeiffer and Lohmann, 2016; Zhang et al., 2013a; Zhang et al., 2014; Wei and Lohmann, 2012] and tectonic time scales [e.g. Knorr et al., 2011; Stepanek and Lohmann, 2012], and under anthropogenic influence [Gierz et al., 2015].

Here, the ECHAM5 simulations were conducted at a T159 spatial resolution (horizontal grid size ca. 80 km x 80

125 km at the equator) with 31 vertical levels (between the surface and 10hPa). This high model resolution is admittedly not
126 required for [all of](#) the climatological questions investigated in this study, [and it should be noted that the skill of GCM's](#)
127 [in predicting orographic precipitation remains limited at this scale \[e.g. Meehl et al. 2007\]](#). However, simulations were
128 conducted at this resolution so that future work can apply the results [in combination with different dynamical and](#)
129 [statistical downscaling methods](#) to quantify changes at large catchment to orogen scales. [The output frequency is](#)
130 [relatively high \(1 day\) to enhance the usefulness of our simulations as input for landscape evolution and other models](#)
131 [that may benefit from daily input](#). The simulations were conducted for five different time periods: present-day (PD), PI,
132 MH, LGM and PLIO.

133 A PD simulation (not shown here) was used to establish confidence in the model performance before conducting
134 [palaeo](#)-simulations and has been compared with the following observation-based datasets: European Centre for
135 Medium-Range Weather Forecasts (ECMWF) re-analyses [ERA40, Uppala et al., 2005], National Centers for
136 Environmental Prediction and National Center for Atmospheric Research (NCEP/NCAR) re-analyses [Kalnay et al.,
137 1996; Kistler et al., 2001], NCEP Regional Reanalysis (NARR) [Mesinger et al., 2006], the Climate Research Unit
138 (CRU) TS3.21 dataset [Harris et al., 2013], High Asia Refined Analysis (HAR30) [MauSSION et al., 2014] and the
139 University of Delaware dataset (UDEL v3.01) [Legates et al., 1990]. (See Mutz et al. [2016] for a detailed comparison
140 with a lower resolution model).

141 The PI climate simulation is an ECHAM5 experiment with PI (reference year 1850) boundary conditions. Sea
142 Surface Temperatures (SST) and Sea Ice Concentration (SIC) are derived from transient coupled ocean-atmosphere
143 simulations [Lorenz and Lohmann, 2004; Dietrich et al., 2013]. Following Dietrich et al. [2013], greenhouse gas
144 (GHG) concentrations ([CO₂: 280 ppm](#)) are taken from ice core based reconstructions of CO₂ [Etheridge et al., 1996],
145 CH₄ [Etheridge et al., 1998] and N₂O [Sowers et al., 2003]. Sea surface boundary conditions for MH originate from a
146 transient, low-resolution, coupled atmosphere-ocean simulation of the mid (6 ka) Holocene [Wei and Lohmann, 2012;
147 Lohmann et al., 2013], where the GHG concentrations ([CO₂: 280 ppm](#)) are taken from ice core reconstructions of
148 GHG's by Etheridge et al. [1996], Etheridge et al. [1998] and Sowers et al. [2003]. GHG's concentrations for the LGM
149 ([CO₂: 185 ppm](#)) have been prescribed following Otto-Bliesner et al. [2006]. Orbital parameters for MH and LGM are
150 set according to Dietrich et al. [2013] and Otto-Bliesner et al. [2006], respectively. LGM land-sea distribution and ice
151 sheet extent and thickness are set based on the PMIP III ([Palaeoclimate Modelling Intercomparison Project](#), phase 3)
152 guidelines (elaborated on by Abe-Ouchi et al [2015]). Following Schäfer-Neth and Paul [2003], SST and SIC for the
153 LGM are based on GLAMAP [Sarnthein et al. 2003] and CLIMAP [CLIMAP project members, 1981] reconstructions
154 for the [for the](#) Atlantic and Pacific/Indian Ocean, respectively. Global MH and LGM vegetation are based on maps of
155 plant functional types by the BIOME 6000 / Palaeovegetation Mapping Project [Prentice et al., 2000; Harrison et al.,
156 2001; Bigelow et al., 2003; Pickett et al., 2004] and model predictions by Arnold et al. [2009]. Boundary conditions for

the PLIO simulation, including GHG concentrations ([CO₂: 405](#)), orbital parameters and surface conditions (SST, SIC, sea land mask, topography and ice cover) are taken from the PRISM (Pliocene Research, Interpretation and Synoptic Mapping) project [Haywood et al., 2010; Sohl et al., 2009; Dowsett et al., 2010], [specifically PRISM3D](#). The PLIO vegetation boundary condition was created by converting the PRISM vegetation reconstruction to the JSBACH plant functional types as described by Stepanek and Lohmann [2012], [but the built-in land surface scheme was used](#). [SST reconstructions can be used as an interface between oceans and atmosphere \[e.g. Li et al. 2016\] instead of conducting the computationally more expensive fully coupled Atmosphere-Ocean GCM experiments. While the use of SST climatologies comes at the cost of capturing decadal-scale variability, and the results are ultimately biased towards the SST reconstructions the model is forced with, the simulated climate more quickly reaches an equilibrium state and the means of atmospheric variables used in this study do no change significantly after the relatively short spin-up period.](#) The palaeoclimate simulations (PI, MH, LGM, PLIO) using ECHAM5 are [therefore](#) carried out for 17 model years, of which the first two years are used for model spin up. The monthly long-term averages (multi-year means for individual months) for precipitation, temperature, as well as precipitation and temperature amplitude, i.e. the mean difference between the hottest and coldest months, have been calculated from the following 15 model years for the analysis presented below.

For further comparison between the simulations, the investigated regions were subdivided (Fig. 1). Western South America was subdivided into four regions: parts of tropical South America (80°-60° W, 23.5°-5° S), temperate South America (80°-60° W, 50°-23.5° S), tropical Andes (80°-60° W, 23.5°-5° S; high-pass filtered), i.e. most of the Peruvian Andes, Bolivian Andes and northernmost Chilean Andes, and temperate Andes (80°-60° W, 50°-23.5° S, high-pass filtered). South Asia was subdivided into three regions: tropical South Asia (40°-120°E, 0°-23.5°N), temperate South Asia (40°-120°E, 23.5°-60°N), and high altitude South Asia (40°-120°E, 0°-60°N; high-pass filtered).

[Our approach of using a single GCM \(ECHAM5\) for our analysis is motivated by, and differs from, previous studies where inter-model variability exists from the use of different GCMs due to different parameterisations in each model. The variability in previous inter-model GCM comparisons exists despite the use of the same forcings \[e.g. see results highlighted in IPCC AR5\]. Similarities identified between these palaeoclimate simulations conducted with different GCMs using similar boundary conditions can establish confidence in the models when in agreement with proxy reconstructions. However, differences identified in inter-model GCM comparisons highlight biases by all or specific GCMs, or reveal sensitivities to one changed parameter, such as model resolution. Given these limitations of GCM modelling, we present in this study a comparison of a suite of ECHAM5 simulations to proxy-based reconstructions \(where possible\) and, to a lesser degree, comment on general agreement or disagreement of our ECHAM5 results with other modelling studies. A detailed inter-model comparison of our results with other GCMs is beyond the scope of this study, and better suited for a different study in a journal with a different focus and audience.](#)

Rather, by using the same GCM and identical resolution for the time slice experiments, we reduce the number of parameters (or model parameterisations) varying between simulations and thereby remove potential sources of error or uncertainty that would otherwise have to be considered when comparing output from different models with different parameterisations of processes, model resolution, and in some cases model forcings (boundary conditions). Nevertheless, the reader is advised to use these model results with the GCM's shortcoming and uncertainties in boundary condition reconstructions in mind. For example, precipitation results may require dynamical or statistical downscaling to increase accuracy where higher resolution precipitation fields are required. Furthermore, readers are advised to familiarise themselves with the palaeogeography reconstruction initiatives and associated uncertainties. For example, while Pliocene ice sheet volume can be estimated, big uncertainties pertaining to their locations remain [Haywood et al. 2010].

2.2 Cluster analysis to document temporal and spatial changes in climatology

~~This section describes the clustering method used in this study.~~ The aim of the clustering approach is to group climate model surface grid boxes together based on similarities in climate. Cluster analyses are statistical tools that allow elements (i) to be grouped by similarities in the elements' attributes. In this study, those elements are spatial units, the elements' attributes are values from different climatic variables, and the measure of similarity is given by a statistical distance. The four basic variables used as climatic attributes of these spatial elements are: near-surface (2m) air temperature, seasonal 2m air temperature amplitude, precipitation rate, and seasonal precipitation rate amplitude. Since monsoonal winds are a dominant feature of the climate in the South Asia region, near surface (10m) speeds of u-wind and v-wind (zonal and meridional wind components, respectively) during the monsoon season (July) and outside the monsoon season (January) are included as additional variables in our analysis of that region. Similarly, u-wind and v-wind speeds during (January) and outside (July) the monsoon season in South America are added to the list of considered variables to take into account the South American Monsoon System (SASM) in the cluster analysis for this region. The long-term monthly means of those variables are used in a hierarchical clustering method, followed by a non-hierarchical k-means correction with randomised re-groupment [Mutz et al., 2016; Wilks, 2011; Paeth, 2004; Bahrenberg et al., 1992].

The hierarchical part of the clustering procedure starts with as many clusters as there are elements (ni), then iteratively combines the most similar clusters to form a new cluster using centroids for the linkage procedure for clusters containing multiple elements. The procedure is continued until the desired number of clusters (k) is reached. One disadvantage of a pure hierarchical approach is that elements cannot be re-categorised once they are assigned to a cluster, even though the addition of new elements to existing clusters changes the clusters' defining attributes and could warrant a re-categorisation of elements. We address this problem by implementation of a (non-hierarchical) k-means

221 clustering correction [e.g. Paeth, 2004]. Elements are re-categorized based on the multivariate centroids determined by
222 the hierarchical cluster analysis in order to minimize the sum of deviations from the cluster centroids. The
223 Mahalanobis distance [e.g. Wilks, 2011] is used as a measure of similarity or distance between the cluster centroids,
224 since it is a statistical distance and thus not sensitive to different variable units. The Mahalanobis distance also accounts
225 for possible multi-collinearity between variables.

226 The end results of the cluster analyses are subdivisions of the climate in the investigated regions into k
227 subdomains or clusters based on multiple climate variables. The region-specific k has to be prescribed before the
228 analyses. A large k may result in redundant additional clusters describing very similar climates, thereby defeating the
229 purpose of the analysis to identify and describe the dominant, distinctly different climates in the region and their
230 geographical coverage. Since it is not possible to know a priori the ideal number of clusters, k was varied between 3 and
231 10 for each region and the results presented below identify the optimal number of visibly distinctly different clusters
232 from the analysis. Optimal k was determined by assessing the distinctiveness and similarities between the climate
233 clusters in the systematic process of increasing k from 3 to 10. Once an increase in k no longer resulted in the addition
234 of another cluster that was climatologically distinctly different from the others, and instead resulted in at least two
235 similar clusters, k of the previous iteration was chosen as the optimal k for the region.

236 The cluster analysis ultimately results in a description of the geographical extent of a climate (cluster)
237 characterised by a certain combination of mean values for each of the variables associated with the climate. For
238 example, climate cluster 1 may be the most tropical climate in a region and thus be characterised by a high precipitation
239 values, high temperature values and low seasonal temperature amplitude. Each of the results (consisting of the
240 geographical extent of climates and mean vectors describing the climate) can be viewed as an optimal classification for
241 the specific region and time. It serves primarily as a means for providing an overview of the climate in each of the
242 regions at different times, reduces dimensionality of the raw simulation output, and identify regions of climatic
243 homogeneity that is difficult to notice by viewing simple maps of each climate variable. Its synoptic purpose is similar
244 to that of the widely known Köppen-Geiger classification scheme [Peel et al., 2007], but we allow for optimal
245 classification rather than prescribe classes, and our selection of variables is more restricted and made in accordance with
246 the focus of this study.

247

248 3. Results

249 Results from our analysis are first presented for general changes in global temperature and precipitation for the
250 different time slices (Fig. 2, 3), which is then followed by an analysis of changes in the climatology of selected orogens.
251 A more detailed description of temperature and precipitation changes in our selected orogens is presented in subsequent
252 subsections (Fig. 4 and following). All differences in climatology are expressed relative to the PI control run. Changes

relative to the PI rather than PD conditions are presented to avoid interpreting an anthropogenic bias in the results and focusing instead on pre-anthropogenic variations in climate. For brevity, near-surface (2m) air temperature and total precipitation rate are referred to as temperature and precipitation.

3.1 Global differences in mean annual temperature

This section describes the differences between simulated MH, LGM, and PLIO annual mean temperature anomalies with respect to PI shown in Fig. 2b, and PI temperature absolute values shown in Fig. 2a. Most temperature differences between the PI and MH climate are within -1°C to 1°C . Exceptions to this are the Hudson Bay, Weddell Sea and Ross Sea regions which experience warming of $1\text{--}3^{\circ}\text{C}$, $1\text{--}5^{\circ}\text{C}$ and $1\text{--}9^{\circ}\text{C}$ respectively. Continental warming is mostly restricted to low-altitude South America, Finland, western Russia, the Arabian Peninsula ($1\text{--}3^{\circ}\text{C}$) and subtropical north Africa ($1\text{--}5^{\circ}\text{C}$). Simulation results show that LGM and PLIO annual mean temperature deviate from the PI means the most. The global PLIO warming and LGM cooling trends are mostly uniform in direction, but the magnitude varies regionally. The strongest LGM cooling is concentrated in [regions where the greatest change in ice extent occurs \(as indicated on Fig. 2\)](#), i.e. Canada, Greenland, the North Atlantic, Northern Europe and Antarctica. Central Alaska shows no temperature changes, whereas coastal South Alaska experiences cooling of $\leq 9^{\circ}\text{C}$. Cooling in the US Pacific northwest is uniform and between 11 and 13°C . Most of high-altitude South America experiences mild cooling of $1\text{--}3^{\circ}\text{C}$, $3\text{--}5^{\circ}\text{C}$ in the central Andes and $\leq 9^{\circ}\text{C}$ in the south. Along the Himalayan orogen, LGM temperature values are $5\text{--}7^{\circ}\text{C}$ below PI values. Much of central Asia and the Tibetan plateau cools by $3\text{--}5^{\circ}\text{C}$, and most of India, low-altitude China and south-east Asia by $1\text{--}3^{\circ}\text{C}$.

In the PLIO climate, parts of Antarctica, Greenland and the Greenland Sea experience the greatest temperature increase ($\leq 19^{\circ}\text{C}$). Most of southern Alaska warms by $1\text{--}5^{\circ}\text{C}$ and $\leq 9^{\circ}\text{C}$ near McCarthy, Alaska. The US Pacific northwest warms by $1\text{--}5^{\circ}\text{C}$. The strongest warming in South America is concentrated at the Pacific west coast and the Andes ($1\text{--}9^{\circ}\text{C}$), specifically between Lima and Chiclayo, and along the Chilean-Argentinian Andes south of Bolivia ($\leq 9^{\circ}\text{C}$). Parts of low-altitude South America to the immediate east of the Andes experience cooling of $1\text{--}5^{\circ}\text{C}$. The Himalayan orogen warms by $3\text{--}9^{\circ}\text{C}$, whereas Myanmar, Bangladesh, Nepal, northern India and northeast Pakistan cool by $1\text{--}9^{\circ}\text{C}$.

3.2 Global differences in mean annual precipitation

Notable differences occur between simulated MH, LGM, PLIO annual mean precipitation anomalies with respect to PI shown in Fig. 3b, and the PI precipitation absolute values shown in Fig. 3a. Of these, MH precipitation deviates the least from PI values. The differences between MH and PI precipitation on land appear to be largest in northern tropical Africa (increase ≤ 1200 mm/a) and along the Himalayan orogen (increase ≤ 2000 mm/a) and in central Indian states (decrease) ≤ 500 mm. The biggest differences in western South America are precipitation increases in central Chile

between Santiago and Puerto Montt. The LGM climate shows the largest deviation in annual precipitation from the PI climate, and precipitation on land mostly decreases. Exceptions are increases in precipitation rates in North American coastal regions, especially in coastal South Alaska (≤ 2300 mm/a) and the US Pacific Northwest (≤ 1700 mm/a). Further exceptions are precipitation increases in low-altitude regions immediately east of the Peruvian Andes (≤ 1800 mm/a), central Bolivia (≤ 1000 mm/a), most of Chile (≤ 1000 mm/a) and northeast India (≤ 1900 mm/a). Regions of notable precipitation decrease are northern Brazil (≤ 1700 mm/a), southernmost Chile and Argentina (≤ 1900 mm/a), coastal south Peru (≤ 700 mm/a), central India (≤ 2300 mm/a) and Nepal (≤ 1600 mm/a).

Most of the precipitation on land in the PLIO climate is higher than those in the PI climate. Precipitation is enhanced by ca. 100-200 mm/a in most of the Atacama desert, by ≤ 1700 mm/a south of the Himalayan orogen and by ≤ 1400 mm/a in tropical South America. Precipitation significantly decreases in central Peru (≤ 2600 mm/a), southernmost Chile (≤ 2600 mm/a) and from eastern Nepal to northernmost northeast India (≤ 2500 mm/a).

3.3 Palaeoclimate characterisation from the cluster analysis and changes in regional climatology

In addition to the above described global changes, the PLIO to PI regional climatology changes substantially in the four investigated regions of: South Asia (section 3.3.1), the Andes (section 3.3.2), South Alaska (section 3.3.3) and the Cascade Range (section 3.3.4). Each climate cluster defines separate distinct climate that is characterized by the mean values of the different climate variables used in the analysis. The clusters are calculated by taking the arithmetic means of all the values (climatic means) calculated for the grid boxes within each region. The regional climates are referred to by their cluster number C_1, C_2, \dots, C_k , where k is the number of clusters specified for the region. The clusters for specific palaeo-climates are mentioned in the text as $C_{i(t)}$, where i corresponds to the cluster number ($i=1, \dots, k$) and t to the simulation time period ($t=PI, MH, LGM, PLIO$). The descriptions first highlight the similarities and then the differences in regional climate. The cluster means of seasonal near-surface temperature amplitude and seasonal precipitation amplitude are referred to as temperature and precipitation amplitude. The median, 25th percentile, 75th percentile, minimum and maximum values for annual mean precipitation are referred to as $P_{md}, P_{25}, P_{75}, P_{min}$ and P_{max} respectively. Likewise, the same statistics for temperature are referred to as $T_{md}, T_{25}, T_{75}, T_{min}$ and T_{max} . These are presented as boxplots of climate variables in different time periods. When the character of a climate cluster is described as “high”, “moderate” and “low”, the climatic attribute’s values are described relative to the value range of the specific region in time, thus high PLIO precipitation rates may be higher than high LGM precipitation rates. The character is presented a raster plots, to allow compact visual representation of it. The actual mean values for each variable in every time-slice and region-specific cluster are included in tables in the supplementary material.

3.3.1 Climate change and palaeoclimate characterisation in South Asia, Central- and East Asia

317 This section describes the regional climatology of the four investigated Cenozoic time slices and how
 318 precipitation and temperature changes from PLIO to PI times in tropical, temperate and high altitude regions. LGM and
 319 PLIO simulations show the largest simulated temperature and precipitation deviations (Fig. 4b) from PI temperature and
 320 precipitation (Fig. 4a) in the South Asia region. LGM temperatures are 1-7°C below PI temperatures and the direction
 321 of deviation is uniform across the study region. PLIO temperature is mostly above PI temperatures by 1-7°C. The
 322 cooling of 3-5°C in the region immediately south of the Himalayan orogen represents one of the few exceptions.
 323 Deviations of MH precipitation from PI precipitation in the region are greatest along the eastern Himalayan orogeny,
 324 which experiences an increase in precipitation (≤ 2000 mm/a). The same region experiences a notable decrease in
 325 precipitation in the LGM simulation, which is consistent in direction with the prevailing precipitation trend on land
 326 during the LGM. PLIO precipitation on land is typically higher than PI precipitation.

327 Annual means of precipitation and temperature spatially averaged for the regional subdivisions and the different
 328 time slice simulations have been compared. The value range P_{25} to P_{75} of precipitation is higher for tropical South Asia
 329 than for temperate and high altitude South Asia (Fig. 5 a-c). The LGM values for P_{25} , P_{md} and P_{75} are lower than for the
 330 other time slice simulations, most visibly for tropical South Asia (ca. 100 mm/a). The temperature range (both $T_{75}-T_{25}$
 331 and $T_{max}-T_{min}$) is smallest in the hot (ca. 21°C) tropical South Asia, wider in the high altitude (ca. -8°C) South Asia, and
 332 widest in the temperate (ca. 2°C) South Asia region (Fig. 5 d-f). T_{md} , T_{25} and T_{75} values for the LGM are ca. 1°C, 1-2°C
 333 and 2°C below PI and MH temperatures in tropical, temperate and high altitude South Asia respectively, whereas the
 334 same temperature statistics for the PLIO simulation are ca. 1°C above PI and MH values in all regional subdivisions
 335 (Fig. 5 d-f). With respect to PI and MH values, precipitation and temperature are generally lower in the LGM and
 336 higher in the PLIO in tropical, temperate and high altitude South Asia.

337 In all time periods, the wettest climate cluster C_1 covers an area along the southeastern Himalayan orogen (Fig. 6
 338 a-d) and is defined by the highest precipitation amplitude (dark blue, Fig. 6 e-h). $C_{5(PI)}$, $C_{3(MH)}$, $C_{4(LGM)}$ and $C_{5(PLIO)}$ are
 339 characterized by (dark blue, Fig. 6e-h) the highest temperatures, u-wind and v-wind speeds during the summer monsoon
 340 in their respective time periods, whereas $C_{4(PI)}$, $C_{5(MH)}$, and $C_{6(LGM)}$ are defined by low temperatures and highest
 341 temperature amplitude, u-wind and v-wind speeds outside the monsoon season (in January) in their respective time
 342 periods (Fig. 6 e-h). The latter 3 climate classes cover much of the more continental, northern landmass in their
 343 respective time periods and represents a cooler climate affected more by seasonal temperature fluctuations (Fig. 6 a-d).
 344 The two wettest climate clusters C_1 and C_2 are more restricted to the eastern end of the Himalayan orogen in the LGM
 345 than during other times, indicating that the LGM precipitation distribution over the South Asia landmass is more
 346 concentrated in this region than in other time slice experiments.

349 This section describes the cluster analysis based regional climatology of the four investigated Late Cenozoic
350 time slices and illustrates how precipitation and temperature changes from PLIO to PI in tropical and temperate low-
351 and high altitude (i.e. Andes) regions in western South America (Fig. 7-9).

352 LGM and PLIO simulations show the largest simulated deviations (Fig. 7b) from PI temperature and
353 precipitation (Fig. 7a) in western South America. The direction of LGM temperature deviations from PI temperatures is
354 negative and uniform across the region. LGM temperatures are typically 1-3°C below PI temperatures across the region,
355 and 1-7°C below PI values in the Peruvian Andes, which also experience the strongest and most widespread increase in
356 precipitation during the LGM (≤ 1800 mm/a). Other regions, such as much of the northern Andes and tropical South
357 America, experience a decrease of precipitation in the same experiment. PLIO temperature is mostly elevated above PI
358 temperatures by 1-5°C. The Peruvian Andes experience a decrease in precipitation (≤ 2600 mm), while the northern
359 Andes are wetter in the PLIO simulation compared to the PI control simulation.

360 PI, MH, LGM and PLIO precipitation and temperature means for regional subdivisions have been compared.
361 The P_{25} to P_{75} range is smallest for the relatively dry temperate Andes and largest for tropical South America and the
362 tropical Andes (Fig. 8 a-d). P_{max} is lowest in the PLIO in all four regional subdivisions even though P_{md} , P_{25} and P_{75} in
363 the PLIO simulation are similar to the same statistics calculated for PI and MH time slices. P_{md} , P_{25} and P_{75} for the LGM
364 are ca. 50 mm/a lower in tropical South America and ca. 50 mm/a higher in the temperate Andes. Average PLIO
365 temperatures are slightly warmer and LGM temperatures are slightly colder than PI and MH temperatures in tropical
366 and temperate South America (Fig. 8 e and f). These differences are more pronounced in the Andes, however. T_{md} , T_{25}
367 and T_{75} are ca. 5°C higher in the PLIO climate than in PI and MH climates in both temperate and tropical Andes,
368 whereas the same temperatures for the LGM are ca. 2-4°C below PI and MH values (Fig. 8 g and h).

369 For the LGM, the model computes drier-than-PI conditions in tropical South America and tropical Andes,
370 enhanced precipitation in the temperate Andes, and a decrease in temperature that is most pronounced in the Andes. For
371 the PLIO, the model predicts precipitation similar to PI, but with lower precipitation maxima. PLIO temperatures
372 generally increase from PI temperatures, and this increase is most pronounced in the Andes.

373 The climate variability in the region is described by six different clusters (Fig. 9 a-d), which have similar
374 attributes in all time periods. The wettest climate C_1 is also defined by moderate to high precipitation amplitudes, low
375 temperatures and moderate to high u-wind speeds in summer and winter in all time periods (dark blue, Fig. 9 e-h). $C_{2(PI)}$,
376 $C_{2(MH)}$, $C_{3(LGM)}$ and $C_{2(PLIO)}$ are characterized by high temperatures and low seasonal temperature amplitude (dark blue,
377 Fig. 9 e-h), geographically cover the north of the investigated region, and represent a more tropical climate. $C_{5(PI)}$,
378 $C_{5(MH)}$, $C_{6(LGM)}$ and $C_{6(PLIO)}$ are defined by low precipitation and precipitation amplitude, high temperature amplitude and
379 high u-wind speeds in winter (Fig. 9 e-h), cover the low-altitude south of the investigated region (Fig. 9 a-d) and
380 represent dry, extra-tropical climates with more pronounced seasonality. In the PLIO simulation, the lower-altitude east

of the region has four distinct climates, whereas the analysis for the other time slice experiments only yield three distinct climates for the same region.

3.3.3 Climate change and palaeoclimate characterization in the St. Elias Range, Southeast Alaska

This section describes the changes in climate and the results from the cluster analysis for South Alaska (Fig. 10-12). As is the case for the other study areas, LGM and PLIO simulations show the largest simulated deviations (Fig. 10b) from PI temperature and precipitation (Fig. 10a). The sign of LGM temperature deviations from PI temperatures is negative and uniform across the region. LGM temperatures are typically 1-9°C below PI temperatures, with the east of the study area experiencing largest cooling. PLIO temperatures are typically 1-5°C above PI temperatures and the warming is uniform for the region. In comparison to the PI simulation, LGM precipitation is lower on land, but higher ($\leq 2300\text{mm}$) in much of the coastal regions of South Alaska. Annual PLIO precipitation is mostly higher ($\leq 800\text{mm}$) than for PI.

P_{md} , P_{25} , P_{75} , P_{min} and P_{max} for South Alaskan mean annual precipitation do not differ much between PI, MH and PLIO climates, while P_{md} , P_{25} , P_{75} and P_{min} decrease by ca. 20-40 mm/a and P_{max} increases during the LGM (Fig. 11a). The Alaskan PLIO climate is distinguished from the PI and MH climates by its higher (ca. 2°C) regional temperature means, T_{25} , T_{75} and T_{md} (Fig. 11b). Mean annual temperatures, T_{25} , T_{75} , T_{min} and T_{max} are lower in the LGM than in any other considered time period (Fig. 11b), and about 3-5°C lower than during the PI and MH.

Distinct climates are present in the PLIO to PI simulations for Southeast Alaska. Climate cluster C_1 is always geographically restricted to coastal southeast Alaska (Fig. 12 a-d) and characterized by the highest precipitation, precipitation amplitude, temperature, and by relatively low temperature amplitude (dark blue, Fig. 12 e-h). Climate C_2 is characterized by moderate to low precipitation, precipitation amplitude, temperature, and by low temperature amplitude. C_2 is either restricted to coastal southeast Alaska (in MH and LGM climates) or coastal southern Alaska (in PI and PLIO climates). Climate C_3 is described by low precipitation, precipitation amplitude, temperature, and moderate temperature amplitude in all simulations. It covers coastal western Alaska and separates climate C_1 and C_2 from the northern C_4 climate. Climate C_4 is distinguished by the highest mean temperature amplitude, by low temperature and precipitation amplitude, and by lowest precipitation.

The geographical ranges of PI climates C_1 - C_4 and PLIO climates C_1 - C_4 are similar. $C_{1(\text{PI/PLIO})}$ and $C_{2(\text{PI/PLIO})}$ spread over a larger area than $C_{1(\text{MH/LGM})}$ and $C_{2(\text{MH/LGM})}$. $C_{2(\text{PI/PLIO})}$ are not restricted to coastal southeast Alaska, but also cover the coastal southwest of Alaska. The main difference in characterization between PI and PLIO climates C_1 - C_4 lies in the greater difference (towards lower values) in precipitation, precipitation amplitude and temperature from $C_{1(\text{PLIO})}$ to $C_{2(\text{PLIO})}$ compared to the relatively moderate decrease in those means from $C_{1(\text{PI})}$ to $C_{2(\text{PI})}$.

3.3.4 Climate change and palaeoclimate characterization in the Cascade Range, US Pacific Northwest

413 This section describes the character of regional climatology in the US Pacific Northwest and its change over time
414 (Fig. 13-15). The region experiences cooling of typically 9-11°C on land during the LGM, and warming of 1-5°C
415 during the PLIO (Fig. 13b) when compared to PI temperatures (Fig. 13a). LGM precipitation increases over water,
416 decreases on land by ≤ 800 mm/a in the North and in the vicinity of Seattle and increases on land by ≤ 1400 mm/a on
417 Vancouver Island, around Portland and the Olympic Mountains, whereas PLIO precipitation does not deviate much
418 from PI values over water and varies in the direction of deviation on land. MH temperature and precipitation deviation
419 from PI values are negligible.

420 P_{md} , P_{25} , P_{75} , P_{min} and P_{max} for the Cascade Range do not notably differ between the four time periods (Fig. 14a).
421 The LGM range of precipitation values is slightly larger than that of the PI and MH with slightly increased P_{md} , while
422 the respective range is smaller for simulation PLIO. The T_{md} , T_{25} , T_{75} and T_{max} values for the PLIO climate are ca. 2°C
423 higher than those values for PI and MH (Fig. 14b). All temperature statistics for the LGM are notably (ca. 13°C) below
424 their analogues in the other time periods (Fig. 14b).

425 PI, LGM and PLIO clusters are similar in both their geographical patterns (Fig. 15 a, c, d) and their
426 characterization by mean values (Fig. 15 e, g, h). C_1 is the wettest cluster and shows the highest amplitude in
427 precipitation. The common characteristics of the C_2 cluster are moderate to high precipitation and precipitation
428 amplitude. C_4 is characterized by the lowest precipitation and precipitation amplitudes, and the highest temperature
429 amplitudes. Regions assigned to clusters C_1 and C_2 are in proximity to the coast, whereas C_4 is geographically restricted
430 to more continental settings.

431 In the PI and LGM climates, the wettest cluster C_1 is also characterized by high temperatures (Fig 10 e, g).
432 However, virtually no grid boxes were assigned to $C_{1(LGM)}$. $C_{1(MH)}$ differs from other climate state's C_1 clusters in that it is
433 also described by moderate to high near surface temperature and temperature amplitude (Fig 10 f), and in that it is
434 geographically less restricted and, covering much of Vancouver Island and the continental coastline north of it (Fig 10
435 b). Near surface temperatures are highest for C_2 in PI, LGM and PLIO climates (Fig 10 e, g, h) and low for $C_{2(MH)}$ (Fig
436 10 f). $C_{2(MH)}$ is also geographically more restricted than C_2 clusters in PI, LGM and PLIO climates (Fig 10 a-d). $C_{2(PI)}$,
437 $C_{2(MH)}$ and $C_{2(LGM)}$ have a low temperature amplitude (Fig 10 e-g), whereas $C_{2(PLIO)}$ is characterized by a moderate
438 temperature amplitude (Fig 10 h).

439

440 4. Discussion

441 In the following, we synthesize our results and compare to previous studies that investigate the effects of
442 temperature and precipitation change on erosion. [Since our results do not warrant merited discussion of subglacial](#)
443 [processes without additional work that is beyond the scope of this study, we instead advise caution in interpreting the](#)
444 [presented precipitation and temperature results in an erosional context where the regions are covered with ice. For](#)

convenience, ice cover is indicated on figures 2,3,47,10 and 13, and a summary of ice cover used as boundary conditions for the different time slice experiments is included in the supplemental material. Where possible, we relate the magnitude of climate change predicted in each geographical study area with terrestrial proxy data.

4.1 Synthesis of temperature changes and implications for weathering and erosion

4.1.1 Temperature changes and implications for weathering and erosion

Changes in temperature can affect physical weathering due to temperature-induced changes in periglacial processes and promote frost cracking and frost creep [e.g., Matsuoka, 2001; Schaller et al., 2002; Matsuoka and Murton, 2008; Delunel et al., 2010; Andersen et al., 2015; Marshall et al., 2015], and also biotic weathering and erosion [e.g. Moulton et al., 1998; Banfield et al., 1999; Dietrich and Perron, 2006]. Quantifying and understanding past changes in temperature is thus vital for our understanding of denudation histories. In the following, we highlight regions in the world where future observational studies might be able to document significant warming or cooling that would influence temperature related changes in physical and chemical weathering over the last ~3 Ma.

Simulated MH temperatures show little deviation (typically < 1°C) from PI temperatures in the investigated regions (Fig. 2b), suggesting little difference in MH temperature-related weathering. The LGM experiences widespread cooling, which is accentuated at the poles. LGM-cooling is accentuated at the poles, in general agreement with studies such as Otto-Bliesner et al. [2006] and Braconnot et al. [2007], and increases in the equator-to-pole pressure gradient and consequently strengthens global atmospheric circulation. Despite this global trend, cooling in coastal South Alaska is higher ($\leq 9^{\circ}\text{C}$) than in central Alaska ($0\pm 1^{\circ}\text{C}$). The larger temperature difference in South Alaska geographically coincides with ice cover (Fig. 10b), and should thus be interpreted in context of a different erosional regime. Cooling in most of the lower-latitude regions in South America and central to southeast Asia is relatively mild. The greatest temperature differences in South America are observed for western Patagonia, which was mostly covered by glaciers. The Tibetan plateau experiences more cooling ($3\text{--}5^{\circ}\text{C}$) than adjacent low-altitude regions ($1\text{--}3^{\circ}\text{C}$) during the LGM.

The PLIO simulation is generally warmer, and temperature differences are shows little to no warming in the tropics and accentuated warming at the poles, as do findings of Salzmann et al. [2011] and Robinson [2009] and Ballantyne [2010] respectively. This would reduce the equator-to-pole sea and land surface temperature gradient, as also reported by Dowsett et al. [2010], and also weaken global atmospheric circulation. Agreement with proxy-based reconstructions, as is the case of the relatively little warming in lower latitudes, is not surprising given that sea surface temperature reconstructions are prescribed in this uncoupled atmosphere simulation. It should be noted that coupled ocean-atmosphere simulations do predict more low-latitude warming [e.g. Stepanek and Lohmann 2012; Zhang et al. 2013b]. Warming in simulation PLIO is present greatest in parts of Canada, and Greenland and Antarctica (up to

19°C), [which geographically coincides with the presence of ice in the PI reference simulation and thus may be attributed to differences in ice cover. It should therefore also be regarded as areas in which process domain shifted from glacial to non-glacial, and consistent with values based on multi-proxy studies \[Ballantyne et al., 2010\]. Due to a scarcity of paleo-botanical proxies in Antarctica, reconstruction-based temperature and ice-sheet extent estimates for a PLIO climate have high uncertainties \[Salzmann et al., 2011\], making model validation difficult. Furthermore, controversy about relatively little warming in the south polar regions compared to the north polar regions remains \[e.g. Hillenbrand and Fütterer, 2002; Wilson et al., 2002\]. Mid-latitude PLIO warming is mostly in the 1-3°C range with notable exceptions of cooling in the northern tropics of Africa and on the Indian subcontinent, especially south of the Himalayan orogen.](#) The warming in simulation PLIO in South Alaska and the US Pacific northwest is mostly uniform and in the range of 1-5°C. [As before, changes in ice cover reveal that the greatest warming may be associated with the absence of glaciers relative to the PI simulation, whereas](#) warming in South America is concentrated at the Pacific west coast and the Andes between Lima and Chiclayo, and along the Chilean-Argentinian Andes south of Bolivia ($\leq 9^\circ\text{C}$).

Overall, annual mean temperatures in the MH simulation show little deviation from PI values. The more significant temperature deviations of the colder LGM and of the warmer PLIO simulations are accentuated at the poles leading to higher and lower equator-to-pole temperature gradients respectively. The largest temperature-related changes (relative to PI conditions) in weathering and subsequent erosion, [in many cases through a shift in the process domain from glacial to non-glacial or vice versa,](#) are therefore to be expected in the LGM and PLIO climates.

4.1.2 Temperature comparison to other studies

[LGM cooling is accentuated at the poles, thus increases the equator-to-pole pressure gradient and consequently strengthens global atmospheric circulation, and is in general agreement with studies such as Otto-Bliesner et al. \[2006\] and Braconnot et al. \[2007\]. The PLIO simulation shows little to no warming in the tropics and accentuated warming at the poles, as do findings of Salzmann et al. \[2011\] and Robinson \[2009\] and Ballantyne \[2010\] respectively. This would reduce the equator-to-pole sea and land surface temperature gradient, as also reported by Dowsett et al. \[2010\], and also weaken global atmospheric circulation. Agreement with proxy-based reconstructions, as is the case of the relatively little warming in lower latitudes, is not surprising given that sea surface temperature reconstructions \(derived from previous coarse resolution coupled ocean-atmosphere models\) are prescribed in this uncoupled atmosphere simulation. It should be noted that coupled ocean-atmosphere simulations do predict more low-latitude warming \[e.g. Stepanek and Lohmann 2012; Zhang et al. 2013b\]. The PLIO warming in parts of Canada and Greenland \(up to 19°C\) and consistent with values based on multi-proxy studies \[Ballantyne et al., 2010\]. Due to a scarcity of palaeobotanical proxies in Antarctica, reconstruction-based temperature and ice-sheet extent estimates for a PLIO climate have high uncertainties](#)

[Salzmann et al., 2011], making model validation difficult. Furthermore, controversy about relatively little warming in the south polar regions compared to the north polar regions remains [e.g. Hillenbrand and Fütterer, 2002; Wilson et al., 2002]. Mid-latitude PLIO warming is mostly in the 1-3°C range with notable exceptions of cooling in the northern tropics of Africa and on the Indian subcontinent, especially south of the Himalayan orogen.

4.2 Synthesis of precipitation changes ~~and implications for orogen denudation~~

4.2.1 Precipitation and implications for weathering and erosion

Changes in precipitation affects erosion through river incision, sediment transport, and erosion due to extreme precipitation events and storms [e.g. Whipple and Tucker, 1999; Hobbey et al., 2010]. Furthermore, vegetation type and cover also co-evolve with variations in precipitation and with changes in geomorphology [e.g. Marston 2010; Roering et al., 2010]. These vegetation changes in turn modify hillslope erosion by increasing root mass and canopy cover, and decreasing water-induced erosion via surface runoff [e.g. Gyssels et al., 2005]. Therefore, understanding and quantifying changes in precipitation in different palaeo-climates is necessary for a more complete reconstruction of orogen denudation histories. A synthesis of predicted precipitation changes is provided below, and highlights regions where changes in river discharge and hillslope processes might be impacted by climate change over the last ~3 Ma.

Most of North Africa is notably wetter during the MH, which is characteristic of the African Humid Period [Sarnthein 1978]. This pluvial regional expression of the Holocene Climatic Optimum is attributed to sudden changes in the strength of the African monsoon caused by orbital-induced changes in summer insolation [e.g. deMenocal et al. 2000]. Southern Africa is characterised by a wetter climate to the east and drier climate to the west of the approximate location of the Congo Air Boundary (CAB), the migration of which has previously been cited as a cause for precipitation changes in East Africa [e.g. Juninger et al. 2014]. In contrast, simulated MH precipitation rates show little deviation from the PI in most of the investigated regions, suggesting little difference in MH precipitation-related erosion. The Himalayan orogen is an exception and shows a precipitation increase of ≤ up to 2000 mm/a. The climate's enhanced erosion potential, that could result from such a climatic change, should be taken into consideration when palaeo-erosion rates estimated from the geological record in this area are interpreted [e.g. Bookhagen et al., 2005]. Specifically, higher precipitation rates (along with differences in other rainfall-event parameters) could increase the probability of mass movement events on hillslopes, especially where hillslopes are close to the angle of failure [e.g. Montgomery, 2001], and modify fluxes to increase shear stresses exerted on river beds and increase stream capacity to enhance erosion on river beds (e.g. by abrasion).

Most precipitation on land is decreased during the LGM due to large-scale cooling and decreased evaporation over the tropics, resulting in an overall decrease in inland moisture transport [e.g., Braconnot et al. 2007]. ~~Coastal~~ North

America, south of the continental ice sheets, is an exception and experiences increases in precipitation. For example, the investigated US Pacific Northwest and the southeastern coast of Alaska ~~are exceptions in that there is experience~~ experience strongly enhanced precipitation of ≤ 1700 mm/a and ≤ 2300 mm/a, respectively. These changes geographically coincide with differences in ice extent. An increase in precipitation in these regions may have had direct consequences on the glaciers' mass balance and equilibrium line altitudes, where the glaciers' effectiveness in erosion is highest [e.g. Egholm et al., 2009; Yanites and Ehlers, 2012]. The differences in the direction of precipitation changes, and accompanying changes in ice cover ~~Reduced precipitation in other parts of southern Alaska result in a stronger south-to-north drying gradient than in the PI simulation. This could~~ would likely result in more regionally differentiated variations in precipitation-specific erosional processes in the St. Elias Range rather than causing systematic offsets for the LGM. Although precipitation is significantly reduced along much of the Himalayan orogen (≤ 1600 mm/a), ~~which is consistent with findings by, e.g., Braconnot et al. [2007],~~ northeast India experiences strongly enhanced precipitation (≤ 1900 mm/a). This could have large implications for studies of uplift and erosion at orogen syntaxes, where highly localized and extreme denudation has been documented [e.g. Koons et al., 2013; Bendick and Ehlers, 2014].

Overall, the PLIO climate is wetter than the PI climate, in particular in the (northern) mid-latitudes, and possibly related to a northward shift of the northern Hadley cell boundary that is ultimately the result of a reduced equator-to-pole temperature gradient [e.g. Haywood et al. 2000, 2013; Dowsett et al. 2010]. ~~A reduction of this gradient by ca. 5°C is indeed present in the PLIO simulation of this study (Fig. 2b).~~ Most of the PLIO precipitation over land increases ~~during the PLIO. This finding agrees well with simulations performed at a lower spatial model resolution [cf. Stepanek and Lohmann, 2012]. PLIO precipitation significantly increases,~~ esp. at the Himalayan orogen by ≤ 1400 mm/a, and decreases from eastern Nepal to Namcha Barwa (≤ 2500 mm/a). Most of the Atacama Desert experiences an increase in precipitation by 100-200 mm/a, which may have to be considered in erosion and uplift history reconstructions for the Andes. A significant increase (~ 2000 mm/a) in precipitation from simulation PLIO to modern conditions is simulated for the eastern margin of the Andean Plateau in Peru and for northern Bolivia. This is consistent with recent findings of a pulse of canyon incision in these locations in the last ~ 3 Ma [Lease and Ehlers, 2013].

Overall, the simulated MH precipitation varies least from PI precipitation. The LGM is generally drier than the PI simulation, even though pockets of a wetter-than-PI climate do exist, such as much of coastal North America. Extra-tropical increased precipitation of the PLIO simulation and decreased precipitation of the LGM climate may be the result of decreased and increased equator-to-pole temperature gradients, respectively.

4.2.2 Precipitation comparison to other studies

The large scale LGM precipitation decrease on land, related to cooling and decreased evaporation over the tropics, and greatly reduced precipitation along much of the Himalayan orogeny, is consistent with previous studies by,

(for example) Braconnot et al. [2007]. The large scale PLIO precipitation increase due to a reduced equator-to-pole temperature gradient, has previously been pointed out by e.g. Haywood et al. [2000, 2013] and Dowsett et al. [2010]. A reduction of this gradient by ca. 5°C is indeed present in the PLIO simulation of this study (Fig. 2b). This precipitation increase over land agrees well with simulations performed at a lower spatial model resolution [cf. Stepanek and Lohmann, 2012]. Section 4.4 includes a more in-depth discussion of how simulated MH and LGM precipitation differences compare with proxy-based reconstructions in South Asia and South America.

4.3 Trends in Late Cenozoic changes in regional climatology

This section describes the major changes in regional climatology and highlights their possible implications on erosion rates.

Himalaya-Tibet, South Asia

In South Asia, cluster-analysis based categorization and description of climates (Fig. 6) remains similar throughout time. However, the two wettest climates (C₁ and C₂) are geographically more restricted to the eastern Himalayan orogen in the LGM simulation. Even though precipitation over the South Asia region is generally lower, this shift indicates that rainfall on land is more concentrated in this region and that the westward drying gradient along the orogen is more accentuated than during other time periods investigated here. While there is limited confidence in the global Atmospheric General Circulation Model's abilities to accurately represent meso-scale precipitation patterns [e.g. Cohen 1990], the simulation warrants careful consideration of possible, geographically non-uniform offsets in precipitation in investigations of denudation and uplift histories.

MH precipitation and temperature in tropical, temperate and high-altitude South Asia is similar to PI precipitation and temperature, whereas LGM precipitation and temperatures are generally lower (by ca. 100 mm/a and 1-2°C respectively), possibly reducing precipitation-driven erosion and enhancing frost-driven erosion in areas pushed into a near-zero temperature range during the LGM.

Andes, South America

Clusters in South America (Fig. 9), which are somewhat reminiscent of the Köppen and Geiger classification [Kraus, 2001], remain mostly the same over the last 3 Ma. In the PLIO simulation, the lower-altitude east of the region is characterized by four distinct climates, which suggests enhanced latitudinal variability in the PLIO climate compared to PI with respect temperature and precipitation.

The largest temperature deviations from PI values are derived for the PLIO simulation in the (tropical and temperate) Andes, where temperatures exceed PI values by 5°C. On the other hand, LGM temperatures in the Andes are

ca. 2-4°C below PI values in the same region (Fig 7 g and h). In the LGM simulation, tropical South America experiences ca. 50 mm/a less precipitation, the temperate Andes receive ca. 50 mm/a more precipitation than in PI and MH simulations. These latitude-specific differences in precipitation changes ought to be considered in attempts to reconstruct precipitation-specific palaeo-erosion rates in the Andes on top of longitudinal climate gradients highlighted by, e.g., Montgomery et al. [2001].

St. Elias Range, South Alaska

South Alaska is subdivided into two wetter and warmer clusters in the south, and two drier, colder clusters in the north. The latter are characterized by increased seasonal temperature variability due to being located at higher latitudes (Fig. 12). The different equator-to-pole temperature gradients for LGM and PLIO may affect the intensity of the Pacific North American Teleconnection (PNA) [Barnston and Livzey, 1987], which has significant influence on temperatures and precipitation, especially in southeast Alaska, and may in turn result in changes in regional precipitation and temperature patterns and thus on glacier mass balance. Changes in the Pacific Decadal Oscillation, which is related to the PNA pattern, has previously been connected to differences in Late Holocene precipitation [Barron and Anderson, 2011]. While this climate cluster pattern appears to be a robust feature for the considered climate states, and hence over the recent geologic history, the LGM sets itself apart from PI and MH climates by generally lower precipitation (20-40 mm) and lower temperatures (3-5°C, Fig. 10, 11), which may favour frost driven weathering during glacial climate states [e.g. Andersen et al., 2015; Marshall et al. 2015] in unglaciated areas, whereas glacial processes would have dominated most of this region as it was covered by ice. Simulation PLIO is distinguished by temperatures that exceed PI and MH conditions by ca. 2°C, and by larger temperature and precipitation value ranges, possibly modifying temperature- and precipitation-dependent erosional processes in the region of South Alaska.

Cascade Range, US Pacific Northwest

In all time slices, the geographic climate patterns, based on the cluster analysis (Fig. 15), represents an increase in the degree of continentality from the wetter coastal climates to the further inland located climates with greater seasonal temperature amplitude and lower precipitation and precipitation amplitude (Fig 15 e-h). The most notable difference between the time slices is the strong cooling during the LGM, when temperatures are ca. 13°C (Fig. 13, 14) below those of other time periods. Given that the entire investigated region was covered by ice (Fig 13), we can assume a shift to glacially dominated processes. possibly leading to enhanced sediment production driven by frost processes, as proposed for parts of the Pacific Northwest by Marshall et al. [2015].

4.4 Comparison of simulated and observed precipitation differences

The predicted precipitation differences reported in this study were compared with observed (proxy record) palaeoprecipitation change. Proxy based precipitation reconstructions for the MH and LGM are presented for South Asia and South America for the purpose of assessing ECHAM5 model performance, and for identifying inconsistencies between neighbouring proxy data. Due to the repeated glaciations, detailed terrestrial proxy records for the time slices investigated here are not available, to the best of our knowledge, for the Alaskan and Pacific NW USA studies. Although marine records and records of glacier extent are available in these regions, the results from them do not explicitly provide estimates of wetter/drier, or colder/warmer conditions that can be spatially compared to the simulation estimates. For these two areas with no available records, the ECHAM5 predicted results therefore provide predictions from which future studies can formulate testable hypotheses to evaluate.

The palaeoclimate changes in terrestrial proxy records compiled here are reported as “wetter than today”, “drier than today” or “the same as today” for each of the study locations, and plotted on top of the simulation-based difference maps as upward facing blue triangles, downward facing red triangles and grey circles respectively (Fig. 16, 17). The numbers listed next to those indicators are the ID numbers assigned to the studies compiled for this comparison and are associated with a citation provided in the figure captions.

In South Asia, 14/26 results from local studies agree with the model predicted precipitation changes for the MH. The model seems able to reproduce the predominantly wetter conditions on much of the Tibetan plateau, but predicts slightly drier conditions north of Chengdu, which is not reflected in local reconstructions. The modest mismatch between ECHAM5 predicted and proxy-based MH climate change in south Asia was also documented by Li et al., [2017], whose simulations were conducted at a coarser (T106) resolution. Despite these model-proxy differences, we note that there are significant discrepancies between the proxy data themselves in neighbouring locations in the MH, highlighting caution in relying solely upon these data for regional palaeoclimate reconstructions. These differences could result from either poor age-constraints in the reported values, or systematic errors in the transfer functions used to convert proxy measurements to palaeoclimate conditions. The widespread drier conditions on the Tibetan Plateau and immediately north of Laos are confirmed by 7/7 of the palaeoprecipitation reconstructions. 23/39 of the reconstructed precipitation changes agree with model predictions for South America during the MH. The model predicted wetter conditions in the central Atacama desert, as well as the drier conditions northwest of Santiago are confirmed by most of the reconstructions. The wetter conditions in southernmost Peru and the border to Bolivia and Chile cannot be confirmed by local studies. 11/17 of the precipitation reconstructions for the LGM are in agreement with model predictions. These include wetter conditions in most of Chile. The most notable disagreement can be seen in northeast Chile at the border to Argentina and Bolivia, where model predicted wetter conditions are not confirmed by reported reconstructions from local sites.

Model performance is, in general, higher for the LGM than for the MH and overall satisfactory given that it

cannot be expected to resolve sub-grid scale differences in reported palaeoprecipitation reconstructions. However, as mentioned above, it should be noted that some locations (MH of south Asia, and MH of north Chile) discrepancies exist between neighbouring proxy samples and highlight the need for caution in how these data are interpreted. Other potential sources of error resulting in disagreement of simulated and proxy-based precipitation estimates are the model's shortcomings in simulating orographic precipitation at higher resolutions, and uncertainties in palaeoclimate reconstructions at the local sites. In summary, although some differences are evident in both the model-proxy data comparison and between neighbouring proxy data themselves, the above comparison highlights an overall good agreement between the model and data for the south Asia and South American study areas. Thus, although future advances in GCM model parameterisations and new or improved palaeoclimate proxy techniques are likely, the palaeoclimate changes documented here are found to be in general robust and provide a useful framework for future studies investigating how these predicted changes in palaeoclimate impact denudation.

4.45 Conclusions

We present a [statistical](#) cluster-analysis-based description of the geographic coverage of possible distinct regional expressions of climates from four different time slices (Fig. 6, 9, 12, 15). These are determined with respect to a selection of variables that characterize the climate of the region and may be relevant to weathering and erosional processes. While the geographic [distribution of](#) climate ~~patterns~~ remains similar throughout time (as indicated by results of four different climate states representative for the climate of the last 3 Ma), results for the PLIO simulation suggests more climatic variability east of the Andes (with respect to near-surface temperature, seasonal temperature amplitude, precipitation, seasonal precipitation amplitude and seasonal u-wind and v-wind speeds). Furthermore, the wetter climates in the South Asia region retreat eastward along the Himalayan orogen for the LGM simulation, this is due to decreased precipitation along the western part of the orogen and enhanced precipitation on the eastern end, possibly signifying more localised high erosion rates.

Most global trends of the high-resolution LGM and PLIO simulations conducted here are in general agreement with previous studies [Otto-Bliesner et al., 2006; Braconnot et al., 2007; Wei and Lohmann, 2012; Lohmann et al., 2013; Zhang et al., 2013b, 2014; Stepanek and Lohmann, 2012]. The MH does not deviate notably from the PI, the LGM is relatively dry and cool, while the PLIO is comparably wet and warm. While the simulated regional changes in temperature and precipitation usually agree with the sign ([or direction](#)) of the simulated global changes, there are region-specific differences in the magnitude and direction. For example, the LGM precipitation of the Tropical Andes does not deviate significantly from PI precipitation, whereas LGM precipitation in the Temperate Andes is enhanced.

[Comparisons to local, proxy-based reconstructions of MH and LGM precipitation in South Asia and South America reveal satisfactory performance of the model in simulating the reported differences. The model performs better](#)

for the LGM than the MH. We note however that compilations of proxy data such as we present here, also identify inconsistencies between neighbouring proxy data themselves, warranting caution in the extent to which both proxy data and palaeoclimate models are interpreted for MH climate change in south Asia, and western South America.

The changes in regional climatology presented here are manifested, in part, by small to large magnitude changes in fluvial and hillslope relevant parameters such as precipitation and temperature. For the regions investigated here we find that precipitation differences between the PI, MH, LGM, and PLIO are in many areas around +/- 200-600 mm/yr, and locally can reach maximums of +/- 1000-2000 mm/yr (Figs. 4, 7, 10, 13). In areas where significant precipitation increases are accompanied by changes in ice extent, such as parts of southern Alaska during the LGM, we would expect a shift in the erosional regime to glacier dominated processes. Temperature differences between these same time periods are around 1-4 °C in many places, but reach maximum values of 8-10 °C. Many of these maxima in the temperature differences geographically coincide with changes in ice sheet extent and must therefore be interpreted as part of a different erosional process domains. However, we also observe large temperature differences (~5°C) in unglaciated areas that would be affected by hillslope, frost cracking, and fluvial processes. The magnitude of these differences are not trivial, and will likely impact fluvial and hillslope erosion and sediment transport, as well as biotic and abiotic weathering. The regions of large magnitude changes in precipitation and temperature documented here (Figs. 4, 7, 10, 13) offer the highest potential for future observational studies interested in quantifying the impact of climate change on denudation and weathering rates.

Acknowledgements

The model simulations presented in this study are freely available to interested persons by contacting S. Mutz or T. Ehlers. We note however that the data files are very large (~4 TB, and too large to archive in journal supplementary material) and require familiarity in reading/plotting NetCDF formatted files. Support from European Research Council (ERC) Consolidator Grant number 615703 provided support for S. Mutz. Additional support is acknowledged from the German science foundation (DFG) priority research program 1803 (EarthShape: Earth Surface Shaping by Biota; grants EH329/14-1 and EH329/17-1). We thank B. Adams and J. Starke for constructive discussions. The DKRZ is thanked for computer time used for some of the simulations presented here. C. Stepanek, M. Werner, and G. Lohmann acknowledge funding by the Helmholtz Climate Initiative ReKlim and the Alfred Wegener Institute's research programme Marine, Coastal and Polar Systems.

732 **Figure Captions**

733

734 **Figure 1** Topography for regions (a) tropical South Asia, (b) temperate South Asia, (c) high altitude South Asia, (d)
735 temperate South America, (e) tropical South America, (f) temperate Andes, (g) tropical Andes-, [SE Alaska and Cas-](#)
736 [cadia](#).

737 **Figure 2** Global PI annual mean near-surface temperatures (a), and deviations of MH, LGM and PLIO annual mean
738 near-surface temperatures from PI values (b). Units are °C and insignificant ($p < 99\%$) differences (as determined by
739 a t-test) are greyed out.

740 **Figure 3** Global PI annual mean precipitation (a), and deviations of MH, LGM and PLIO annual mean near-surface
741 temperatures from PI values (b). Units are mm/yr.

742 **Figure 4** PI annual mean near-surface temperatures (a), and deviations of MH, LGM and PLIO annual mean near-sur-
743 face temperatures from PI values (b) for the South Asia region. Insignificant ($p < 99\%$) differences (as determined
744 by a t-test) are greyed out.

745 **Figure 5** PI, MH, LGM and PLIO annual mean precipitation in (a) tropical South Asia, (b) temperate South Asia, and
746 (c) high-altitude South Asia; PI, MH, LGM and PLIO annual mean temperatures in (d) tropical South Asia, (e) tem-
747 perate South Asia, and (f) high-altitude South Asia. For each time slice, the minimum, lower 25th percentile, median,
748 upper 75th percentile and maximum are plotted.

749 **Figure 6** Geographical coverage and characterization of climate classes C_1 - C_6 based on cluster-analysis of 8 variables
750 (near surface temperature, seasonal near surface temperature amplitude, total precipitation, seasonal precipitation
751 amplitude, u-wind in January and July, v-wind in January and July) in the South Asia region. The geographical cov-
752 erage of the climates C_1 - C_6 is shown on the left for PI (a), MH (b), LGM (c) and PLIO (d); the complementary,
753 time-slice specific characterization of C_1 - C_6 for PI (e), MH (f), LGM (g) and PLIO (h) is shown on the right.

754 **Figure 7** PI annual mean near-surface temperatures (a), and deviations of MH, LGM and PLIO annual mean near-sur-
755 face temperatures from PI values (b) for western South America. Insignificant ($p < 99\%$) differences (as determined
756 by a t-test) are greyed out.

757 **Figure 8** PI, MH, LGM and PLIO annual mean precipitation in (a) tropical South America, (b) temperate South Amer-
758 ica, (c) tropical Andes, and (d) temperate Andes; PI, MH, LGM and PLIO annual mean temperatures in (e) tropical

759 South America, (f) temperate South America, (g) tropical Andes, and (h) temperate Andes. For each time slice, the
760 minimum, lower 25th percentile, median, upper 75th percentile and maximum are plotted.

761 **Figure 9** Geographical coverage and characterization of climate classes C₁- C₆ based on cluster-analysis of 8 variables
762 (near surface temperature, seasonal near surface temperature amplitude, precipitation, seasonal precipitation amp-
763 litude, u-wind in January and July, v-wind in January and July) in western South America. The geographical cover-
764 age of the climates C₁- C₆ is shown on the left for PI (a), MH (b), LGM (c) and PLIO (d); the complementary, time-
765 slice specific characterization of C₁- C₆ for PI (e), MH (f), LGM (g) and PLIO (h) is shown on the right.

766 **Figure 10** PI annual mean near-surface temperatures (a), and deviations of MH, LGM and PLIO annual mean near-sur-
767 face temperatures from PI values (b) for the South Alaska region. Insignificant ($p < 99\%$) differences (as determined
768 by a t-test) are greyed out.

769 **Figure 11** PI, MH, LGM and PLIO annual mean precipitation (a), and mean annual temperatures (b) in South Alaska.
770 For each time slice, the minimum, lower 25th percentile, median, upper 75th percentile and maximum are plotted.

771 **Figure 12** Geographical coverage of climate classes C₁- C₄ based on cluster-analysis of 4 variables (near surface tem-
772 perature, seasonal near surface temperature amplitude, total precipitation, seasonal total precipitation amplitude) in
773 southern Alaska. The geographical coverage of the climates C₁- C₄ is shown on the left for PI (a), MH (b), LGM (c)
774 and PLIO (d); the complementary, time-slice specific characterization of C₁- C₆ for PI (e), MH (f), LGM (g) and
775 PLIO (h) is shown on the right.

776 **Figure 13** PI annual mean near-surface temperatures (a), and deviations of MH, LGM and PLIO annual mean near-sur-
777 face temperatures from PI values (b) for the US Pacific Northwest. Insignificant ($p < 99\%$) differences (as determ-
778 ined by a t-test) are greyed out.

779 **Figure 14** PI, MH, LGM and PLIO annual mean precipitation (a), and annual mean temperatures (b) in the Cascades,
780 US Pacific Northwest. For each time slice, the minimum, lower 25th percentile, median, upper 75th percentile and
781 maximum are plotted.

782 **Figure 15** Geographical coverage and characterization of climate classes C₁- C₄ based on cluster-analysis of 4 variables
783 (near surface temperature, seasonal near surface temperature amplitude, total precipitation, seasonal total precipita-
784 tion amplitude) in the Cascades, US Pacific Northwest. The geographical coverage of the climates C₁- C₄ is shown
785 on the left for PI (a), MH (b), LGM (c) and PLIO (d); the complementary, time-slice specific characterization of C₁-

786 C₆ for PI (e), MH (f), LGM (g) and PLIO (h) is shown on the right.

787 **Figure 16** [Simulated annual mean precipitation deviations of MH \(left\) and LGM \(right\) from PI values in South Asia,](#)
788 [and temporally corresponding proxy-based reconstructions, indicating wetter \(upward facing blue triangles\), drier](#)
789 [\(downward facing red triangles\) or similar \(grey circles\) conditions in comparison with modern climate. MH proxy-](#)
790 [based precipitation differences are taken from Mügler et al. \(2010\) \(66\), Wischnewski et al. \(2011\) \(67\), Mischke et](#)
791 [al. \(2008\), Wischnewski et al. \(2011\), Herzsuh et al. \(2009\) \(68\), Yanhong et al. \(2006\) \(69\), Morrill et al. \(2006\)](#)
792 [\(70\), Wang et al. \(2002\) \(71\), Wuennemann et al. \(2006\) \(72\), Zhang et al. \(2011\), Morinaga et al. \(1993\),](#)
793 [Kashiwaya et al. \(1995\) \(73\), Shen et al. \(2005\) \(74\), Liu et al. \(2014\) \(75\), Herzsuh et al. \(2006\) \(76\), Zhang and](#)
794 [Mischke \(2009\) \(77\), Nishimura et al. \(2014\) \(78\), Yu and Lai \(2014\) \(79\), Gasse et al. \(1991\) \(80\), Van Campo et](#)
795 [al. \(1996\) \(81\), Demske et al. \(2009\) \(82\), Kramer et al. \(2010\) \(83\), Herzsuh et al. \(2006\) \(84\), Hodell et al.](#)
796 [\(1999\)\(85\), Hodell et al. \(1999\) \(86\), Shen et al. \(2006\) \(87\), Tang et al. \(2000\) \(88\), Tang et al. \(2000\) \(89\), Zhou](#)
797 [et al. \(2002\) \(90\), Liu et al. \(1998\) \(91\), Asashi \(2010\)\(92\), Kotila et al. \(2009\) \(93\), Kotila et al. \(2000\) \(94\), Wang](#)
798 [et al. \(2002\) \(95\), Hu et al. \(2014\) \(96\), Hodell et al. \(1999\) \(97\), Hodell et al. \(1999\) \(98\).](#)

799 **Figure 17** [Simulated annual mean precipitation deviations of MH \(left\) and LGM \(right\) from PI values in South Amer-](#)
800 [ica, and temporally corresponding proxy-based reconstructions, indicating wetter \(upward facing blue triangles\),](#)
801 [drier \(downward facing red triangles\) or similar \(grey circles\) conditions in comparison with modern climate. MH](#)
802 [proxy-based precipitation differences are taken from Bird et al. \(2011\) \(1\), Hansen et al \(1994\) \(2\), Hansen et al](#)
803 [\(1994\) \(3\), Hansen et al \(1994\) \(4\), Hansen et al \(1994\) \(5\), Hansen et al \(1994\) \(6\), Hillyer et al. \(2009\) \(7\),](#)
804 [D’Agostino et al. \(2002\) \(8\), Baker et al. \(2001\) \(9\), Schwalb et al \(1999\) \(10\), Schwalb et al \(1999\) \(11\), Schwalb](#)
805 [et al \(1999\) \(12\), Schwalb et al \(1999\) \(13\), Moreno et al \(2009\) \(14\), Pueyo et al \(2011\) \(15\), Mujica et al \(2015\)](#)
806 [\(16\), Fritz et al. \(2004\) \(17\), Gayo et al. \(2012\) \(18\), Latorre et al. \(2006\) \(19\), Latorre et al. \(2003\) \(20\), Quade et al](#)
807 [\(2008\) \(21\), Bobst et al. \(2001\) \(22\), Grosjean et al. \(2001\) \(23\), Betancourt et al. \(2000\) \(24\), Latorre et al. \(2002\)](#)
808 [\(25\), Rech et al. \(2003\) \(26\), Diaz et al. \(2012\) \(27\), Maldonado et al \(2005\) \(28\), Diaz et al. \(2012\) \(29\), Lamy et](#)
809 [al. \(2000\) \(30\), Kaiser et al. \(2008\) \(31\), Maldonado et al. \(2010\) \(32\), Villagrán et al. \(1990\) \(33\), Méndez et al.](#)
810 [\(2015\) \(34\), Maldonado et al. \(2006\) \(35\), Lamy et al. \(1999\) \(36\), Jenny et al. \(2002\) \(37\), Jenny et al. \(2002b\)](#)
811 [\(38\), Villa-Martínez et al. \(2003\) \(39\), Bertrand et al. \(2008\) \(40\), De Basti et al. \(2008\) \(41\), Lamy et al. \(2009\)](#)
812 [\(42\), Lamy et al. \(2002\) \(43\), Szeicz et al. \(2003\) \(44\), de Porras et al. \(2012\) \(45\), de Porras et al. \(2014\) \(46\),](#)
813 [Markgraf et al. \(2007\) \(47\), Siani et al. \(2010\) \(48\), Gilli et al. \(2001\) \(49\), Markgraf et al. \(2003\) \(50\), Stine et al.](#)
814 [\(1990\) \(51\).](#)

817 **References**

818

819 Abe-Ouchi, A., Saito, F., Kageyama, M., Bracannot, P., Harrison, S. P., Lambeck, K., Otto-Bliesner, B. L., Peltier,
 820 W.R., Tarasov, L., Peterschmitt, J.-Y., Takahashi, K.: Ice-sheet configuration in the CMUP5/PMIP3 Last Glacial
 821 Maximum experiments. *Geosci. Model Dev.*, 8, 3621-3637, doi:10.5194/gmd-8-3621-2015, 2015

822 [Andersen, J., Egholm, D.L., Knudsen, M.F., Jansen, J., Nielsen, S.B., The periglacial engine of mountain erosion – Part](#)
 823 [1: Rates of frost cracking and frost creep., *Earth Surface Dynamics*, 3\(4\), 447-462, 2015.](#)

824 Arnold, L., Breon, F.M., and Brewer, S: The earth as an extrasolar planet: the vegetation spectral signature today and
 825 during the last Quaternary climatic extrema, *Int. J. Astrobiol.*, 8, 81–94. [http://dx.doi.org/10.1017/](http://dx.doi.org/10.1017/S1473550409004406)
 826 [S1473550409004406](http://dx.doi.org/10.1017/S1473550409004406), 2009.

827 [Asahi, K.: Equilibrium-line altitudes of the present and Last Glacial Maximum in the eastern Nepal](#)
 828 [Himalayas and their implications for SW monsoon climate, *Quatern. Int.*, 212, 26-34,](#)
 829 [doi:10.1016/j.quaint.2008.08.004, 2010.](#)

830 Bahrenberg, G., Giese, E., and Nipper, J.: Multivariate Statistik. *Statistische Methoden in der Geographie 2*, Stuttgart,
 831 1992.

832 [Baker, P. A., Seltzer, G. O., Fritz, S. C., Dunbar, R. B., Grove, M. J., Tapia, P. M., Cross L., Rowe H. D., and](#)
 833 [Baroda, J. P.: The History of South America Tropical Precipitation for the Past 25,000 Years, *Earth and*](#)
 834 [Atmospheric Sciences, 291, 640-643, doi:10.1126/science.291.5504.640, 2001.](#)

835 Ballantyne, A.P., Greenwood, D.R., Sinninghe Damste, J.S., Csank, A.Z., Eberle, J.J., and Rybczynski, N.:
 836 Significantly warmer Arctic surface temperatures during the Pliocene indicated by multiple independent proxies,
 837 *Geology* 38 (7), 603–606, 2010.

838 Banfield, J.F., Barker, W.W., Welch, S.A., and Taunton, A.: Biological impact on mineral dissolution: application of
 839 the lichen model to understanding mineral weathering in the rhizosphere, *Proceedings of the National Academy of*
 840 *Sciences*, 96, 3404-3411, 1999.

841 [Barnston, A. G. and Livezey, R. E.: Classification, Seasonality and Persistence of Low-Frequency](#)
 842 [Atmospheric Circulation Patterns, *Mon. Weather Rev.*, 115, 1083-1126, doi:10.1175/1520-](#)
 843 [0493\(1987\)1151083:CSAPOL2.0.CO;2, 1987.](#)

844 [Barron, J.A., and Anderson, L.: Enhanced Late Holocene ENSO/PDO expression along the margins of the](#)
 845 [eastern North Pacific. *Quaternary International*, 235, 3-12, 2011.](#)

846 Bendick, R., and Ehlers, T.A.: Extreme localized exhumation at syntaxes initiated by subduction geometry, *Geophys.*
 847 *Res. Lett.*, 41(16), 2014GL061026, doi:10.1002/2014GL061026, 2014.

848 [Bertrand, S., Charlet F., Charlier B., Renson V., and Fagel N.: Climate variability of southern Chile since the](#)
 849 [Last Glacial Maximum: a continuous sedimentological records from Lago Puyehue \(40°S\), *J. Paleolimnol.*,](#)

850 | [39, 179-195, doi:10.1007/s10933-007-9117-y, 2008.](#)

851 | [Betancourt, J. L., Latorre C., Rech J. A., Quade J., and Rylander K.A.: A 22,000 Year Record of Monsoonal](#)
852 | [Precipitation from Northern Chile's Atacama Desert, *Science*, 289, 1542-1546, doi: 10.1126/](#)
853 | [science.289.5484.1542, 2000.](#)

854 | Bigelow, N. H., Brubaker, L. B., Edwards, M. E., Harrison, S. P., Prentice, I. C., Anderson, P. M., Andreev, A. A.,
855 | Bartlein, P. J., Christensen, T. R., Cramer, W., Kaplan, J. O., Lozhkin, A. V., Matveyeva, N. V., Murray, D. V.,
856 | McGuire, A. D., Razzhivin, V. Y., Ritchie, J. C., Smith, B., Walker, D. A., Gajewski, K., Wolf, V., Holmqvist, B.
857 | H., Igarashi, Y., Kremenetskii, K., Paus, A., Pisaric, M. F. J., and Vokova, V. S.: Climate change and Arctic ecosys-
858 | tems I. Vegetation changes north of 55°N between the last glacial maximum, mid-Holocene and present. *Journal of*
859 | *Geophysical Research - Atmospheres*, 108(D19), doi: 10.1029/2002JD002558, 2003.

860 | [Bird, B. W., Abbott M. B., Rodbell D. T., and Vuille M.: Holocene tropical South American hydroclimate re-](#)
861 | [vealed from a decadal resolved lake sediment \$\delta^{18}\text{O}\$ record, *Earth Planet. Sc. Lett.*, 310, 192-202,](#)
862 | [doi:10.1016/j.epsl.2011.08.040, 2011.](#)

863 | [Bobst, A. L., Lowenstein, T. K., Jordan, T. E., Godfrey, L. V., Ku, T.-L., and Luo, S.: A 106 ka paleoclimate](#)
864 | [record from drill core of the Salar de Atacama, northern Chile, *Palaeogeogr. Palaeocl.*, 173, 21-42,](#)
865 | [doi:10.1016/S0031-0182\(01\)00308, 2001.](#)

866 | Braconnot, P., Otto-Bleisner, B., Harrison, S.P., Joussaume, S., Peterschmitt, J.-Y., Abe-Ouchi, A., Crucifix, M.,
867 | Driesschaert, E., Fichefet, T., Hewitt, C.D., Kagayama, M., Kitoh, A., Loutre, M.-F., Marti, O., Merkel, U.,
868 | Ramstein, G., Valdes, P., Weber, L., Yu, Y., and Zhao, Y.: Results of PMIP2 coupled simulations of the mid-
869 | Holocene and Last Glacial maximum, part 1: experiments and large-scale features, *Clim Past* 3:261–277, 2007.

870 | Böhner, J.: General climatic controls and topoclimatic variations in Central and High Asia, *Boreas*, 35(2), 279-295,
871 | 2006.

872 | Bookhagen, B., Thiede, R.C., and Strecker, M.R.: Late Quaternary intensified monsoon phases control landscape
873 | evolution in the northwest Himalaya, *Geology*, 33(2), 149-152. doi: 10.1130/G20982.1, 2005.

874 | Boos, W. R., and Kuang, Z.: Dominant control of the South Asian monsoon by orographic insulation versus plateau
875 | heating, *Nature*, 463, 218-222, 2010.

876 | Braun, J.: A simple model for regolith formation by chemical weathering: Regolith Formation, *Journal of Geophysical*
877 | *Research Earth's Surface*, DOI: 10.1002/2016JF003914, 2016.

878 | Caves, J.: Late Miocene Uplift of the Tian Shan and Altai and Reorganization of Central Asia Climate, *GSA*
879 | [Today](#), doi:10.1130/gsatg305a.1, 2017.

880 | CLIMAP Project Members: Seasonal Reconstruction of the Earth's Surface at the Last Glacial Maximum.
881 | *Map and Chart Series*, Vol. 36, Geological Society of America, 18 pp., 1981.

882 | Cohen, S.J.: Bringing the global warming issue close to home: The challenge of regional impact studies. *Bulletin of the*
883 | *American Meteorological Society*, 71: 520 – 526., 1990.

886 | [D'Agostino, K., Seltzer, G., Baker, P., Fritz, S., and Dunbar, R.: Late-Quaternary lowstands of Lake Titicaca: evidence from high-resolution seismic data, *Palaeogeogr. Palaeoclimatol.*, 179, 97-111, doi:10.1016/S0031-0182\(01\)00411-4, 2002.](#)

889 | [De Batist, M., Fagel N., Loutre M. F., and Chapron E.: A 17,900-year multi-proxy lacustrine record of Lago](#)

890 | [Puyehue \(Chilean Lake District\): introduction, *J. Paleolimnol.*, 39, 151-161, doi:10.1007/s10933-007-](#)

891 | [9113-2, 2007.](#)

892 | [de Porras, M. E., Maldonado, A., Abarzua, A. M., Cardenas, M. L., Francois, J. P., Martel-Cea, A., Stern, C.](#)

893 | [R., Mendez, C., and Reyes, O.: Postglacial vegetation, fire and climate dynamics at Central Chilean](#)

894 | [Patagonia \(Lake Shaman, 44°S\), *Quaternary Sci. Rev.*, 50, 71-85, doi:10.1016/j.quascirev.2012.06.015;](#)

895 | [2012.](#)

896 | [de Porras, M. E., Maldonado, A., Quintana, F. A., Martel-Cea, A., Reyes, O., and Méndez, C.: Environmental](#)

897 | [and climatic changes in central Chilean Patagonia since the Late Glacial \(Mallín El Embudo, 44° S\), *Clim.*](#)

898 | [Past](#), 10, 1063–1078, doi:10.5194/cp-10-1063-2014, 2014.

899 | Delunel, R., van der Beek, P. A., Carcaillet, J., Bourlès, D. L., and Valla, P.G.: Frost-cracking control on catchment de-

900 | nudation rates: Insights from in situ produced ¹⁰Be concentrations in stream sediments (Ecrins–Pelvoux massif,

901 | French Western Alps), *Earth and Planetary Science Letters*, 293(1–2), 72–83, doi:10.1016/j.epsl.2010.02.020,

902 | 2010.

903 | [DeMenocal, P., Ortiz, J., Guilderson, T., Adkins, J., Samthein, M., Baker, L., and Yarusinsky, M.: Abrupt on-](#)

904 | [set and termination of the African Humid Period:: rapid climate responses to gradual insolation forcing, *Quaternary Sci. Rev.*, 19, 347-361, doi:10.1016/S0277-3791\(99\)00081-5, 2000.](#)

905 | [Demske, D., Tarasov, P. E., Wünnemann, B., and Riedel, F.: Late glacial and Holocene vegetation, Indian](#)

906 | [monsoon and westerly circulation in the Trans-Himalaya recorded in the lacustrine pollen sequence from](#)

907 | [Tso Kar, Ladakh, NW India, *Palaeogeogr. Palaeoclimatol.*, 279, 172-185, doi:10.1016/j.palaeo.2009.05.008,](#)

908 | [2009.](#)

909 | [Diaz, F.P., Latorre, C., Maldonado, A., Quade, J., and Betancourt, J.L.: Rodent middens reveal episodic,](#)

910 | [long-distance plant colonizations across the hyperarid Atacama Desert over the last 34,000 years, *J.*](#)

911 | [Biogeogr.](#), 39, 510-525, doi:10.1111/j.1365-2699.2011.02617.x, 2012.

912 | [Dietrich, W. E., and Perron, J.T.: The search for a topographic signature of life, *Nature*, 439\(7075\), 411–418,](#)

913 | [doi:10.1038/nature04452, 2006.](#)

914 | [Dietrich, S., Werner, M., Spanghel, T., and Lohmann, G.: Influence of orbital forcing and solar activity on water iso-](#)

915 | [topes in precipitation during the mid and late Holocene, *Clim. Past*, 9, 13-26. doi:10.5194/cp-9-13-2013, 2013.](#)

916 | [Dettman, D.L., Fang, X.M., Garzione, C.N., and Li, J.J.: Uplift-driven climate change at 12 Ma: a long delta O-18 re-](#)

917 | [cord from the NE margin of the Tibetan plateau. *Earth and Planetary Science Letters*, 214\(1-2\), 267-277, 2003.](#)

918 | [Dowsett, H.J., Robinson, M., Haywood, A., Salzmann, U., Hill, D., Sohl, L., Chandler, M., Williams, M., Foley, K.,](#)

919 | [and Stoll, D.: The PRISM3D paleoenvironmental reconstruction. *Stratigraphy*, 7, 123–139, 2010.](#)

920 | [Egholm, D.L., Nielsen, S.B., Pedersen, V.K., Lesemann, J.: Glacial effects limiting mountain height, *Nature*, 460\(7257\).](#)

921 | [Egholm, D.L., Nielsen, S.B., Pedersen, V.K., Lesemann, J.: Glacial effects limiting mountain height, *Nature*, 460\(7257\).](#)

922 | [Egholm, D.L., Nielsen, S.B., Pedersen, V.K., Lesemann, J.: Glacial effects limiting mountain height, *Nature*, 460\(7257\).](#)

923 | [884-887, 2009.](#)

924 | Ehlers, T.A., and Poulsen, C.J.: Influence of Andean uplift on climate and paleoaltimetry estimates, *Earth and Planet-*
925 *ary Science Letters*, 281(3-4), 238-248, 2009.

926 Etheridge, D.M., Steele, L., Langenfelds, R., Francey, R., Barnola, J., and Morgan, V.: Natural and anthropogenic
927 changes in atmospheric CO₂ over the last 1000 years from air in Antarctic ice and firm, *J Geophys Res* 101:4115–
928 4128, 1996.

929

930 Etheridge, D.M., L. Steele, R. Francey, and R. Langenfelds (1998), Atmospheric methane between 1000 a.d. and
931 present: evidence of anthropogenic emissions and climatic variability. *J Geophys Res*, 103:15979–15993

932

933 Feng, R., Poulsen, C.J., Werner, M., Chamberlain, C.P., Mix, H.T., and Mulch, A.: Early Cenozoic evolution of topo-
934 graphy, climate, and stable isotopes in precipitation in the North American Cordillera, *American Journal of Science*,
935 313(7), 613–648, 2013.

936 | [Feng, R., Poulsen, C.J., Werner, M., 2016. Tropical circulation intensification and tectonic extension recorded](#)
937 [by Neogene terrestrial d18O records of the western United States. *Geology* 44. doi:10.1130/G38212.1](#)
938

939 | [Feng, R., Poulsen, C.J., 2016. Refinement of Eocene lapse rates, fossil-leaf altimetry, and North American](#)
940 [Cordilleran surface elevation estimates. *Earth Planet. Sci. Lett.* doi:10.1016/j.epsl.2015.12.022](#)
941

942 | [Fritz, S. C., Baker, P. A., Lowenstein, T. K., Seltzer, G. O., Rigsby, C. A., Dwyer, G. S., Tapia, P. M., Arnold,](#)
943 [K. K., Ku, T. L., and Luo, S: Hydrologic variation during the last 170,000 years in the southern hemisphere](#)
944 [tropics of South America, *Quaternary Res.*, 61, 95 – 104, doi:10.1016/j.yqres.2003.08.007, 2004.](#) Gasse, F.,
945 Arnold, M., Fontes, J. C., Fort, M., Gibert, E., Huc, A., Li, B., Li, Y., Liu, Q., Melleres, F., Van Campo, E.,
946 Wang, F., and Zhang, Q.: A 13,000-year climate record from western Tibet, *Nature*, 353, 742-745,
947 [doi:10.1016/j.quaint.2006.02.001, 1991.](#)

948 | [Gayo E. M., Latorre, C., Santoro, C. M., Maldonado, A., and De Pol-Holz, R.: Hydroclimate variability in the](#)
949 [low-elevation Atacama Desert over the last 2500 yr, *Clim. Past*, 8, 287-306, doi:10.5194/cp-8-287-2012,](#)
950 [2012.](#)

951 | Gierz, P., Lohmann, G., and Wei, W.: Response of Atlantic Overturning to future warming in a coupled atmosphere-
952 ocean-ice sheet model, *Geophysical Research Letters*, 42, 6811-6818, doi:10.1002/2015GL065276, 2015.

953 | [Gilli, A., Ariztegui, D., Bradbury, J. P., Kelts, K. R., Markgraf, V., and McKenzie, J. A.: Tracking abrupt cli-](#)
954 [mate change in the Southern Hemisphere: a seismic stratigraphic study of Lago Cardiel, Argentina](#)
955 [\(49°S\). *Terra Nova*, 13, 443-448. doi:10.1046/j.1365-3121.2001.00377.x , 2001.](#)

956 Glotzbach, C., van der Beek, P., Carcaillet, J., and Delunel, R.: Deciphering the driving forces of erosion rates on mil-
957 lennial to million-year timescales in glacially impacted landscapes: An example from the Western Alps, *Journal of*
958 *Geophysical Research: Earth Surface*, 118, 1491-1515, 2013.

959 Gong, X., Knorr, G., Lohmann, G., and Zhang, X.: Dependence of abrupt Atlantic meridional ocean circulation changes
960 on climate background states, *Geophysical Research Letters*, 40 (14), 3698-3704, doi:10.1002/grl.50701, 2013.

961 | [Grosjean, M., Van Leeuwen, J., Van der Knaap, W., Geyh, M., Ammann, B., Tanner, W., Messerli, B.,](#)

962 [Núñez, L., Valero-Garcés, B., and Veit, H. : A 22,000 14C year BP sediment and pollen record of climate](#)
963 [change from Laguna Miscanti \(23°S\), northern Chile, *Global Planet. Change*, 28, 35–51, doi:10.1016/](#)
964 [S0921-8181\(00\)00063-1, 2001.](#)

965 Gysels, G., Poesen, J., Bochet, E., and Li, Y.: Impact of plant roots on the resistance of soils to erosion by water: a re-
966 view, *Progress in Physical Geography*, 29, 189–217. <http://doi.org/10.1191/0309133305pp443ra>, 2005.

967 [Hansen, B. C. S., Seltzer, G. O., and Wright Jr., H.E.: Late Quaternary vegetational change in the central](#)
968 [Peruvian Andes, *Palaeogeogr. Palaeocl.*, 109, 263–285, doi:10.1016/0031-0182\(94\)90179-1, 1994.](#)

969 Harris, I., Jones, P.D., Osborn, T.J., and Lister, D.H.: Updated high-resolution grids of monthly climatic observations -
970 the CRU TS3.10 Dataset, *International Journal of Climatology*, doi:10.1002/joc.3711, 2013.

971 Harrison, S. P., Yu, G., Takahara, H., and Prentice, I. C.: Palaeovegetation - Diversity of temperate plants in east Asia.
972 *Nature* 413, 129–130, 2001.
973

974 Harrison, S.P., Bartlein, P.J., Brewer, S., Prentice, I.C., Boyd, M., Hessler, I., Holmgren, K., Izumi, K., and Willis, K.:
975 Climate model benchmarking with glacial and mid-Holocene climates, *Climate Dynamics*, 43, 671–688. doi
976 10.1007/s00382-013-1922-6, 2013.

977 Haywood, A.M., Valdes, P.J., and Sellwood, B.W.: Global scale palaeoclimate reconstruction of the middle Pliocene
978 climate using the UKMO GCM: initial results. *Global and Planetary Change*, 25 (3–4), 239–256, 2000.

979 Haywood, A.M., Dowsett, H.J., Otto-Bliesner, B., Chandler, M.A., Dolan, A.M., Hill, D.J., Lunt, D.J., Robinson, M.M.,
980 Rosenbloom, N., Salzmann, U., and Sohl, L.E.: Pliocene Model Intercomparison Project (PlioMIP): experimental
981 design and boundary conditions (Experiment 1), *Geoscientific Model Development* (3), 227–242, 2010.
982

983 Haywood, A.M., Hill, D.J., Dolan, A.M., Otto-Bliesner, B., Bragg, F., Chan, W.-L., Chandler, M.A., Contoux, C., Jost,
984 A., Kamae, Y., Lohmann, G., Lunt, D.J., Abe-Ouchi, A., Pickering, S.J., Ramstein, G., Rosenbloom, N.A., Sohl, L.,
985 Stepanek, C., Yan, Q., Ueda, H., and Zhang, Z.: Large-scale features of Pliocene climate: results from the Pliocene
986 Model Intercomparison Project, *Clim. Past*, 9, 191–209. doi:10.5194/cp-9-191-2013, 2013.
987

988 Herman, F., Seward, D., Valla, P.G., Carter, A., Kohn, B., Willett, S.D., and Ehlers, T.A.: Worldwide acceleration of
989 mountain erosion under a cooling climate, *Nature*, 504, 423–426. doi:10.1038/nature12877, 2013.

990 [Herzschuh, U., Kuerschner, H., and Mischke, S.: Temperature variability and vertical vegetation belt shifts](#)
991 [during the last ~50,000 yr in the Qilian Mountains \(NE margin of the Tibetan Plateau, China\), *Quaternary*](#)
992 [Res., 66, 133–146, doi:10.1016/j.yqres.2006.03.001, 2006a.](#)

993 [Herzschuh, U., Winter, K., Wuennemann, B., and Li, S.: A general cooling trend on the central Tibetan](#)
994 [Plateau throughout the Holocene recorded by the lake Zigetang pollen spectra, *Quatern. Int.*, 154, 113–](#)
995 [121, doi:10.1016/j.quaint.2006.02.005, 2006b.](#)

996
997 [Herzschuh, U., Kramer A., Mischke S., and Zhang C.: Quantitative climate and vegetation trends since the](#)
998 [late glacial on the northeastern Tibetan Plateau deduced from Koucha lake pollen spectra, *Quaternary*](#)
999 [Res., 71, 162–171, doi:10.1016/j.yqres.2008.09.003, 2009.](#)

- 1000 Hillenbrand, C.-D., and Fütterer, D.K.: Neogene to Quaternary deposition of opal on the continental rise west of the
1001 Antarctic Peninsula, ODP Leg 178, Sites 1095, 1096, and 1101. In: Barker, P.F., Camerlenghi, A., Acton, G.D.,
1002 Ramsay, A.T.S. (Eds.), Proceedings of the Ocean Drilling Programme, Scientific Results, 178. Texas A and M Uni-
1003 versity, College Station, Texas, pp. 1–40 (CD-ROM), 2002.
- 1004 [Hillyer, R., Valencia, B. G., Bush, M.B., Silman, M.R., and Steinitz-Kannan, M.: A 24,700-yr paleolimnological](#)
1005 [history from the Peruvian Andes, Quaternary Res., 71, 71-82, doi:10.1016/j.yqres.2008.06.006, 2009.](#)
- 1006 Hobley, D.E., Sinclair, H.D., and Cowie, P.A.: Processes, rates, and time scales of fluvial response in an ancient post-
1007 glacial landscape of the northwest Indian Himalaya. *Geological Society of America Bulletin*, 122, 1569-1584, 2010.
- 1008 [Hodell, D. A., Brenner, M., Kanfoush, S. L., Curtis, J. H., Stoner, J. S., Song, X., Wu, Y., and Whitmore, T. J.:](#)
1009 [Paleoclimate of southwestern China for the past 50,000 yr inferred from lake sediment records, Quatern-](#)
1010 [ary Res., 52, 369-380, doi:10.1006/qres.1999.2072, 1999.](#)
- 1011 [Hu, G., Yi, C.-L., Zhang, J.-F., Liu, J.-L., Jiang, T., and Qin, X.: Optically stimulated luminescence dating of a](#)
1012 [moraine and a terrace in Laohugou valley, western Qilian Shan, northeastern Tibet, Quaternary Interna-](#)
1013 [tional 321, 37-49, doi:10.1016/j.quaint.2013.12.019, 2014.](#)
- 1014 Insel, N., Poulsen, C.J., and Ehlers, T.A.: Influence of the Andes Mountains on South American moisture transport,
1015 convection, and precipitation, *Climate Dynamics*, 35 (7-8), 1477-1492, 2010.
- 1016 Jeffery, M.L., Ehlers, T.A., Yanites, B.J., and Poulsen, C.J.: Quantifying the role of paleoclimate and Andean Plateau
1017 uplift on river incision: PALEOCLIMATE ROLE IN RIVER INCISION, *Journal of Geophysical Research: Earth*
1018 *Surface*, 118(2), 852–871, doi:10.1002/jgrf.20055, 2013.
- 1019 [Jenny, B., Valero-Garces, B. L., Urrutia, R., Kelts, K., Veit, H., and Geyh, M.: Moisture changes and](#)
1020 [fluctuations of the Westerlies in Mediterranean Central Chile during the last 2000 years: The Laguna](#)
1021 [Aculeo record \(33°50' S\), Quatern. Int., 87, 3-18, doi:10.1016/S1040-6182\(01\)00058-1, 2002a.](#)
- 1022 [Jenny, B., Valero-Garcés, B.L., Villa-Martínez, R., Urrutia, R., Geyh, M. A., and Veit, H.: Early to Mid-Holo-](#)
1023 [cene Aridity in Central Chile and the Southern Westerlies: The Laguna Aculeo Record \(34°S\), Quaternary](#)
1024 [Res., 58, 160–170, doi:10.1006/qres.2002.2370, 2002b.](#)
- 1025 Jungclauss, J. H., Lorenz, S. J., Timmreck, C., Reick, C. H., Brovkin, V., Six, K., Segschneider, J., Giorgetta, M.A.,
1026 Crowley, T.J., Pongratz, J., Krivova, N.A., Vieira, L.E., Solanki, S.K., Klocke, D., Botzet, M., Esch, M., Gayler,
1027 V., Haak, H., Raddatz, T.J., Roeckner, E., Schnur, R., Widmann, H., Claussen, M., Stevens, B., and Marotzke, J.:
1028 Climate and carbon-cycle variability over the last millennium. *Climate of the Past*, 6, 723-737. doi:10.5194/cp-6-723-
1029 2010, 2010.
- 1030 [Junginger, A., Roller, S., Olaka, L. A., and Trauth, M. H.: The effects of solar irradiation changes on the mi-](#)
1031 [gration of the Congo Air Boundary and water levels of paleo-Lake Suguta, Northern Kenya Rift, during the](#)
1032 [African Humid Period \(15–5 ka BP\), Palaeogeogr. Palaeoclimatol., 396, 1-16, doi:10.1016/](#)
1033 [j.palaeo.2013.12.007, 2014.](#)
- 1034 [Kaiser, J., Schefuss, E., Lamy, F., Mohtadi, M., and Hebbeln, D.: Glacial to Holocene changes in sea surface](#)
1035 [temperature and coastal vegetation in north central Chile : high versus low latitude forcing, Quaternary](#)

1036 | [Sci. Rev., 27, 2064–2075, doi:10.1016/j.quascirev.2008.08.025, 2008.](#)

1037 Kalnay, E., Kanamitsu, M., Kistler, R., Collins, W., Deaven, D., Gandin, L., Iredell, M., Saha, S., White, G., Woollen,
 1038 J., Zhu, Y., Chelliah, M., Ebisuzaki, W., Higgins, W., Janowiak, J., Mo, K.C., Ropelewski, C., Wang, J., Leetmaa,
 1039 A., Reynolds, R., Jenne, R., and Joseph, D.: The NCEP/NCAR 40-year reanalysis project. *Bulletin of the American*
 1040 *Meteorological Society*, 77(3), 437–471, 1996.

1041 [Kashiwaya, K., Masuzawa, T., Morinaga, H., Yaskawa, K., Yuan, B. Y., Liu, J. Q., and Gu, Z.: Changes in](#)
 1042 [hydrological conditions in the central Qing-Zang \(Tibetan\) Plateau inferred from lake bottom sediments.](#)
 1043 [Earth Planet. Sc. Lett., 135, 31–39, doi:10.1016/0012-821X\(95\)00136-Z, 1995.](#)

1044 [Kent-Corson, M., Sherman, L., Mulch, A. and Chamberlain, C.: Cenozoic topographic and climatic response](#)
 1045 [to changing tectonic boundary conditions in Western North America, Earth Planet. Sc. Lett., 252\(3–4\),](#)
 1046 [453–466, doi:10.1016/j.epsl.2006.09.049, 2006.](#)

1047 Kistler, R., Collins, W., Saha, S., White, G., Woollen, J., Kalnay, E., Chelliah, M., Ebisuzaki, W., Kanamitsu, M.,
 1048 Kousky, V., Van den Dool, H., Jenne, R., and Fiorino, M.: The NCEP–NCAR 50–Year Reanalysis: Monthly Means
 1049 CD–ROM and Documentation. *Bulletin of the American Meteorological Society*, 82(2), 247–267, 2001.

1050 Kirchner, J.W., Finkel, R.C., Riebe, C.S., Granger, D.E., Clayton, J.L., King, J.G., and Megahan, W.F.: Mountain
 1051 erosion over 10 yr, 10 k.y., and 10 m.y. time scales, *Geology*, 29 (7), 591–594, 2001.

1052 Knorr, G., Butzin, M., Micheels, A., and Lohmann, G.: A Warm Miocene Climate at Low Atmospheric CO₂ levels.
 1053 *Geophysical Research Letters*, 38, L20701, doi:10.1029/2011GL048873, 2011.

1054 Koons, P.O., Zeitler, P.K., and Hallet, B.: 5.14 Tectonic Aneurysms and Mountain Building, in *Treatise on Geomor-*
 1055 *phology*, pp. 318–349, Elsevier, 2013.

1056 [Kotlia, B. S., Sharma, C., Bhalla, M. S., Rajagopalan, G., Subrahmanyam, K., Bhattacharya, A., and](#)
 1057 [Valdiya, K. S.: Paleoclimatic conditions in the late Pleistocene Wadda Lake, eastern Kumaun Himalaya](#)
 1058 [\(India\), Palaeogeogr. Palaeocl., 162, 105–118, doi:10.1016/S0031-0182\(00\)00107-3, 2000.](#)

1059 [Kramer, A., Herzs Schuh, U., Mischke, S., and Zhang, C.: Late glacial vegetation and climate oscillations on](#)
 1060 [the southeastern Tibetan Plateau inferred from the lake Naleng pollen profile, Quaternary Res., 73, 324–](#)
 1061 [335, doi:10.1016/j.yqres.2009.12.003, 2010.](#)

1062 Kraus, H.: Die Atmosphäre der Erde. Eine Einführung in die Meteorologie. Berlin, 2001.

1063 Kutzbach, J.E., Guetter, P.J., Ruddiman, W.F., and Prell, W.L.: Sensitivity of Climate to Late Cenozoic Uplift in
 1064 Southern Asia and the American West - Numerical Experiments, *Journal of Geophysical Research-Atmospheres*,
 1065 94(D15), 18393–18407, 1989.

1066 Kutzbach, J.E., Prell, W.L., and Ruddiman, W.F.: Sensitivity of Eurasian Climate to Surface Uplift of the Tibetan Plat-
 1067 eau, *Journal of Geology*, 101(2), 177–190, 1993.

1068 | [Lamy, F. and Kaiser, J.: Past Climate Variability in South America and Surrounding Regions, Chapter 6:](#)

1069 | [Glacial to Holocene Paleoceanographic and Continental Paleoclimate Reconstructions Based on ODP](#)
1070 | [Site 1233/GeoB 3313 Off southern Chile, 2009.](#)

1071 | [Lamy, F., Hebbeln, D., and Wefer, G.: High Resolution Marine Record of Climatic Change in Mid-latitude](#)
1072 | [Chile during the Last 28,000 Years Based on Terrigenous Sediment Parameters, *Quaternary Res.*, 51,](#)
1073 | [83-93, doi:10.1006/qres.1998.2010, 1999.](#)

1074 | [Lamy, F., Klump, J., Hebbeln, D., and Wefer, G.: Late Quaternary rapid climate change in northern Chile,](#)
1075 | [Terra Nova, 12, 8-13, doi:10.1046/j.1365-3121.2000.00265.x, 2000.](#)

1076 | [Lamy, F., Rühlemann, C., Hebbeln, D. and Wefer, G.: High- and low-latitude climate control on the position](#)
1077 | [of the southern Peru-Chile Current during the Holocene, *Paleoceanography*, 17, 16-1-16-10,](#)
1078 | [doi:10.1029/2001PA000727, 2002.](#)

1079 | [Latorre, C., Betancourt, J., Rylander, K., and Quade, J.: Vegetation invasions into absolute desert: A 45 000](#)
1080 | [yr rodent midden record from the Calama-Salar de Atacama basins, northern Chile \(lat 22° - 24°S\), *Geol.*](#)
1081 | [Soc. Am. Bull., 114, 349-366, doi:10.1130/0016-7606\(2002\)114<0349:VIIADA>2.0.CO;2, 2002.](#)

1082 | [Latorre, C., Betancourt, J.L., Rylander, K.A., Quade, J., and Matthei, O.: A vegetation history from the arid](#)
1083 | [prepuna of northern Chile \(22-23°S\) over the last 13500 years, *Palaeogeogr. Palaeocl.*, 194, 223-246,](#)
1084 | [doi:10.1016/S0031-0182\(03\)00279-7, 2003.](#)

1085 | [Latorre, C., Betancourt, J.L., and Arroyo, M.T.K.: Late Quaternary vegetation and climate history of a peren-](#)
1086 | [nial river canyon in the Río Salado basin \(22°S\) of northern Chile, *Quaternary Res.*, 65, 450-466,](#)
1087 | [doi:10.1016/j.yqres.2006.02.002, 2006.](#)

1088 | [Lechler, A. and Niemi, N.: Sedimentologic and isotopic constraints on the Paleogene paleogeography and](#)
1089 | [paleotopography of the southern Sierra Nevada, California, *Geology*, 39\(4\), 379-382,](#)
1090 | [doi:10.1130/g31535.1, 2011.](#)

1091 | [Lechler, A., Niemi, N., Hren, M. and Lohmann, K.: Paleoelevation estimates for the northern and central](#)
1092 | [proto-Basin and Range from carbonate clumped isotope thermometry, *Tectonics*, 32\(3\), 295-316,](#)
1093 | [doi:10.1002/tect.20016, 2013.](#)

1094 | Lease, R.O., and Ehlers, T.A.: Incision into the Eastern Andean Plateau During Pliocene Cooling, *Science*, 341(6147),
1095 | 774-776, doi:10.1126/science.1239132, 2013.

1096 | Legates, D.R., and Willmott, C.J.: Mean Seasonal and Spatial Variability in Gauge-Corrected, Global Precipitation, *In-*
1097 | *ternational Journal of Climatology* 10(2), 111-127. doi: 10.1002/joc.3370100202, 1990.

1098 | Li, J., Ehlers, T.A., Werner, M., Mutz, S.G., Steger, C., Paeth, H.: Late quaternary climate, precipitation $\delta^{18}\text{O}$, and In-
1099 | dian monsoon variations over the Tibetan Plateau. *Earth and Planetary Science Letters* 457, 412-422, 2017.

1100 | [Liu, X., Colman, S. M., Brown, E. T., An, Z., Zhou, W., Jull, A. J. T., Huang, Cheng, Y., P., Liu, W., and Xu,](#)
1101 | [H.: A climate threshold at the eastern edge of the Tibetan plateau, *Geophys. Res. Lett.*, doi:](#)
1102 | [10.1002/2014GL060833, 2014.](#)

1103 | [Licht, A., Quade, J., Kowler, A., de los Santos, M., Hudson, A., Schauer, A., Huntington, K., Copeland, P.](#)
1104 | [and Lawton, T.: Impact of the North American monsoon on isotope paleoaltimeters: Implications for the](#)
1105 | [paleoaltimetry of the American southwest, *Am. J. Scie*, 317\(1\), 1-33, doi:10.2475/01.2017.01, 2017.](#)

1106 Lohmann, G., Pfeiffer, M., Laepple, T., Leduc, G., and Kim, J.-H.: A model-data comparison of the Holocene global
1107 sea surface temperature evolution. *Clim. Past*, 9, 1807-1839, doi:10.5194/cp-9-1807-2013, 2013.
1108

1109 Lorenz, S.J., and Lohmann, G.: Acceleration technique for Milankovitch type forcing in a coupled atmosphere-ocean
1110 circulation model: method and application for the Holocene. *Climate Dynamics* (2004) 23: 727. doi:10.1007/
1111 s00382-004-0469-y, 2004.
1112

1113 [Maldonado, A. and Villagrán, C.: Climate variability over the last 9900 cal yr BP from a swamp forest pollen
1114 record along the semiard coast of Chile, *Quaternary Res.*, 66, 146-258, doi:10.1016/j.yqres.2006.04.003,
1115 2006.](#)

1116 [Maldonado, A. J., Betancourt, J. L., Latorre, C., and Villagrán, C.: Pollen analyses from a 50000-yr rodent
1117 midden series in the southern Atacama Desert \(25°30' S\), *J. Quaternary Sci.*, 20, 493-507,
1118 doi:10.1002/jqs.936, 2005.](#)

1119 [Maldonado, A., Méndez, C., Ugalde, P., Jackson, D., Seguel, R., and Latorre, C.: Early Holocene climate
1120 change and human occupation along the semiarid coast of north-central Chile, *J. Quaternary Sci.*, 25,
1121 985–988, doi:10.1002/jqs.1385, 2010.](#)

1122 [Markgraf, V., Bradbury, J. P., Schwalb, A., Burns, S., Stern, C., Ariztegui, D., Gilli, D., Anselmetti, F. S.,
1123 Stine, S., and Maidana, N.: Holocene palaeoclimates of southern Patagonia: limnological and
1124 environmental history of Lago Cardiel, Argentina, *Holocene*, 13, 581–591,
1125 doi:10.1191/0959683603hl648rp, 2003.](#)

1126 [Markgraf, V., Whitlock, C., and Haberle, S.: Vegetation and fire history during the last 18,000 cal yr B.P. in
1127 Southern Patagonia: Mallín Pollux, Coyhaique, Province Aisén \(45°41'30" S, 71°50'30" W, 640 m
1128 elevation\), *Palaeogeogr. Palaeocl.*, 254, 492–507, doi:10.1016/j.palaeo.2007.07.008, 2007.](#)

1129 [Maroon, E. A., Frierson, D. M. W., and Battisti, D. S.: The tropical precipitation response to Andes
1130 topography and ocean heat fluxes in an aquaplanet model, *J. Climate*, 28, 381–398, doi:10.1175/JCLI-D-
1131 14-00188.1, 2015.](#)

1132 [Maroon, E. A., Frierson, D. M. W., Kang, S. M., and Scheff, J.: The precipitation response to an idealized
1133 subtropical continent, *J. Climate*, 29, 4543–4564, doi:10.1175/JCLI-D-15-0616.1, 2016.](#)

1134 Marshall, J.A., Roering, J.J., Bartlein, P.J., Gavin, D.G., Granger, D.E., Rempel, A.W., Praskievicz, S.J., and Hales,
1135 T.C.: Frost for the trees: Did climate increase erosion in unglaciated landscapes during the late Pleistocene? *Science
1136 Advances*, 1, 1-10, 2015.

1137 Marston, R.A.: Geomorphology and vegetation on hillslopes: Interactions, dependencies, and feedback loops, *Geomor-
1138 phology*, 116(3–4), 206–217. doi:http://doi.org/10.1016/j.geomorph.2009.09.028, 2010.

1139 Matsuoka, N., and Murton, J.: Frost weathering: Recent advances and future directions. *Permafr. Periglac. Process.* 19,
1140 195–210, 2008.

1141 Matsuoka, N.: Solifluction rates, processes and landforms: A global review. *Earth Science Reviews* 55, 107–134, 2001.

1142 Maussion, F., Scherer, D., Mölg, T., Collier, E., Curio, J., and Finkelnburg, R.: Precipitation seasonality and variability
1143 over the Tibetan Plateau as resolved by the High Asia Reanalysis, *J. Climate*, 27, 1910-1927, doi:10.1175/JCLI-D-
1144 13-00282.1, 2014

1145 [Méndez, C., Gil, A., Neme, G., Nuevo Delaunay, A., Cortegoso, V., Huidobro, C., Durán, and Maldano, A.:
1146 Mid Holocene radiocarbon ages in the Subtropical Andes \(~29° - 35° S\), climatic change an implicaton for
1147 human space organization, *Quatern. Int.*, 356, 15-26, doi:10.1016/j.quaint.2014.06.059, 2015.](#)

1148 Mesinger, F., DiMego, G., Kalnay, E., Mitchell, K., Shafran, P.C., Ebisuzaki, W., Jovic, D., Woollen, J., Rogers, E.,
1149 Berbery, E.H., Ek, M.B., Fan, Y., Grumbine, R., Higgins, W., Li, H., Lin, Y., Manikin, G., Parrish, D., and Shi, W.:
1150 North American Regional Reanalysis, *Bulletin of the American Meteorological Society*, 87, 343–
1151 360.[doi:10.1175/BAMS-87-3-343](https://doi.org/10.1175/BAMS-87-3-343), 2006.

1152 [Methner, K., Fiebig, J., Wacker, U., Umhoefer, P., Chamberlain, C. and Mulch, A.: Eocene-Oligocene proto-](#)
1153 [Cascades topography revealed by clumped \(\$\Delta 47\$ \) and oxygen isotope \(\$\delta 18\text{O}\$ \) geochemistry \(Chumstick](#)
1154 [Basin, WA, USA\), *Tectonics*, 35\(3\), 546-564, \[doi:10.1002/2015tc003984\]\(https://doi.org/10.1002/2015tc003984\), 2016.](#)

1155 [Mischke S., Kramer M., Herzsich U., Shang H., Erzinger J., and Zhang C.: Reduced early holocene](#)
1156 [moisture availability in the Bayan Har Mountains, northeastern Tibetan Plateau, inferred from a multi-](#)
1157 [proxy lake record, *Palaeogeogr. Palaeoclimatol.*, 267, 59-76, \[doi:10.1016/j.palaeo.2008.06.002\]\(https://doi.org/10.1016/j.palaeo.2008.06.002\), 2008.](#)

1158 Molnar, P., Boos, W.R., and Battisti, D.S.: Orographic Controls on Climate and Paleoclimate of Asia: Thermal and
1159 Mechanical Roles for the Tibetan Plateau, *Annual Review of Earth and Planetary Sciences*, 38, 77-102, 2010.

1160 Molnar, P., and England, P.: Late Cenozoic uplift of mountain ranges and global climate change: chicken or egg?,
1161 *Nature*, 346, 29-34, 1990.

1162 Montgomery, D.R.: Slope distributions, threshold hillslopes, and steady-state topography, *American Journal of Science*,
1163 301, 432-454, 2001.

1164 Montgomery, D.R., Balco, G., and Willett, S.D.: Climate, tectonics, and the morphology of the Andes, *Geology*, 29(7),
1165 579-582, 2001.

1166 Moon, S., Chamberlain, C.P., Blisniuk, K., Levine, N., Rood, D.H., Hilley, G.E.: Climatic control of denudation in the
1167 deglaciated landscape of the Washington Cascades, *Nature Geoscience*, 4, 469-473, 2011.

1168 [Moreno, A., Santoro, C. M., and Latorre, C.: Climate change and human occupation in the northernmost](#)
1169 [Chilean Altiplano over the last ca. 11500 cal. a BP, *Quaternary Sci.*, 24, 373–382, \[doi:10.1002/jqs.1240\]\(https://doi.org/10.1002/jqs.1240\),](#)
1170 [2009.](#)

1171 [Morinaga, H., Itota, C., Isezaki, N., Goto, H., Yaskawa, K., Kusakabe, M., Liu, J., Gu, Z., Yuan, B., and Cong,](#)
1172 [S.: Oxygen-18 and carbon-13 records for the last 14,000 years from lacustrine carbonates of Siling-Co](#)
1173 [\(lake\) in the Qinghai-Tibetan Plateau, *Geophys. Res. Lett.*, 20, 2909-2912, \[doi:10.1029/93GL02982\]\(https://doi.org/10.1029/93GL02982\),](#)
1174 [1993.](#)

1175 [Morrill, C., Overpeck, J. T., Cole, J. E., Liu, K., Shen, C., and Tang, L.: Holocene variations in the Asian mon-](#)
1176 [soon inferred from the geochemistry of lake sediments in central Tibet, *Quaternary Res.*, 65, 232-243,](#)
1177 [doi:10.1016/j.yqres.2005.02.014, 2006.](#)

1178 Moulton, K.L., and Berner, R.A.: Quantification of the effect of plants on weathering: studies in Iceland, *Geology*, 26,
1179 895-898, 1998.

1180 [Muegler, I., Gleixner, G., Guenther, F., Maeusbacher, R., Daut, G., Schuett, B., Berking, J., Schwalb, A.,](#)
1181 [Schwark, L., Xu, B., Yao, T., Zhu, L., and Yi, C.: A multi-proxy approach to reconstruct hydrological](#)
1182 [changes and Holocene climate development of Nam Co, Central Tibet, *J. Paleolimnol.*, 43, 625-648,](#)
1183 [doi:10.1007/s10933-009-9357-0, 2010.](#)

1184 [Mujica, M. I., Latorre, C., Maldonado, A., González-Silvestre, L., Pinto, R., De Pol-Holz, R., and Santoro, C.](#)
1185 [M.: Late Quaternary climate change, relict populations and present-day refugia in the northern Atacama](#)
1186 [Desert: a case study from Quebrada La Higuera \(18° S\), J. Biogeogr. , 42, 76–88, doi:10.1111/jbi.12383,](#)
1187 [2015.](#)

1188 [Mulch, A., Sarna-Wojcicki, A., Perkins, M. and Chamberlain, C.: A Miocene to Pleistocene climate and](#)
1189 [elevation record of the Sierra Nevada \(California\), P. Natl. Acad. Sci. USA, 105\(19\), 6819-6824,](#)
1190 [doi:10.1073/pnas.0708811105, 2008.](#)

1191 [Mulch, A., Chamberlain, C., Cosca, M., Teyssier, C., Methner, K., Hren, M. and Graham, S.: Rapid change in](#)
1192 [high-elevation precipitation patterns of western North America during the Middle Eocene Climatic Op-](#)
1193 [timum \(MECO\), Am. J. Scie, 315\(4\), 317-336, doi:10.2475/04.2015.02, 2015.](#)

1194

1195 Mutz, S.G., Ehlers, T.A., Li, J., Steger, C., Peath, H., Werner, M., Poulsen, C.J.: Precipitation $\delta^{18}\text{O}$ over the South Asia
1196 Orogen from ECHAM5-wiso Simulation: Statistical Analysis of Temperature, Topography and Precipitation.
1197 *Journal of Geophysical Research-Atmospheres*, 121(16),9278-9300, doi: 10.1002/2016JD024856, 2016.

1198 [Nishimura, M., Matsunaka, T., Morita, Y., Watanabe, T., Nakamura, T., Zhu, L., Nara, W. F., Imai, A., Izutsu,](#)
1199 [Y., and Hasuike, N.: Paleoclimatic changes on the southern Tibetan Plateau over the past 19,000 years](#)
1200 [recorded in lake Pumoyum Co. and their implications for the southwest monsoon evolution, Palaeogeogr.](#)
1201 [Palaeocl., 396, 75-92, doi:10.1016/j.palaeo.2013.12.015, 2014.](#)

1202 Otto-Bliesner, B.L., Brady, C.B., Clauzet, G., Tomas, R., Levis, S., and Kothavala, Z.: Last Glacial Maximum and
1203 Holocene Climate in CCSM3. *Journal of Climate*, 19, 2526-2544, 2006.

1204 Paeth, H.: Key Factors in African Climate Change Evaluated by a Regional Climate Model, *Erdkunde*, 58, 290-315,
1205 2004.

1206 [Peel, M.C., Finlayson, B.L., McMahon, T.A.: Updated world map of the Koppen- Geiger climate classification.](#)
1207 [Hydrol. Earth Syst. Sci. 11, 1633–1644, 2007.](#)

1208

1209 Pfeiffer, M., and Lohmann, G.: Greenland Ice Sheet influence on Last Interglacial climate: global sensitivity studies
1210 performed with an atmosphere-ocean general circulation model. *Climate of the Past*, 12, pp. 1313-1338,
1211 doi:10.5194/cp-12-1313-2016, 2016.

1212 Pickett, E.J., Harrison, S.P., Flenley, J., Grindrod, J., Haberle, S., Hassell, C., Kenyon, C., MacPhail, M., Martin, H.,
1213 Martin, A.H., McKenzie, M., Newsome, J.C., Penny, D., Powell, J., Raine, J.I., Southern, W., Stevenson, J., Sutra,
1214 J.-P., Thomas, I., van der Kaars, S., Ward, J.: Pollen-based reconstructions of biome distributions for Australia,
1215 South-East Asia and the Pacific (SEAPAC region) at 0, 6000 and 18,000 14C years B.P.. *Journal of Biogeography*,
1216 31, 1381–1444, doi: 10.1111/j.1365-2699.2004.01001.x, 2004.

1217

1218 [Pingel, H., Mulch, A., Alonso, R., Cottle, J., Hynek, S., Poletti, J., Rohrmann, A., Schmitt, A., Stockli, D. and](#)
1219 [Strecker, M.: Surface uplift and convective rainfall along the southern Central Andes \(Angastaco Basin,](#)
1220 [NW Argentina\), Earth Planet. Sc. Lett., 440, 33-42, doi:10.1016/j.epsl.2016.02.009, 2016.](#)

1221

1222 Prentice, I. C., Jolly, D., and BIOME 6000 Participants. (2000). Mid-Holocene and glacial-maximum vegetation geo-
1223 graphy of the northern continents and Africa. *Journal of Biogeography* 27, 507-519.

- 1224
- 1225 [Pueyo, J. J., Sáez, A., Giralt, S., Valero-Garcés, B.L., Moreno, A., Bao, R., Schwalb, A., Herrera, C., Klo-](#)
- 1226 [sowska, B., and Taberner, C.: Carbonate and organic matter sedimentation and isotopic signatures in](#)
- 1227 [Lake Chungará, Chilean Altiplano, during the last 12.3 kyr, *Palaeogeogr. Palaeocl.*, 307, 339-355,](#)
- 1228 [doi:10.1016/j.palaeo.2011.05.036, 2011.](#)
- 1229 [Quade, J., Rech, J. A., Betancourt, J. L., Latorre, C., Quade, B., Rylander, K. A., and Fisher, T.: Paleowet-](#)
- 1230 [lands and regional climate change in the central Atacama Desert, northern Chile, *Quaternary Res.*, 69,](#)
- 1231 [343-360, doi:10.1016/j.yqres.2008.01.003, 2008.](#)
- 1232 Raymo, M.E., and Ruddiman, W.F.: Tectonic forcing of late cenozoic climate. *Nature*, 359(6391), 117-122, 1992.
- 1233 [Rech, J. A., Pigati, J. S., Quade, J., and Betancourt, J. L.: Re-evaluation of mid-Holocene deposits at](#)
- 1234 [Quebrada Puripica, northern Chile, *Palaeogeogr. Palaeocl.*, 194, 207-222, doi:0.1016/S0031-](#)
- 1235 [0182\(03\)00278-5, 2003.](#)
- 1236 Robinson, M.M.: New quantitative evidence of extreme warmth in the Pliocene Arctic, *Stratigraphy* 6, 265–275, 2009.
- 1237 Roeckner, E., Bäuml, G., Bonaventura, L., Brokopf, R., Esch, M., Giorgetta, M., Hagemann, S., Kirchner, I., Korn-
- 1238 blueh, L., Manzini, E., Rhodin, A., Schlese, U., Schulzweida, U., and Tompkins, A.: The atmospheric general circu-
- 1239 lation model ECHAM5. Part I: Model description. Rep. 349Rep., 127 pp, Max Planck Institute for Meteorology,
- 1240 Hamburg, 2003.
- 1241 Roering, J.J., Marshall, J., Booth, A.M., Mort, M., and Jin, Q.: Evidence for biotic controls on topography and soil pro-
- 1242 duction, *Earth and Planetary Science Letters*, 298(1–2), 183–190, doi:10.1016/j.epsl.2010.07.040, 2010.
- 1243 Salzmann, U., Williams, M., Haywood, A.M., Johnson, A.L.A., Kender, S., and Zalasiewicz, J.: Climate and environ-
- 1244 ment of a Pliocene warm world. *Palaeogeography, Palaeoclimatology, Palaeoecology*, 309 (1-8), 2011.
- 1245 [Sarnthein, M.: Sand deserts during glacial maximum and climatic optimum, *Nature*, 272, 43–46,](#)
- 1246 [doi:10.1038/272043a0, 1978.](#)
- 1247 Sarnthein, M., Gersonde, R., Niebler, S., Pflaumann, U., Spielhagen, R., Thiede, J., Wefer, G., Weinelt, M.: Overview
- 1248 of Glacial Atlantic Ocean Mapping (GLAMAP 2000), *Paleoceanography*, 18(2), doi:10.1029/2002PA000769,
- 1249 2003.
- 1250 Schäfer-Neth C., and Paul, A.: The Atlantic Ocean at the last glacial maximum: objective mapping of the GLAMAP
- 1251 sea-surface conditions. In: Wefer G, Mulitza S, Ratmeyer V (eds) *The South Atlantic in the late quaternary: recon-*
- 1252 *struction of material budgets and current systems.* Springer, Berlin, pp 531–548, 2003.
- 1253 Schaller, M., von Blanckenburg, F., Veldkamp, A., Tebbens, L.A., Hovius, N., and Kubik, P.W.: A 30 000 yr record of
- 1254 erosion rates from cosmogenic ¹⁰Be in Middle European river terraces, *Earth and Planetary Science Letters*,
- 1255 204(1), 307–320, 2002.
- 1256 Schaller, M., and Ehlers T.A.: Limits to quantifying climate driven changes in denudation rates with cosmogenic radio-
- 1257 nuclides, *Earth and Planetary Science Letters*, v. 248, pp. 153-167. doi:10.1016/j.epsl.2006.05.027, 2006.

1258 [Schwalb, A., Burns, S., and Kelts, K.: Holocene environments from stable isotope stratigraphy of ostracods](#)
1259 [and authigenic carbonate in Chilean Altiplano Lakes, *Palaeogeogr. Palaeoclimatol.*, 148, 153-168, doi:10.1016/](#)
1260 [S0031-0182\(98\)00181-3, 1999.](#)

1261 [Shen J., Liu X. Q., Wang S. M., and Matsumoto R.: Palaeoclimatic changes in the Qinghai Lake area during](#)
1262 [the last 18,000 years, *Quatern. Int.*, 136, 131-140, doi:10.1016/j.quaint.2004.11.014, 2005.](#)

1263 [Shen C., Liu K., Tang L., and Overpeck J. T.: Quantitative relationships between modern pollen rain and cli-](#)
1264 [mate in the Tibetan Plateau. *Rev. Palaeobot. Palynol.*, 140, 61–77, doi:10.1016/j.revpalbo.2006.03.001,](#)
1265 [2006.](#)

1266 [Siani, G., Colin, C., Michel, E., Carel, M., Richter, T., Kissel, C., and Dewilde, F.: Late Glacial to Holocene](#)
1267 [terrigenous sediment record in the Northern Patagonian margin: Paleoclimate implications, *Palaeogeogr.*](#)
1268 [Palaeoclimatol.](#), 297, 26-36, doi:10.1016/j.palaeo.2010.07.011, 2010.

1269 Simmons, A.J., Burridge, D.M., Jarraud, M., Girard, C., and Wergen, W.: The ECMWF Medium-Range prediction
1270 models development of the numerical formulations and the impact of increased resolution, *Meteorology and Atmo-*
1271 *spheric Physics*, 40(1-3), 28-60, 1989.

1272 Sohl, L.E., Chandler, M.A., Schmunk, R.B., Mankoff, K., Jonas, J.A., Foley, K.M., and Dowsett, H.J.: PRISM3/GISS
1273 topographic reconstruction, *U.S. Geological Survey Data Series*, 419, 6p., 2009.

1274

1275 Sowers T., Alley, R.B., and Jubenville, J.: Ice core records of atmospheric N₂O covering the last 106,000 years. *Sci-*
1276 *ence*, 301:945–948, 2003.

1277

1278 Stepanek, C., and Lohmann, G.: Modelling mid-Pliocene climate with COSMOS , *Geosci. Model Dev.* , 5 , pp. 1221-
1279 1243 . doi:10.5194/gmd-5-1221-2012, 2012.

1280 [Stine, S. and Stine M.: A record from Lake Cardiel of climate change in southern South America, *Nature*,](#)
1281 [345, 705-708, doi:10.1038/345705a0,1990.](#)

1282 [Szeicz, J. M., Haberle, S. G., and Bennett, K. D.: Dynamics of North Patagonian rainforests from fine-resolu-](#)
1283 [tion pollen, charcoal and tree-ring analysis, *Chonos Archipelago, Southern Chile, Austral Ecol.*, 28, 413–](#)
1284 [422, doi:10.1046/j.1442-9993.2003.01299.x , 2003.](#)

1285 Takahashi, K., and Battisti, D.: Processes controlling the mean tropical pacific precipitation pattern. Part I: The Andes
1286 and the eastern Pacific ITCZ. *Journal of Climate*, 20(14), 3434-3451, 2007a.

1287 Takahashi, K., and Battisti, D.: Processes controlling the mean tropical pacific precipitation pattern. Part II: The SPCZ
1288 and the southeast pacific dry zone. *Journal of Climate*, 20(23), 5696-5706, 2007b.

1289 [Tang, L., Shen, S., Liu, K., and Overpeck, J. T.: Changes in south Asian monsoon: new high-resolution pa-](#)
1290 [leoclimatic records from Tibet, China, *Chinese Sci. Bull.*, 45, 87-91, doi:10.1007/BF02884911, 2000.](#)

1291 Thiede, R.C., and Ehlers, T.A.: Large spatial and temporal variations in Himalayan denudation. *Earth and Planetary*
1292 *Science Letters*, 374, 256-257. doi:10.1016/j.epsl.2013.03.004, 2013.

- 1293 Thomas, A.: The climate of the Gongga Shan range, Sichuan Province, PR China. *Arctic and Alpine Research*, 29(2),
1294 226-232, 1997.
- 1295 Uppala, S.M., Kållberg, P.W., Simmons, A.J., Andrae, U., da Costa Bechtold, V., Fiorino, M., Gibson, J.K., Haseler, J.,
1296 Hernandez, A., Kelly, G.A., Li, X., Onogi, K., Saarinen, S., Sokka, N., Allan, R.P., Andersson, E., Arpe, K.,
1297 Balmaseda, M.A., Beljaars, A.C.M., van de Berg, L., Bidlot, J., Bormann, N., Caires, S., Chevallier, F., Dethof, A.,
1298 Dragosavac, M., Fisher, M., Fuentes, M., Hagemann, S., Hólm, E., Hoskins, B.J., Isaksen, L., Janssen, P.A.E.M.,
1299 Jenne, R., McNally, A.P., Mahfouf, J.-F., Morcrette, J.-J., Rayner, N.A., Saunders, R.W., Simon, P., Sterl, A.,
1300 Trenberth, K.E., Untch, A., Vasiljevic, D., Viterbo, P., and Woollen, J.: The ERA-40 re-analysis. *Quart. J. R.*
1301 *Meteorol. Soc.*, 131, 2961-3012, 2005.
- 1302
- 1303 von Blanckenburg, F., Bouchez, J., Ibarra, D.E., and Maher, K.: Stable runoff and weathering fluxes into the oceans
1304 over Quaternary climate cycles, *Nature Geoscience*, 8(7), 538–542, doi:10.1038/ngeo2452, 2015.
- 1305 Valla, P.G., Shuster, D.L., and van der Beek, P.A.: Significance increase in relief of European Alps during mid-Pleisto-
1306 cene glaciations. *Nature Geoscience*, 4, 688–692. doi:10.1038/ngeo1242, 2011.
- 1307 [Van Campo, E., Cour, P., and Huang, S.: Holocene environmental changes in Bangong Co basin \(Western](#)
1308 [Tibet\). Part 2: The pollen record, *Palaeogeogr. Palaeoclimatol.*, 120, 49-63, doi:10.1016/0031-0182\(95\)00033-](#)
1309 [X, 1996.](#)
- 1310
- 1311 [Villagrán, C. and Varela, J.: Palynological Evidence for Increased Aridity on the Central Chilean Coast during](#)
1312 [the Holocene, *Quaternary Res.*, 34, 198–207, doi:10.1016/0033-5894\(90\)90031-F, 1990.](#)
- 1313 [Villa-Martínez, R., Villagrán, C., and Jenny, B.: The last 7500 cal yr B.P. of westerly rainfall in Central Chile](#)
1314 [inferred from a high-resolution pollen record from Laguna Aculeo \(34°S\), *Quaternary Res.*, 60, 284-293,](#)
1315 [doi:https://doi.org/10.1016/j.yqres.2003.07.007, 2003.](#)
- 1316 Wei, W., and Lohmann, G.: Simulated Atlantic Multidecadal Oscillation during the Holocene. *Journal of Climate*, 25,
1317 6989–7002. doi: http://dx.doi.org/10.1175/JCLI-D-11-00667.1, 2012.
- 1318 [Wang, R.L., Scarpitta, S. C., Zhang, S. C., and Zheng, M. P.: Later Pleistocene/Holocene climate conditions](#)
1319 [of Qinghai-Xizhang Plateau \(Tibet\) based on carbon and oxygen stable isotopes of Zabuye Lake sedi-](#)
1320 [ments, *Earth Planet. Sc. Lett.*, 203, 461-477, doi:10.1016/S0012-821X\(02\)00829-4, 2002.](#)
- 1321 Whipple, K.X., Kirby, E., and Broecklehurst, S.H.: Geomorphic limits to climate-induced increases in topographic re-
1322 lief. *Nature*, 401, 39-43. doi:10.1038/43375, 1999.
- 1323 Whipple, K.X., and Tucker, G.E.: Dynamics of the stream-power river incision model: Implications for height limits of
1324 mountain ranges, landscape response timescales, and research needs, *Journal of Geophysical Research-Solid Earth*,
1325 104, 17661-17674, 1999.
- 1326 Whipple, K. X.: The influence of climate on the tectonic evolution of mountain belts, *Nat. Geosci.*, 2, doi:10.1038/
1327 ngeo413, 2009.
- 1328 Wilks, D.S.: Statistical methods in the atmospheric sciences - 3rd ed. Academic Press, Oxford, 2011.

- 1329 Willett, S.D., Schlunegger, F., and Picotti, V.: Messinian climate change and erosional destruction of the central
1330 European Alps. *Geology*, 34(8), 613-616, 2006.
- 1331 Wilson, G.S., Barron, J.A., Ashworth, A.C., Askin, R.A., Carter, J.A., Curren, M.G., Dalhuisen, D.H., Friedmann, E.I.,
1332 Fyodorov-Davidov, D.G., Gilichinsky, D.A., Harper, M.A., Harwood, D.M., Hiemstra, J.F., Janecek, T.R., Licht,
1333 K.J., Ostroumov, V.E., Powell, R.D., Rivkina, E.M., Rose, S.A., Stroeve, A.P., Stroeve, P., van der Meer, J.J.M.,
1334 Wizevich, M.C.: The Mount Feather Diamict of the Sirius Group: an accumulation of indicators of Neogene Ant-
1335 arctic glacial and climatic history, *Palaeogeography, Palaeoclimatology, Palaeoecology*, 182 (1–2), 117–131, 2002.
- 1336 [Wischnewski, J., Mischke, S., Wang, Y., and Herzschuh, U.: Reconstructing climate variability on the](#)
1337 [northeastern Tibetan Plateau since the last lateglacial – a multi-proxy, dual-site approach comparing](#)
1338 [terrestrial and aquatic signals, *Quaternary Science Reviews*, 30, 82-97,](#)
1339 [doi:10.1016/j.quascirev.2010.10.001, 2011.](#)
- 1340 [Wünnemann, B., Mischke, S., and Chen, F.: A Holocene sedimentary record from Bosten lake, China, *Pa-*](#)
1341 [laeogeogr. Palaeocl., 234, 223-238, doi:10.1016/j.palaeo.2005.10.016, 2006.](#)
- 1342 [Yanhong, W., Lücke, A., Zhangdong, J., Sumin, W., Schleser, G.H., Battarbee, R.W., and Weilan, X.: Holo-](#)
1343 [cene climate development on the central Tibetan Plateau: A sedimentary record from Cuoe Lake, *Palaeo-*](#)
1344 [geogr. Palaeocl., 234, 328-340, doi:10.1016/j.palaeo.2005.09.017, 2006](#)
- 1345 Yanites, B.J., and Ehlers, T.A.: Global climate and tectonic controls on the denudation of glaciated mountains. *Earth*
1346 *and Planetary Science Letters*, 325, 63-75, 2012.
- 1347 [Yu, L. and Lai, Z.: Holocene climate change inferred from stratigraphy and OSL chronology of Aeolian sedi-](#)
1348 [ments in the Qaidam Basin, northeastern Qinghai-Tibetan Plateau, *Quaternary Res.*, 81, 488-499,](#)
1349 [doi:10.1016/j.yqres.2013.09.006, 2014.](#)
- 1350 [Zhang, C. and Mischke, S.: A lateglacial and Holocene lake record from the Nianbaoyeze Mountains and in-](#)
1351 [ferences of lake, glacier and climate evolution on the eastern Tibetan Plateau, *Quaternary Sci. Rev.*, 28,](#)
1352 [1970-1983, doi:10.1016/j.quascirev.2009.03.007, 2009.](#)
- 1353 [Zhang, J., Chen, F., Holmes, J. A., Li, H., Guao, X., Wang, J., Li, S., Lu, Y., Zhao, Y., and Qiang, M.: Holo-](#)
1354 [cene monsoon climate documented by oxygen and carbon isotopes from lake sediments and peat bogs](#)
1355 [in China: a review and synthesis, *Quaternary Sci. Rev.*, 30, 1973-1987, doi:10.1016/](#)
1356 [j.quascirev.2011.04.023, 2011.](#)
- 1357 Zhang, X., Lohmann, G., Knorr, G., and Xu X.: Different ocean states and transient characteristics in Last Glacial Max-
1358 imum simulations and implications for deglaciation. *Clim. Past*, 9, 2319-2333, doi:10.5194/cp-9-2319-2013, 2013a.
- 1359 Zhang, R., Yan, Q., Zhang, Z.S., Jiang, D., Otto-Bliesner, B.L., Haywood, A.M., Hill, D.J., Dolan, A.M., Stepanek, C.,
1360 Lohmann, G., Contoux, C., Bragg, F., Chan, W.-L., Chandler, M.A., Jost, A., Kamae, Y., Abe-Ouchi, A., Ramstein,
1361 G., Rosenbloom, N.A., Sohl, L., and Ueda, H.: East Asian monsoon climate simulated in the PlioMIP. *Clim. Past*, 9,
1362 2085-2099, doi:10.5194/cp-9-2085-2013, 2013b.
- 1363
- 1364 Zhang, X., Lohmann, G., Knorr, G., and Purcell C.: Abrupt glacial climate shifts controlled by ice sheet changes.

1365 *Nature*, 512 (7514), 290-294, doi:10.1038/nature13592, 2014.

1366 Zhisheng, A., Kutzbach, J.E., Prell, W.L., and Porter, S.C.: Evolution of Asian monsoons and phased uplift of the South
1367 Asian plateau since Late Miocene times. *Nature*, 411(6833), 62-66, 2001.

1368 [Zhou, W. J., Lu, X. F., Wu, Z. K., Deng, L., Jull, A. J. T., Donahue, D. J., and Beck, W.: Peat record reflecting](#)
1369 [Holocene climate change in the Zoigê Plateau and AMS radiocarbon dating, Chinese Sci. Bull., 47, 66-](#)
1370 [70, doi:10.1360/02tb9013, 2002.](#)

1371

1372

1373

1374

1375

1376

1377

1378

1379

1380

1381

1382

1383

1384

1385

1386

1387

1388

1389

1390

1391

1392

1393

1394

1395

1396

1397

1398

1399

1400

1401

1402

1403

1404

1405

1406

1407

1408

1409

1410

1411

1412

1413

1414

1415

1416

1417

1418

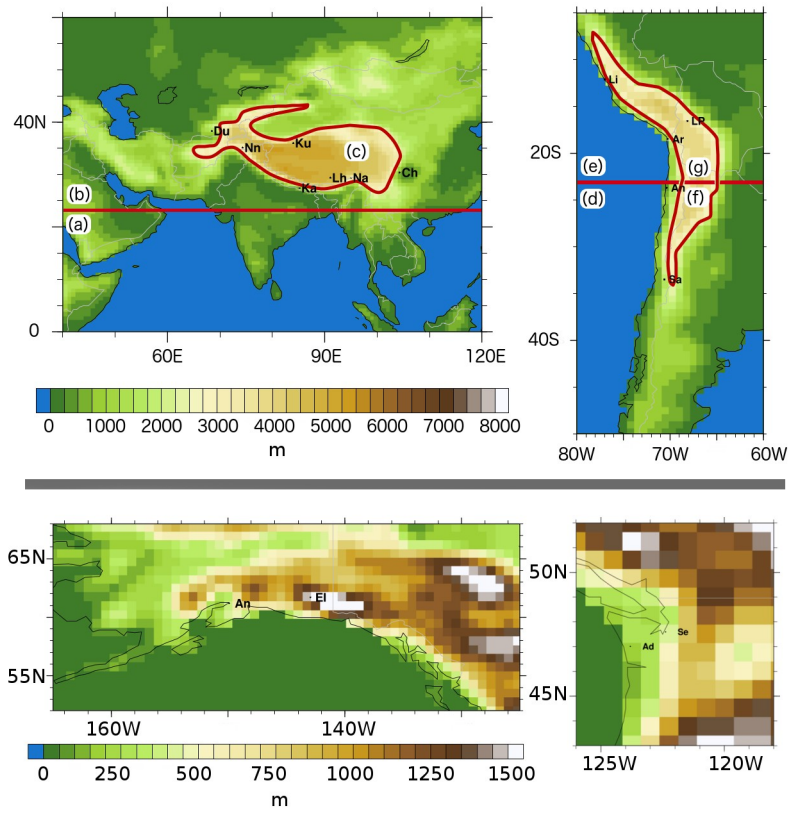


Figure 1

1478
1479
1480
1481
1482
1483
1484
1485
1486
1487
1488
1489
1490
1491
1492
1493
1494
1495
1496
1497
1498
1499
1500
1501
1502
1503
1504
1505
1506
1507
1508
1509
1510
1511
1512
1513
1514
1515
1516
1517
1518
1519
1520
1521
1522
1523
1524
1525
1526
1527
1528
1529
1530
1531
1532
1533
1534
1535
1536
1537

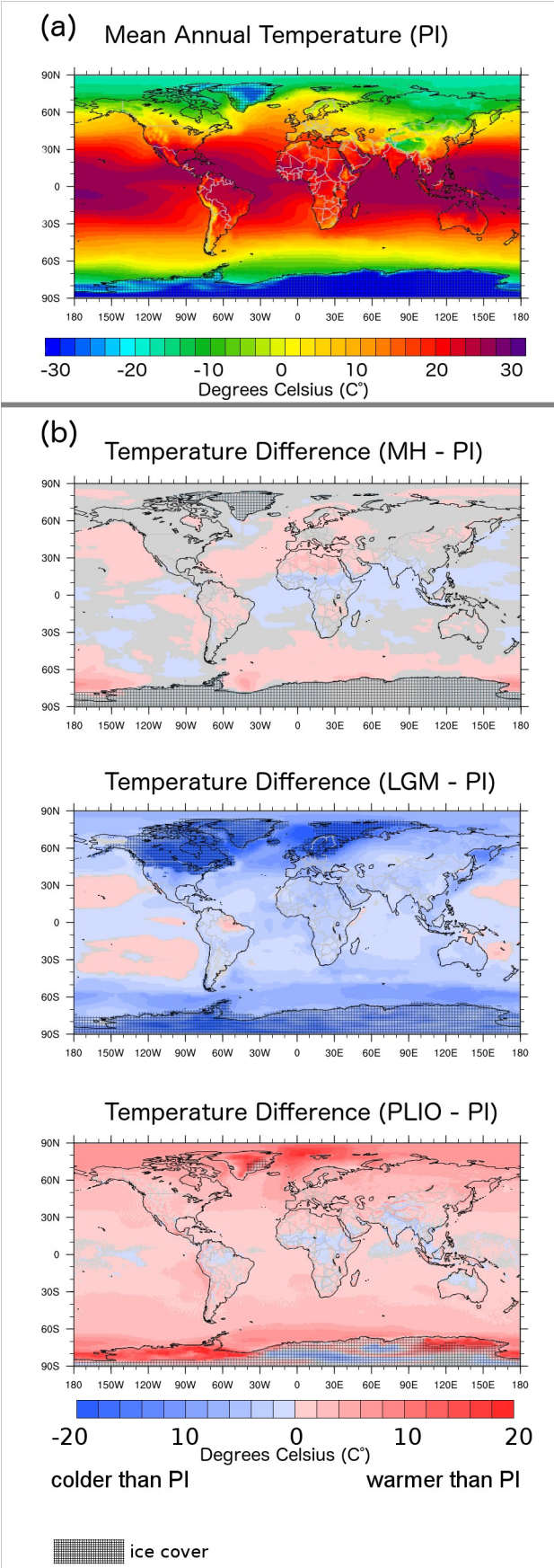


Figure 2

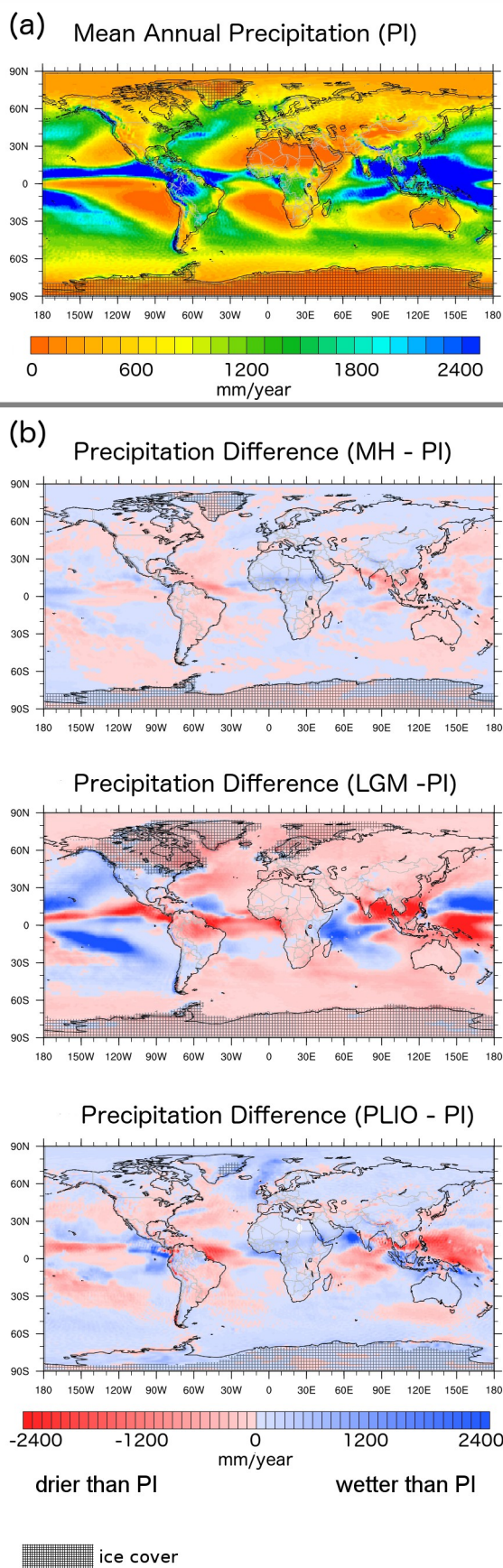


Figure 3

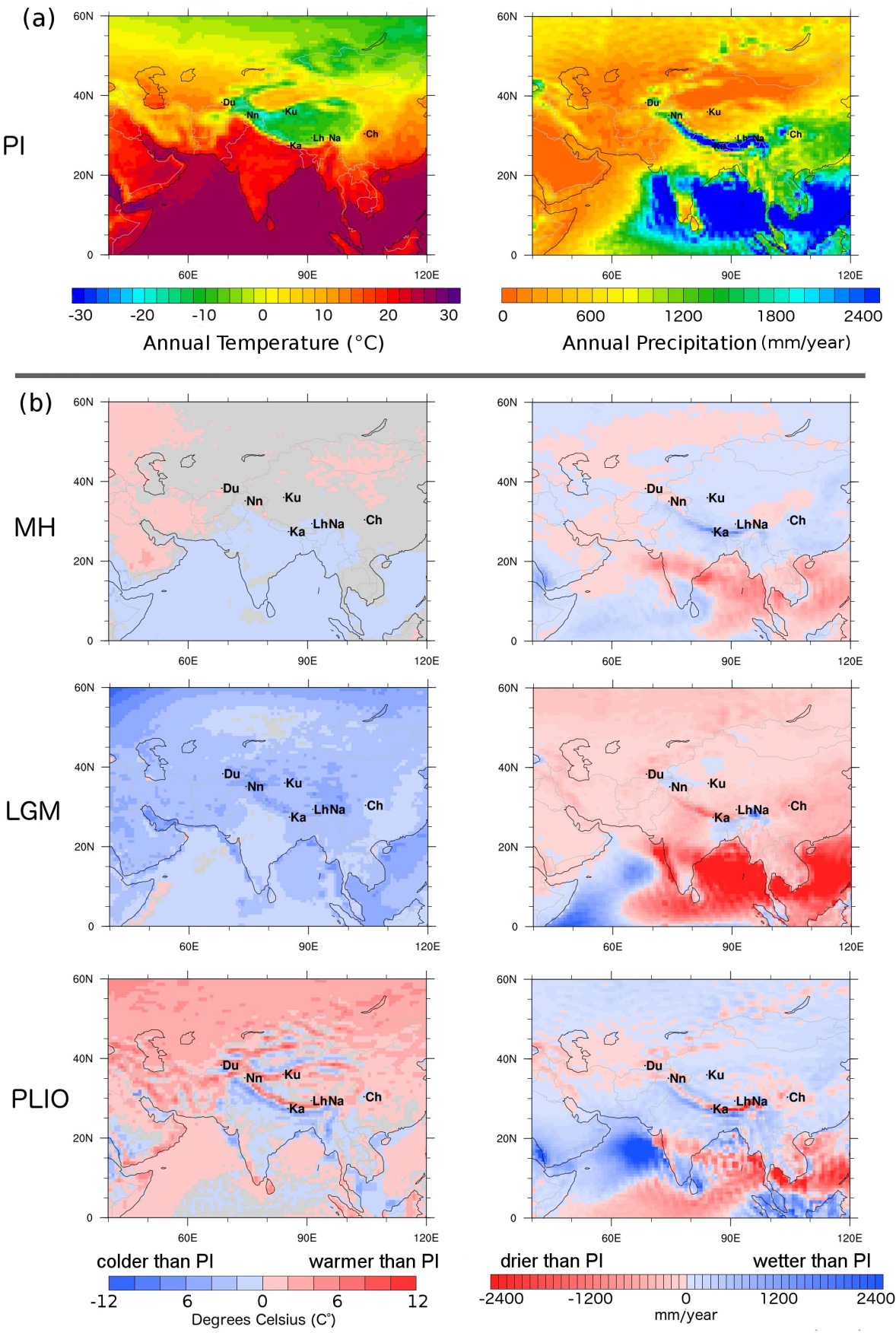


Figure 4

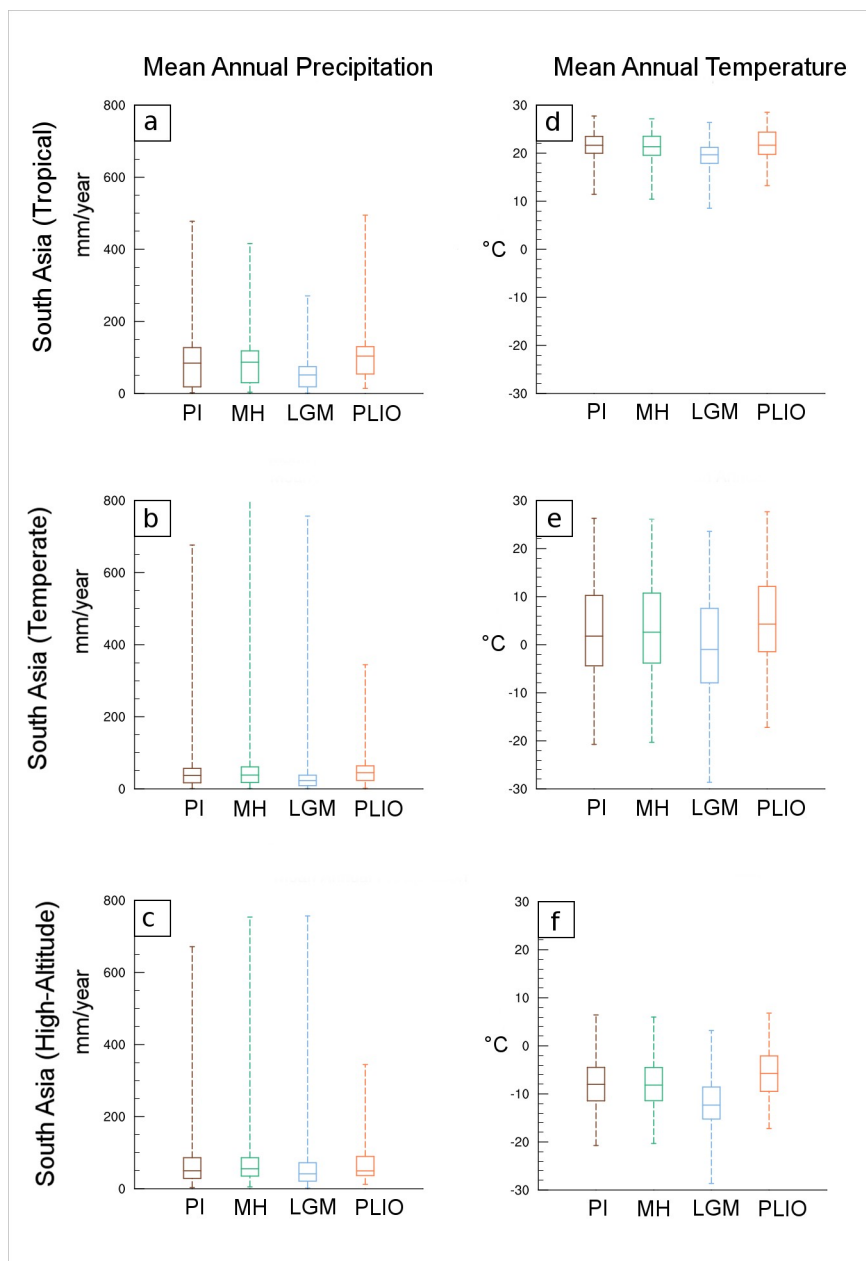


Figure 5

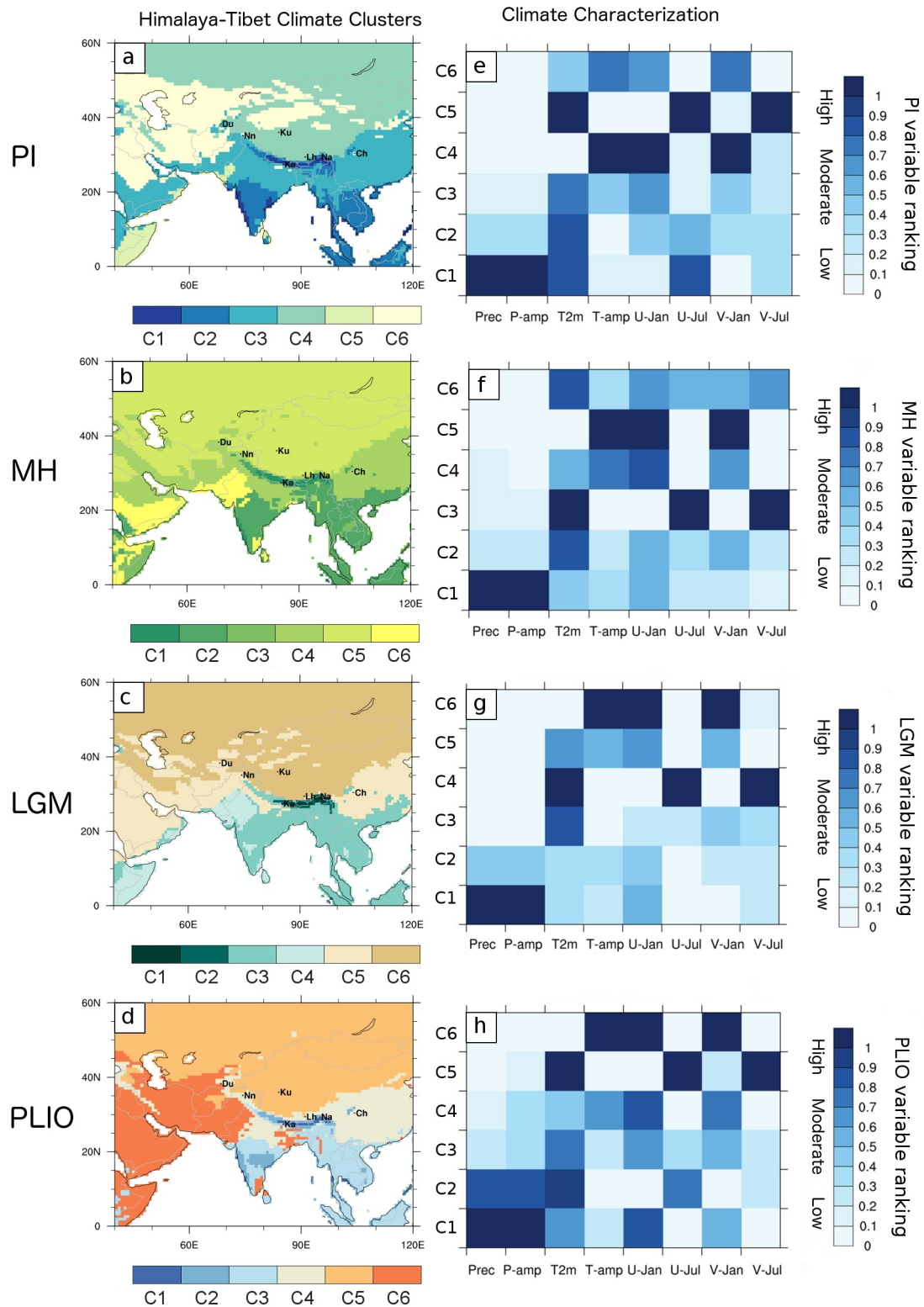


Figure 6

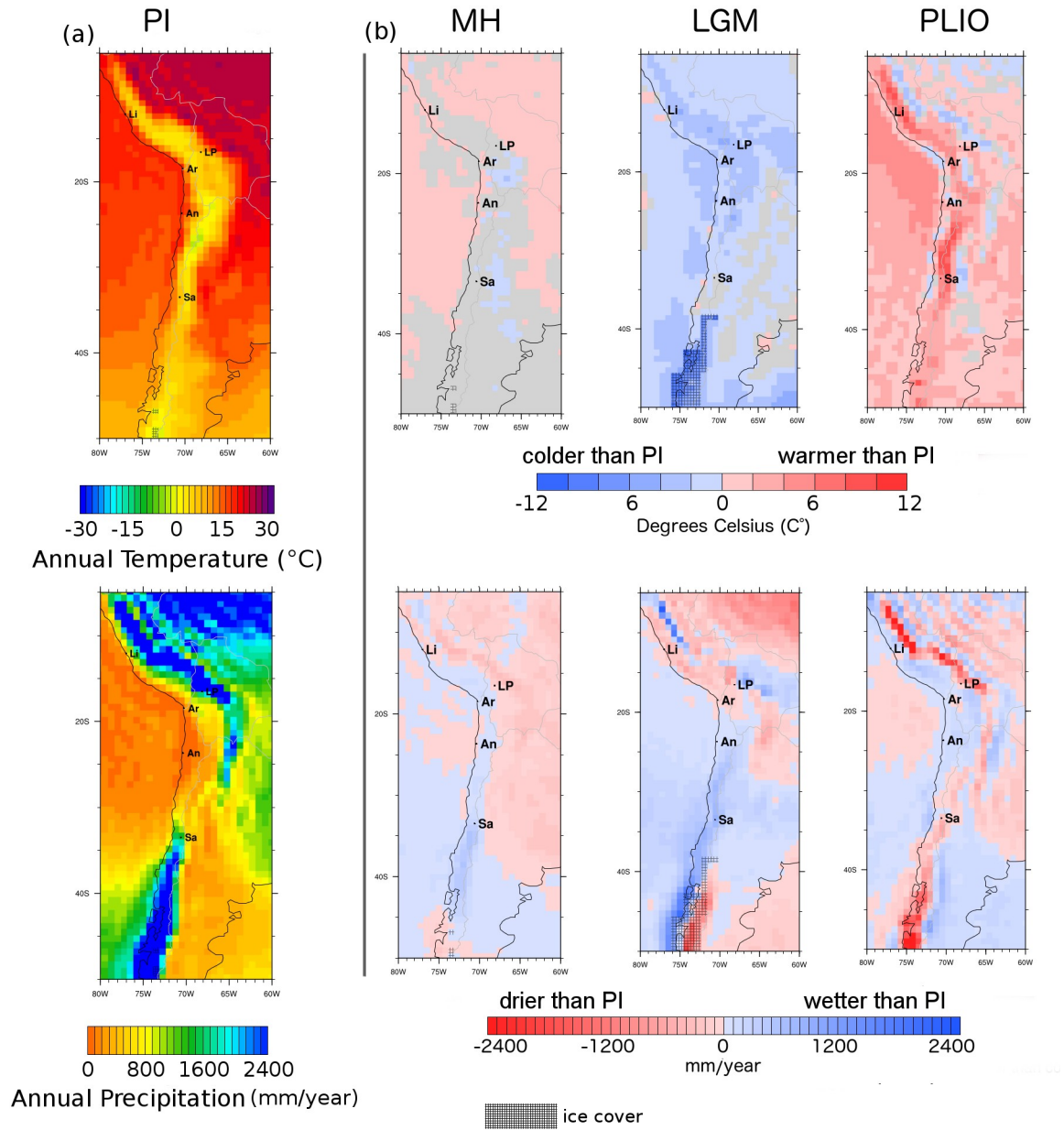


Figure 7

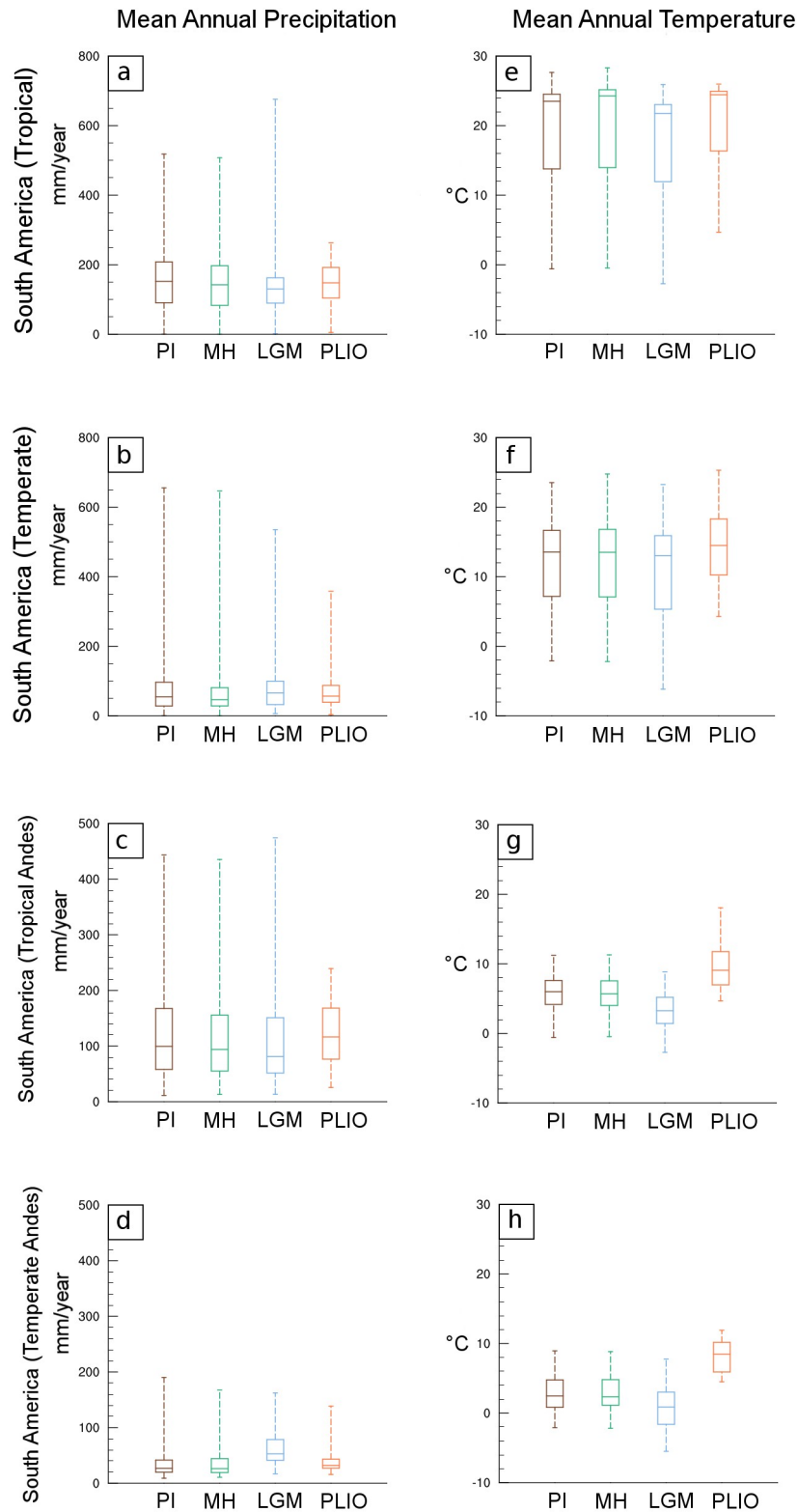


Figure 8

Andes Climate Clusters

Climate Characterization

PI

MH

LGM

PLIO

PI variable ranking

MH variable ranking

LGM variable ranking

PLIO variable ranking

C1 C2 C3 C4 C5 C6

Prec P-amp T2m T-amp U-Jan U-Jul V-Jan V-Jul

High Moderate Low

0 0.1 0.2 0.3 0.4 0.5 0.6 0.7 0.8 0.9 1

Figure 9

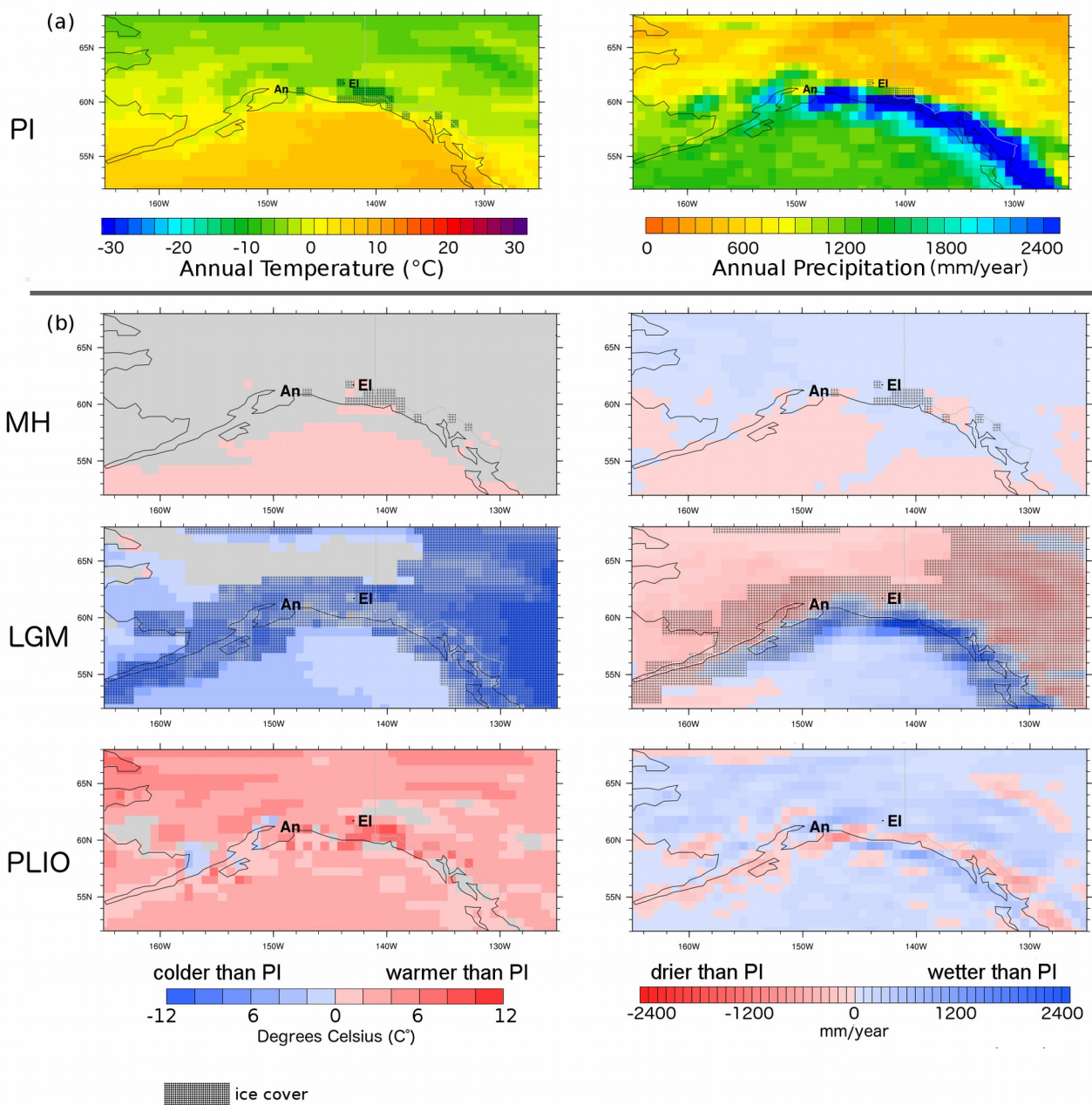


Figure 10

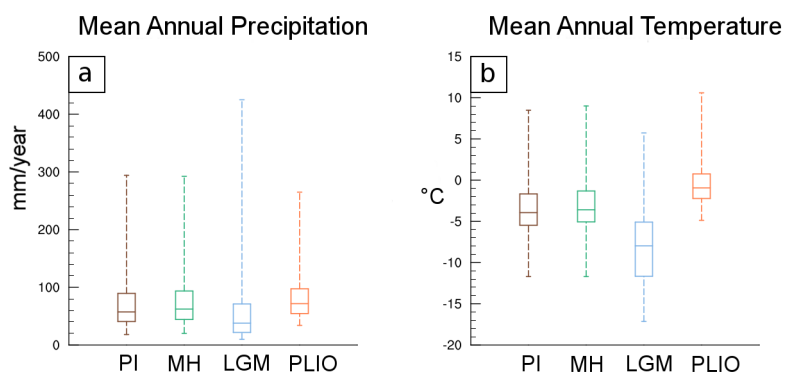
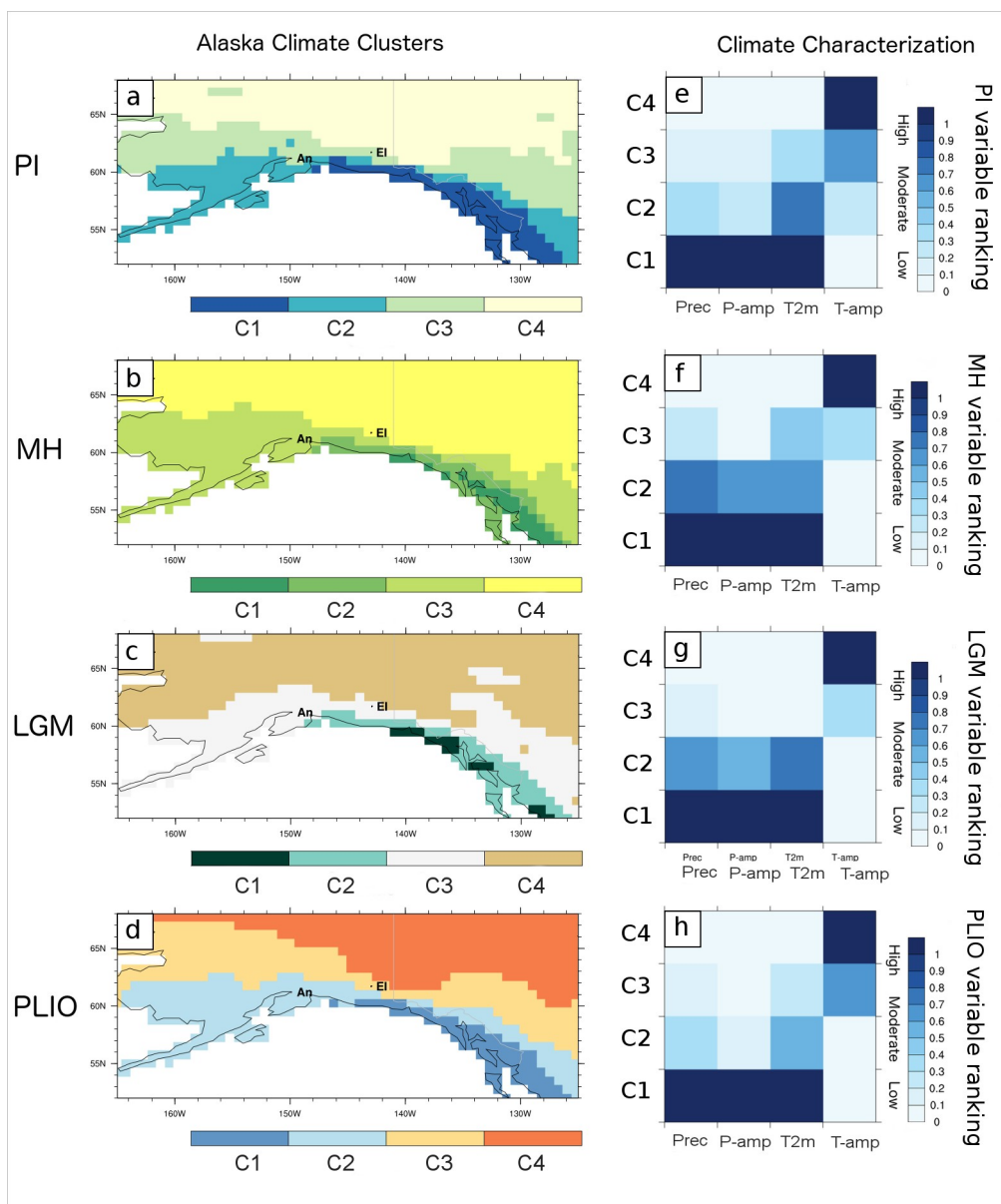


Figure 11

1920
1921
1922
1923
1924
1925
1926
1927
1928
1929
1930
1931
1932
1933
1934
1935
1936
1937
1938
1939
1940
1941
1942
1943
1944
1945
1946
1947
1948
1949
1950
1951
1952
1953
1954
1955
1956
1957
1958
1959
1960
1961
1962
1963
1964
1965
1966
1967
1968
1969
1970
1971
1972
1973
1974
1975
1976
1977
1978
1979



1980
1981
1982
1983
1984
1985
1986
1987
1988
1989
1990
1991
1992
1993
1994
1995
1996
1997
1998
1999
2000
2001
2002
2003
2004
2005
2006
2007
2008
2009
2010
2011
2012
2013
2014
2015
2016
2017
2018
2019
2020
2021
2022
2023
2024
2025
2026
2027
2028
2029
2030
2031
2032
2033
2034
2035
2036
2037
2038
2039

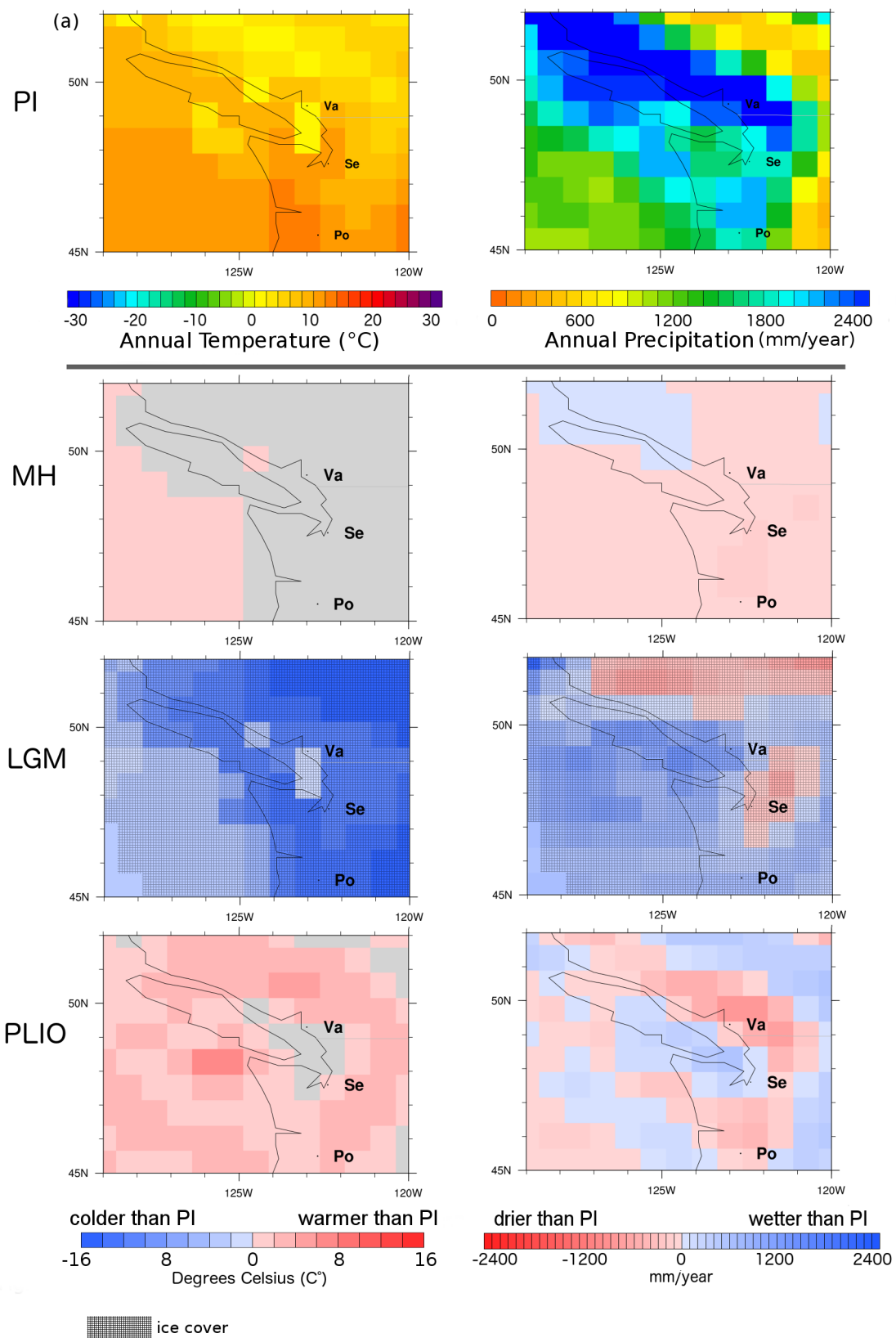


Figure 13

2040
2041
2042
2043
2044
2045
2046
2047
2048
2049
2050
2051
2052
2053
2054
2055
2056
2057
2058
2059
2060
2061
2062
2063
2064
2065
2066
2067
2068
2069
2070
2071
2072
2073
2074
2075
2076
2077
2078
2079
2080
2081
2082
2083
2084
2085
2086
2087
2088
2089
2090
2091
2092
2093
2094
2095
2096
2097
2098
2099

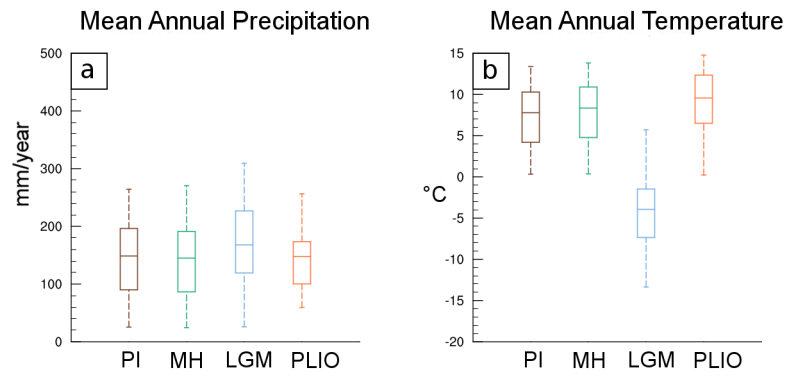


Figure 14

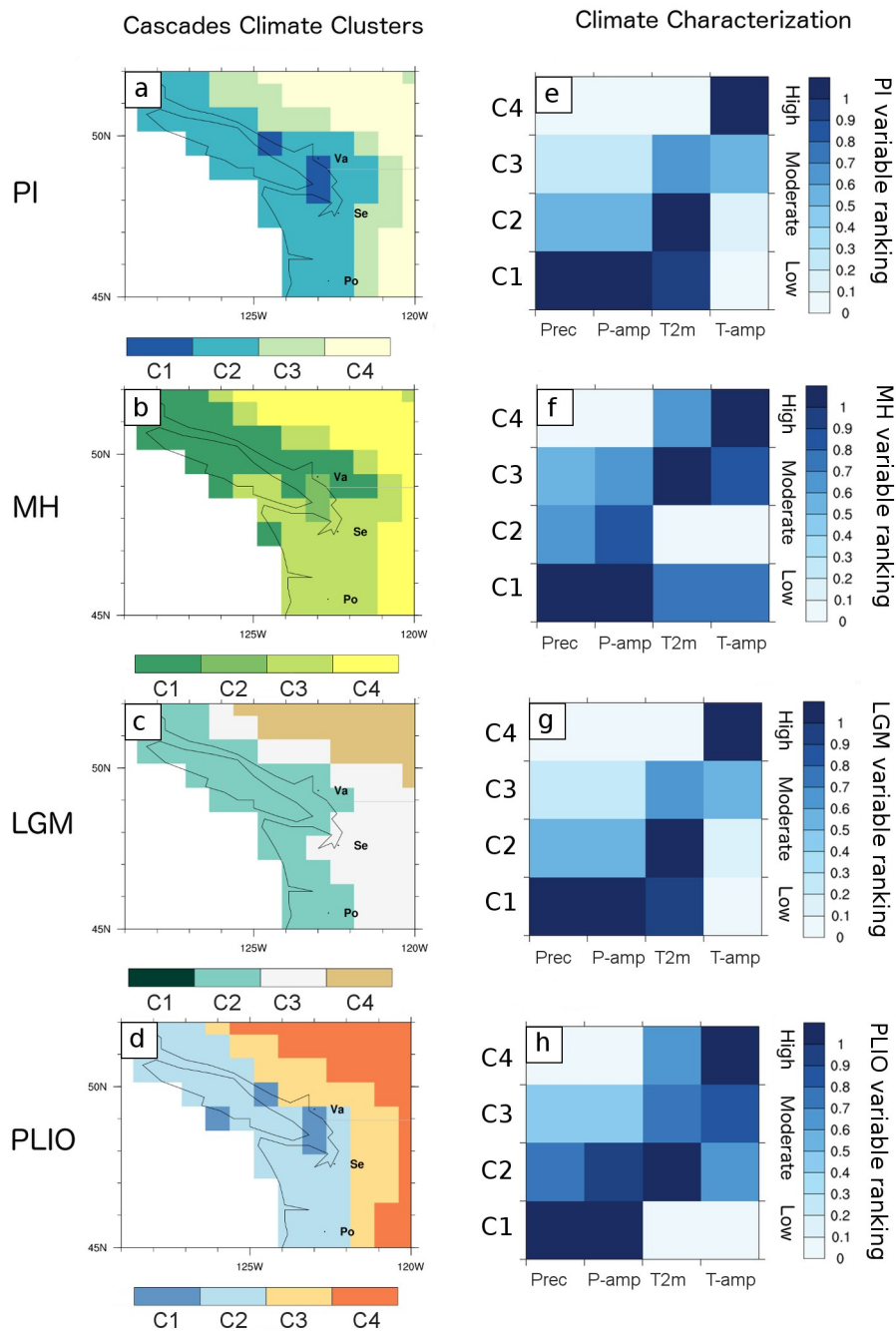


Figure 15

2100
2101
2102
2103
2104
2105
2106
2107

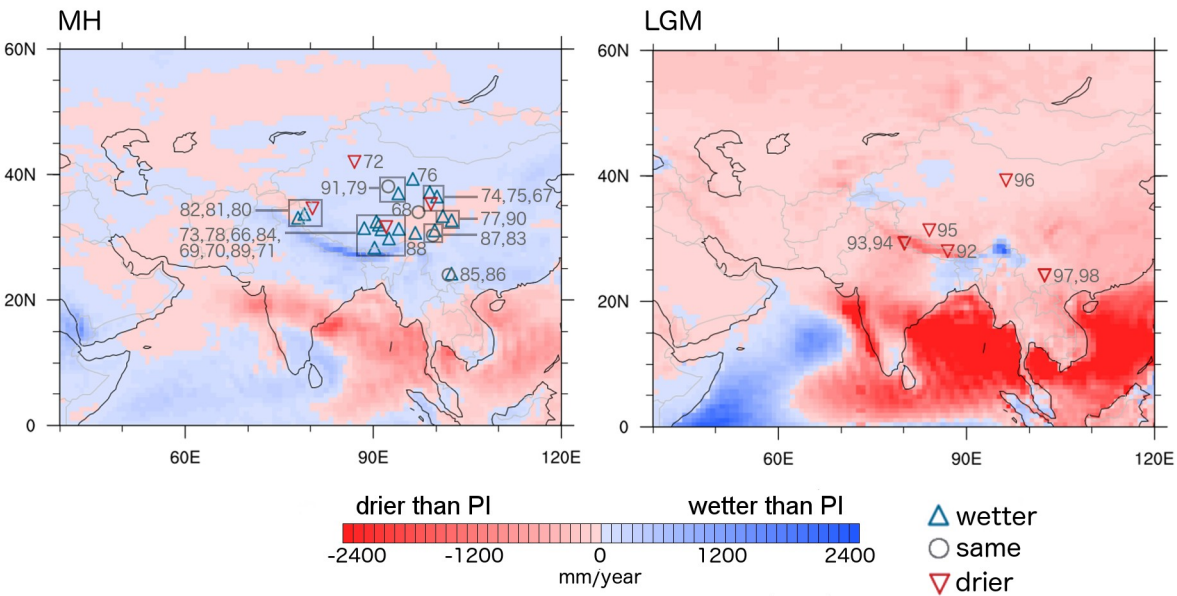


Figure 16

2108
2109
2110
2111
2112
2113
2114
2115
2116
2117
2118
2119
2120
2121
2122
2123
2124
2125
2126
2127
2128
2129
2130
2131
2132
2133
2134
2135
2136
2137
2138
2139
2140
2141
2142
2143
2144
2145
2146
2147

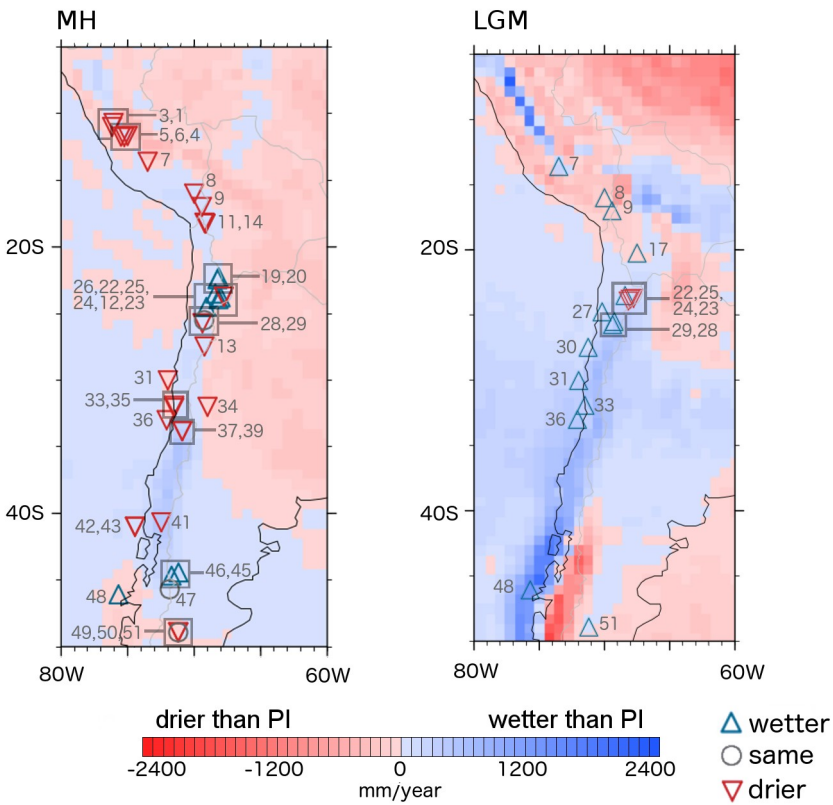
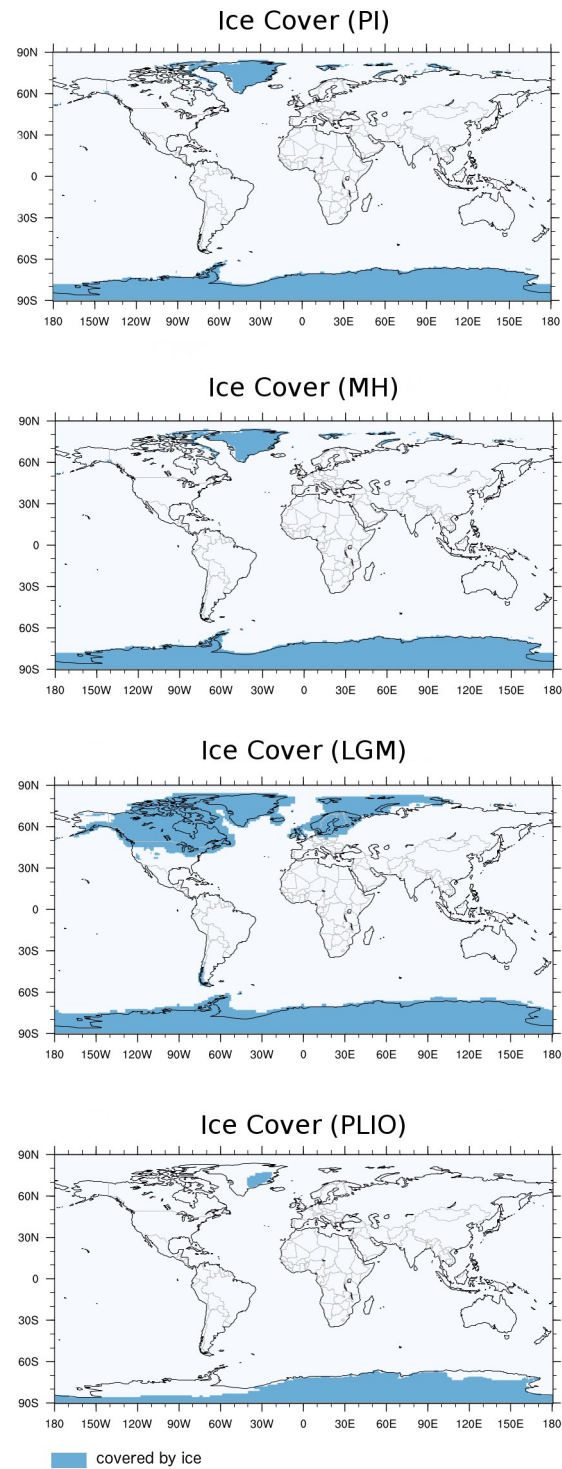


Figure 17

2148
2149
2150
2151
2152
2153
2154
2155
2156
2157
2158
2159
2160
2161
2162
2163
2164
2165
2166
2167
2168
2169
2170
2171
2172
2173
2174
2175
2176
2177
2178
2179
2180
2181
2182
2183
2184
2185
2186
2187
2188
2189
2190
2191
2192
2193
2194
2195



Supplemental Figure S1